

**Vacuum Ultraviolet Surface Modification of
Organic Materials**

Kim, Young-Jong

**Vacuum Ultraviolet Surface Modification of
Organic Materials**

**A Doctoral Dissertation by
Kim, Young-Jong**

2008

Department of Materials Science and Engineering,
Kyoto University,
In partial fulfillment of the requirements for the degree of
DOCTOR OF ENGINEERING

Contents

Chapter 1 Introduction

1.1 Photochemical surface processing	1
1.1.1 Excimer ultraviolet (UV) sources	1
1.1.2 Surface modification of organic materials with excimer lasers	2
1.1.3 Surface modification of organic materials with VUV lamps	3
1.2 VUV surface modification of organic monolayers	7
1.2.1 Self-assembled monolayers (SAMs)	7
1.2.2 Organosilane self-assembled monolayers on Si	9
1.2.3 Formation of multilayers by self-assembly	11
1.2.4 Photochemical micropatterning of organosilane SAMs	12
1.3 VUV surface modification of synthetic resins	13
1.3.1 General introduction to plastics	13
1.3.2 Cyclo-olefin polymer (COP)	15
1.3.3 Applications of COP	16
1.4 Aim of the study	18
1.4.1 Background	18
1.4.2 Aim of this thesis	19
1.4.3 Scope	20

Chapter 2 Surface chemical conversion of organosilane SAMs

2.1 Introduction	25
2.2 Experimental procedure	27
2.3 Results and discussion	29
2.3.1 Surface chemical conversion of a alkylsilane monolayer	29
2.3.2 Stacking of a second alkylsilane SAM	36
2.4 Summary	38

Chapter 3 Organosilane self-assembled multilayer formation

3.1 Introduction	43
3.2 Experimental procedure	45
3.3 Results and discussion	48
3.3.1 Growth mechanism of a solid-immobilized multilayer	48
3.3.2 Surface analysis of monolayer/multilayers	51

3.4 Summary	62
-------------------	----

Chapter 4 Surface modification and bonding of cyclo-olefin polymer (COP)

4.1 Introduction	66
4.2 Experimental procedure	68
4.3 Results and discussion	70
4.3.1 Water contact angle of direct and remote VUV-light treated COP surface ...	70
4.3.2 Chemical composition of direct and remote VUV-light treated COP surface	71
4.3.3 Topography of direct and remote VUV-light treated COP surface	82
4.3.4 Temporal change of VUV-light treated COP surface	85
4.3.5 Photochemical activation bonding of COP	88
4.4 Summary	91

Chapter 5 Conclusions95

Chapter 1

Introduction

1.1 Photochemical surface processing

1.1.1 Excimer ultraviolet (UV) sources

There have been growing attention on the UV photochemistry of material surfaces owing to its key roles in practical applications, e.g., surface cleaning, surface modification, thin film deposition, etching, etc., as well as to fundamental scientific interests in surface photochemical phenomena. Among a number of requirements for the light source applied to UV photochemical surface processing, the availability of photons with a sufficiently high energy is of primary importance. In most cases, photon energies from 3 to 10 eV, which correspond to UV, deep UV (DUV) and vacuum UV (VUV) lights, are employed. The low-pressure mercury discharge lamp has been used as a DVU-VUV light source with a strong resonance line at 254 nm and a weaker line at 185 nm. Moderate intensities at shorter wavelengths are available from the deuterium lamp with an intense atomic line at 122 nm and a dissociation continuum peaking at about 160 nm. Radiations with a few of wavelengths are obtained from rare-gas resonance lines in low pressure discharges, that is, Ar at 107 nm, Kr at 124 nm and Xe at 147 nm, although only lower photon fluxes are available compared with the other light sources. Although synchrotron radiation is favourable for the light source of DUV-VUV photochemistry, it requires a huge facility and, thus, cannot be adopted to desktop experiments and the most of industry fields. Accordingly, there has been an increasing demand for compact DUV and VUV light sources having a light intensity sufficient for surface processing.

Promising light sources applicable to the DUV-VUV photochemical surface

modification have been developed in these two decades. The light sources depend on radiation from excimers consisting of rare-gas and/or halogen atoms. Excimer lasers with wavelengths of 157 nm (F₂), 193 nm (ArF), 222 nm (KrCl), 248 nm (KrF), 308 nm (XeCl) and 351 nm (XeF) have attracted attention as DUV-VUV light sources with a high photon flux. For example, in the microelectronics industry, KrF and ArF lasers have commercially employed in photolithography systems as their light source promoting photochemical reactions of photoresist.

1.1.2 Surface modification of organic materials with excimer lasers

Since the discovery of laser ablation, that is, the light-stimulated thin layer removal from organic polymer surfaces, in 1982 [1,2], scientific interests on the physics and chemistry of organic polymers irradiated with intense DUV light from an excimer laser have emerged. The ablative photo-decomposition process renders important potential applications in microelectronics, optics, packaging technology and surgery. For example, polyimides (PIs) and fluoropolymers were modified in order to offer desirable properties for microcircuit fabrication [3]. Polymethylmetacrylate (PMMA) was modified by this process as resist films in photolithography [4]. The method was employed for the pre-treatment of plastic substrates for metalization toward applications in the automotive industry and the fields of electromagnetic shielding, semiconductor manufacturing and packaging [3,5].

Controlled modification of polymeric materials based on the interaction of energetic particle beams, photons and plasmas with the materials has become a field of considerable technical importance. The adhesion of coating films on polymers can be enhanced when the polymer surface are properly modified. Furthermore, wettability and printability of polymers can be improved as well through changes in morphology and chemical properties of the

polymer surfaces. Area-selective processing of polymeric materials by excimer lasers has become a growing field of applied research [6]. A considerable number of theoretical and experimental works have been conducted in order to elucidate the observed phenomena. A wide variety of polymers, e.g., (PMMA, PI, polyethyleneterephthalate (PET), polytetrafluoroethylene (PTFE), polyethylene (PE), polycarbonate (PC), etc.) have been provided for samples of laser ablation. Most of the etching studies were performed using pulsed excimer lasers. Table 1.1 summarizes a part of the published results. Several models have been suggested to describe the laser ablation of polymers [7,8].

1.1.3 Surface modification of organic materials with VUV lamps

Surface modification based on UV radiation is not restricted to the use of high UV intensities obtainable from excimer lasers nor is submicron patterning dependent on coherent monochromatic illumination realized by the expensive photolithography systems. Instead of excimer lasers radiating a pulsed and intense DUV or VUV light, the use of DUV-VUV lamps for surface processing has a particular advantage that it can be adopted to surface modification at once with a relatively wide area compared with the excimer laser processing. One problem of the lamps is window materials especially at wavelengths shorter than 160 nm, that is, the cut-off wavelength of high-purity quartz. Available materials (MgF_2 , CaF_2 , LiF) show lifetimes of an insufficient length because of the radiation-induced colour center formation. This effect leads to a decrease in transmission with VUV exposure time. LiF has an additional disadvantage as being hygroscopic. To avoid problems on window materials, windowless UV sources have been proposed [9-11], for example by passing the photons through a small orifice between the discharge generating the UV radiation and the reaction chamber. A wide-area windowless VUV lamp was developed by Yu et al. [12]. It uses an

electron-beam-generated plasma disk to excite hydrogen, nitrogen or helium spectral lines at about 120 nm. Recent developments in DUV-VUV light source are excimer lamps which radiate an incoherent UV light of a fairly narrow-bandwidth at a number of different wavelengths. The excimer lamps provide DUV-VUV lights of a sufficiently high intensity for material surface modification. They can be used as sealed lamps or also in windowless internal lamp configurations. As already shown in several practical applications, the excimer lamps bear substantial potentials for photochemical surface processing.

Among various DUV-VUV lamps, Xe excimer lamp radiating VUV light at 172 nm in wavelength has an advantage in window material. Quartz can be used for the window material of this lamp. Therefore, the lamp is practically important and promising as a light source for VUV surface processing. There are distinct differences in characteristics between excimer lasers and the Xe excimer lamp. The excimer lasers radiate a pulsed and coherent light with a relatively high intensity, while the excimer lamp radiates a continuous and incoherent light with a moderate intensity. Consequently, surface modification mechanisms of organic materials with the VUV excimer lamp are considered to be rather different from those with the excimer lasers, that is, laser ablation. Reliance on knowledge of photophysics and photochemistry, UV photons in resonance with electronic transitions in unsaturated hydrocarbon monolayer, e.g., π - π^* transition, induces photolysis of aromatic-silane monolayers [13], while direct photolysis of saturated hydrocarbons requires σ - σ^* transition in C-H or C-C bonds. Such excitations are induced by VUV light less than 160 nm in wavelength [14]. Therefore, the VUV light at 172 nm is rarely absorbed with saturated hydrocarbon [15]. Consequently, organic materials consisting of saturated hydrocarbon molecules are considered hardly etched only by VUV-irradiation at 172 nm. Indeed, saturated hydrocarbon polymers such as PE and polypropylene (PP) were not etched with

VUV-irradiation at 172 nm in vacuum [16]. VUV-etching of PE proceeds effectively in the presence of atmospheric oxygen molecules [17]. On the contrary, PMMA distinctly absorbs the VUV light [15]. Its optical density at 172 nm is more than 6 times of that of PE. Thus, PMMA is readily photoetched with UV or VUV irradiation even without atmospheric oxygen [16,17]. This is most certainly due to photoexcitation and decomposition of the oxygen-containing parts of PMMA.

Here, we discuss on the role of atmospheric oxygen in the VUV processing at 172 nm. The VUV light of 172 nm in wavelength excites atmospheric oxygen molecules resulting in the generation of oxygen atoms in the singlet and triplet states, [O(1D) and O(3P), respectively] as described in the Equation 1.1 [18].



These oxygen atoms, particularly O(1D), have a strong oxidative reactivity. Thus, when an alkyl monolayer is employed as a sample for VUV surface modification at 172 nm in the presence of atmospheric oxygen molecules, $-\text{CH}_3$ groups terminating its surface are oxidized to be in forms of $-\text{COOH}$, $-\text{CHO}$ and so forth. The monolayer surface, thus, becomes more hydrophilic. Such oxygen containing functional groups are decomposed by VUV-excitation as similarly to PMMA. The oxidation and subsequent decomposition reactions of the alkyl chains proceed simultaneously, resulting in the etching of the monolayer.

Ye et al. have reported similar results on UV photodegradation of alkylsiloxane monolayer based on the irradiation at 254 nm containing a VUV light at 183 nm with an intensity of 3% of the total intensity [19]. They concluded as well that atomic oxygen species generated through UV photochemistry of atmospheric oxygen were crucial for oxidation and

etching of the alkylsilane monolayers.

Table 1.1. UV-induced etching of polymers.

Polymer	Ambient	Light sources (λ)	Remarks
PET	Air	ArF* (193 nm)	1.2 $\mu\text{m}/\text{pulse}$
	Vacuum		(0.37 J/cm ²)
	Vacuum	ArF* (193 nm), low pressure mercury lamp (185, 254 nm)	XPS, SEM
PI	Air	ArF*, KrF*, XeCl* (193, 248, 308 nm)	Etch rate, UV, model
		XeCl* (308 nm)	IR, SEM
	Vacuum	F ₂ *, ArF*, XeCl* (157, 193, 308 nm)	MS
PMMA	Air	KrF*, XeCl*, XeF* (248, 308, 351 nm)	Threshold fluence, UV, IR GC/MS
	Vacuum		
	Air	KrF* (248 nm)	Etch rate, Model, incubation
PMMA, PET, PI	Air	ArF*, KrF*, XeCl* (193, 248, 308 nm)	Etch rate, SEM, LIF, model
		XeCL* (308 nm)	Etch rate, SEM, model
		Ar ion laser (300-330, 350-380 nm)	Etch rate, SEM
		ArF*, KrF*, XeCl*, XeF* (193, 248, 308, 351 nm)	Etch rate, UV, SEM
		ArF* (193 nm), low pressure mercury lamp (185, 254 nm)	Etch rate, XPS, SEM
PMMA, PI	Vacuum	Xe ₂ *, KrCl*, XeCl*	Etch rate, MS
PET, PTFE	Air	(172, 222, 308 nm)	UV, SEM, XPS
PTFE (Teflon)	Air	KrF* (248 nm)	Etch rate, SEM
α -MePS, PMMA	Air	ArF*, KrF* (193, 248 nm)	Etch rate, IR, UV, SEM
		ArF* (193 nm)	Etch rate, XPS
PC, PET, PS	Air	ArF*, KrF* (193, 248 nm), low pressure mercury lamp (185, 254 nm)	Etch rate
	Vacuum		
PE, PET, PI	Helium	F ₂ * (157 nm)	Threshold fluence
Mylar, PI,	Air, Helium	ArF*, KrF*, XeF*	Threshold fluence,
PMMA	Vacuum	(193, 248, 351 nm)	SEM

PS: polystyrene, α -MePS: poly(methylstyrene), GC: gas chromatography, LIF: laser induced fluorescence.

1.2 VUV surface modification of organic monolayers

1.2.1 Self-assembled monolayers (SAMs)

In recent years organized molecular systems have attracted growing attention. The techniques presently available for the construction of such systems include Langmuir-Blodgett (LB) [20,21] and self-assembly [22-24] deposition methods, by which well-ordered monomolecular layers can be formed on hydrophilic surfaces. These systems are believed to have technological potentials in both optical and molecular electronics [25,26]. Organized molecular films are also of particular interest in the field of, for example, smart surface coatings for tribology and advanced technique of nanofabrication. Therefore, they provide the opportunity to develop novel materials with improved performance and/or properties. Particularly, self-assembling, in which minute elements such as atoms, molecules and clusters are spontaneously organized into an ordered array of the elements, is a key process of the bottom-up nanotechnology [27-30]. One of the promising material processes on the basis of self-assembly is the fabrication of organic thin films with a monomolecular thickness. Although, it has been well-known that some types of organic molecules adsorb on a particular substrate and form a monolayer since several tens of years ago [31-33], such types of organic monolayers have recently named as self-assembled monolayers (SAMs). Due to immobilization of the molecules to the substrate through chemical bondings and the presence of intermolecular attractive interactions, the SAMs are more stable mechanically, chemically and thermodynamically compared with similar monolayers fabricated by the Langmuir-Blodgett technique.

However, the formation of SAMs depends on unique chemical reactions between a substrate and organic molecules. Hence, specific pairs of a substrate and a precursor are

required to fabricate SAMs. Typical examples for these SAM formation pairs are summarized in Table 1.2. Among various materials, Si is most important in micro ~ nano electronics and mechatronics. Thus, SAMs on Si are of special interest in order to integrate Si micro ~ nanodevices with organic molecules. As described in Section 1.2.2, there have been major methods preparing SAMs on Si.

Table 1.2. Pairs of precursors and substrates.

Precursor molecules	Substrate materials
Organosulfurs	Metals/compound semiconductors
alkylthiol: R-SH	Au, Ag, Cu, Pt, Pd, Hg, Fe, GaAs, InP
dialkyldisulfide: RS-SR'	
thioisocyanide: R-SCN etc.	
Fatty acid	Oxide
R-COOH	Al ₂ O ₃ , AgO, CuO
Phosphonic acid	Oxide
R-PO ₃ H ₂	ZrO ₂ , TiO ₂ , Al ₂ O ₃ , Ta ₂ O ₅ , etc.
Organosilanes:	Oxide
R-SiX ₃ (X = Cl, OCH ₃ , OC ₂ H ₅)	glass, mica, SiO ₂ , SnO ₂ , GeO ₂ , ZrO ₂ , TiO ₂ , Al ₂ O ₃ , ITO, PZT, etc.
Unsaturated hydrocarbons	Silicon
alkene, alkyne: R-CH = CH ₂ , R-C≡H	hydrogen-terminated Si: Si-H
Alchols, Aldehydes	halogen-terminated Si: Si-X (X = Cl, Br, I)
R-OH, R-CHO	

1.2.2 Organosilane self-assembled monolayers on Si

A molecule consisting of one Si atom connected with four functional groups, SiX_4 , is named as “silane”. A molecule in which at least one of these four functional groups are substituted with organic functional groups, that is, $\text{SiR}_n\text{X}_{4-n}$, is organosilane. Organosilane molecules react with hydroxyl groups on an oxide surface so as to be fixed on the surface as illustrated in Figure 1.1. This surface modification chemistry has been practically used as the silane coupling reaction for preparing organic layers on inorganic materials surfaces [34]. Sagiv and co-workers have reported, for the first time, that SAMs could be formed from organosilane molecules with one long alkyl chain in each of the molecules [35,36]. On a Si substrate, such a SAM can be formed as well by covering the substrate with its oxide. As shown in Figure 1.1, a trace amount of water is necessary to form organosilane SAMs. Halogen or alkoxy groups in an organosilane molecule are converted to hydroxyl ($-\text{OH}$) groups by hydrolysis. Dehydration reaction between these silanol ($\text{Si}-\text{OH}$) sites in the molecule with $-\text{OH}$ groups on the surface oxide of a Si substrate immobilizes the molecules on the oxide through siloxane ($\text{Si}-\text{O}-\text{Si}$) bonds.

There are three types of organosilane precursor molecules which have one, two or three reactive sites. When a SAM is formed from organosilane molecules with a single reactive site, the molecular density assembled into the SAM remains to be relatively low due to steric hindrance between methyl ($-\text{CH}_3$) groups of adjacent molecules. On the other hand, when a SAM is formed from organosilane molecules each of which has three reactive sites, its growth behavior is complicated somewhat. Since two $\text{Si}-\text{OH}$ groups remain in the organosilane molecule after that is immobilized on the substrate, the molecule is further linked with adjacent organosilane molecules through $\text{Si}-\text{O}-\text{Si}$ bonds as illustrated in Figure 1.2. This type of organosilane SAM is more closely packed and stable mechanically, chemically and

thermally due to the siloxane network laterally connecting molecules in the SAM in addition to the chemical attachment to the substrate.

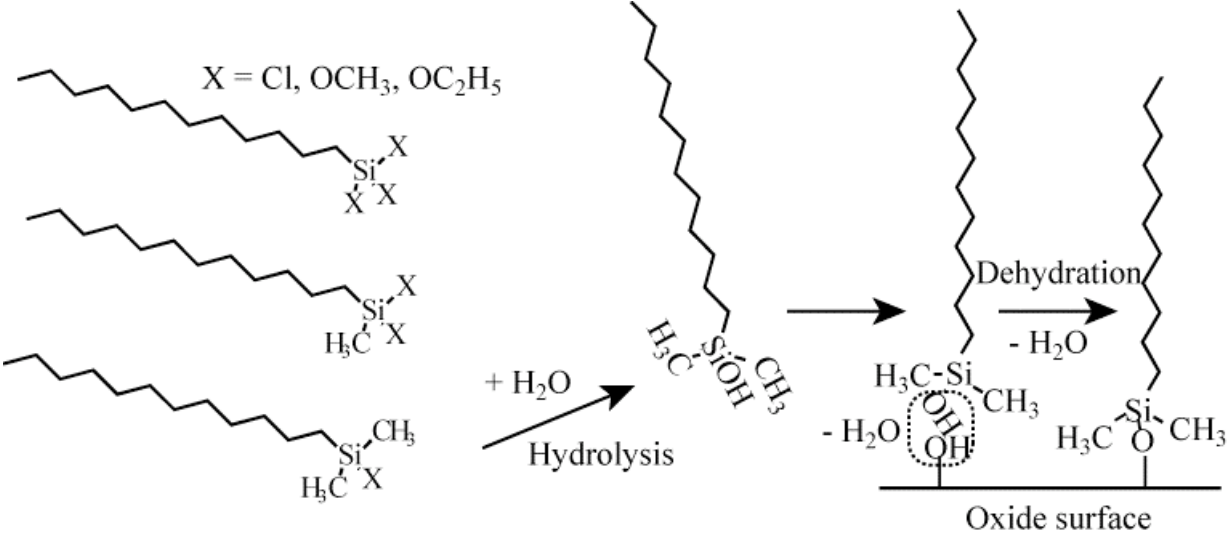


Figure 1.1. Organosilane SAMs.

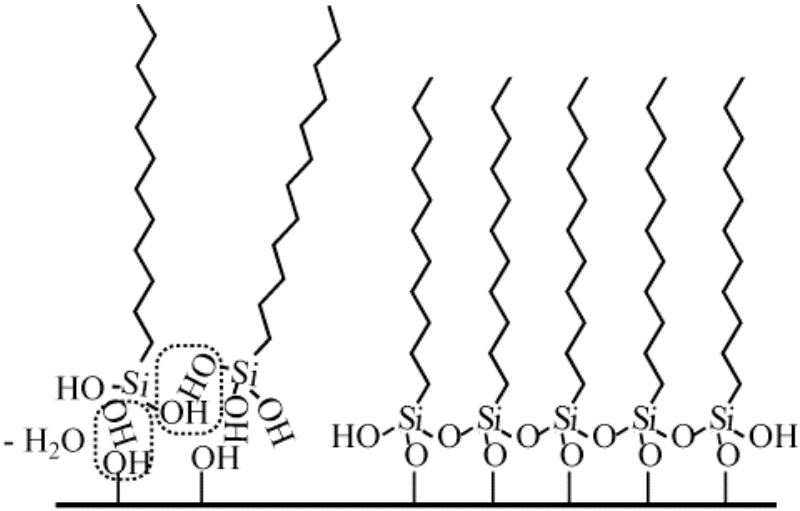


Figure 1.2. SAM formation from tri-functional organosilane molecules.

1.2.3 Formation of multilayers by self-assembly

As schematically illustrated in Figure 1.2, the formation of the organosilane SAM essentially relies on the in situ formation of a polysiloxane monolayer, by which the alkyl monolayer is connected to the substrate surface via Si–O–Si bonds. Since the presence of –OH groups on the substrate is crucial for the SAM formation, the construction of a self-assembled multilayer requires that each monolayer surface being modified to bear a hydroxylated surface. On this modified SAM surface, another SAM can be stacked (Figure 1.3). Such hydroxylated surfaces can be prepared by a chemical reaction and the conversion of a nonpolar terminal group to a hydroxyl group. Examples of such reactions are a reduction of a surface ester group [37], a hydrolysis of a protected surface hydroxyl group, and a hydroboration-oxidation of a terminal double bond [38,39].

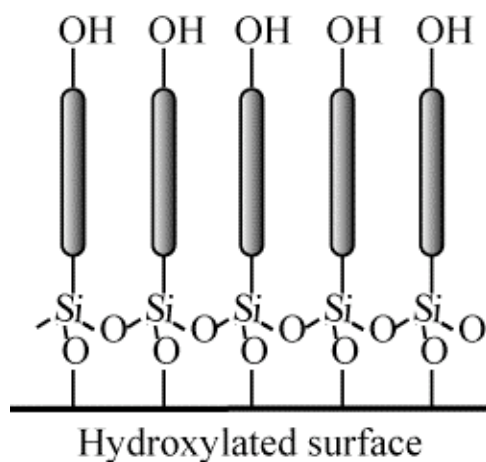


Figure 1.3. A hydroxy-terminated SAM.

A close inspection of Figure 1.4 reveals that the self-assembly multilayer structure is similar to a Z-type LB multilayer [20]. However, there is a significant difference between the

self-assembly system and an LB Z-film. Here, the film is connected to the substrate surface, the molecules in the monolayers are connected to each other, and the monolayers are bonded to each other by strong chemical bonds. In other words, an self-assembly multilayer is a three-dimensional polymer network, which explains its excellent material properties.

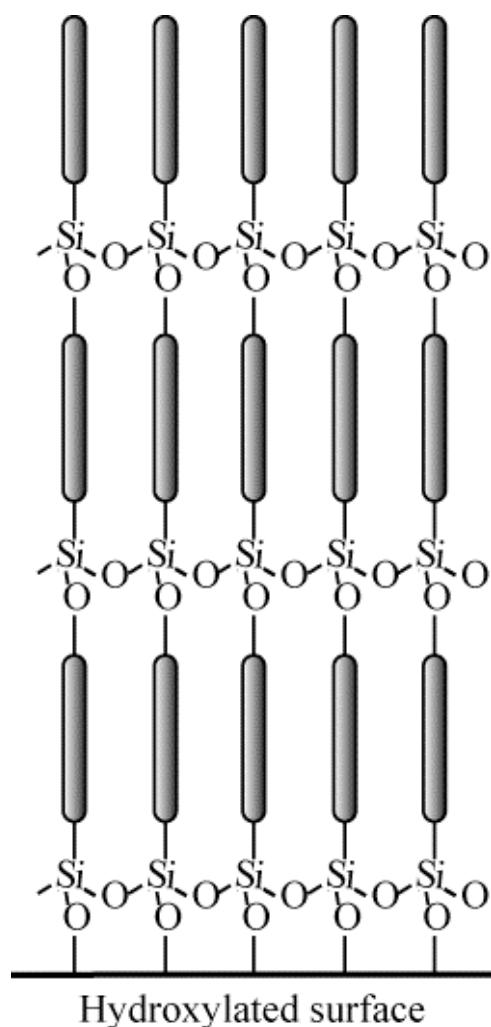


Figure 1.4. Self-assembly multilayers.

1.2.4 Photochemical micropatterning of organosilane SAMs

Much attention is denoted to the micropatterning of SAMs [13,40-61] for construction

of microstructures. The micro-contact printing method [62], by which a micropatterned SAM is directly formed on a substrate using an elastomeric stamp, has been applied to organosilane SAMs as well [46,49]. However, conventional photolithography using photomasks [13,42,55,57-61] and other lithographic tools employing electron beams [43,45], ion beams [44], neutral atomic beams [50], or scanning probe microscopes [48, 51-56] have been more frequently used in order to micropattern homogeneously prepared organosilane SAMs. Among various patterning methods, photolithography is most practical, since it can transfer an entire pattern on a photomask to a SAM by a single exposure. Photopatterning of organosilane SAMs has been conducted so far using deep ultra-violet light near 200 nm or longer in wavelength based on the particular photochemistry of aromatic, mercapto and chloride organosilane SAMs [13,42,58]. In these cases, photopatterning of SAMs was based on photochemistries of particular chemical parts in the SAMs, that is, the aromatic rings, S-H and C-Cl groups. Although these approaches are successful, the photochemistries are not applicable to photopatterning of alkylsilane and, in particular, fluoroalkylsilane SAMs, in spite of the fact that these SAMs are widely used for surface modification since more hydrophobic surfaces than those with the aromatic, mercapto and chloride SAMs are prepared.

1.3 VUV surface modification of synthetic resins

1.3.1 General introduction to plastics

A word of “plastics” (known in engineering as technopolymer) is the general term for a wide range of synthetic or semisynthetic polymerization products. They are composed of organic condensation or addition polymers and may contain other substances to improve performance or reduce costs. There are many natural polymers generally considered to be

“plastics”. Plastics can be formed into objects, films, or fibers. Their name is derived from the malleability, or plasticity, of many of them. The “s” in “plastics” is there to distinguish between the polymer and the way a material deforms.

Although plastics can be classified in many ways, most commonly, they are named due to their polymer backbones, for example, polyvinyl chloride, PE, PMMA, silicones, and polyurethanes. Other classifications include thermoplastic, thermoset, elastomer, engineering plastic, addition or condensation or polyaddition (depending on polymerization process used), and glass transition temperature (T_g). Some plastics are partially crystalline and partially amorphous in molecular structure, giving them both a melting point, that is, the temperature at which the attractive intermolecular forces are overcome, and one or more glass transitions, that is, temperatures above which the extent of localized molecular flexibility is substantially increased. Typical so-called semi-crystalline plastics are PE, PP, polyvinylchloride, polyamides, polyesters and some polyurethanes. Many plastics are completely amorphous, such as polystyrene and its copolymers, PMMA, and all thermosets.

As described above, plastics are polymers: long chains of atoms bonded to one another. Common thermoplastics range from 20,000 to 500,000 in molecular weight, while thermosets are assumed to have infinite molecular weight. These chains are made up of many repeating molecular units, known as “repeat units”, derived from “monomers”; each polymer chain will have several 1000’s of repeat units. The vast majority of plastics are composed of polymers of carbon and hydrogen alone or with oxygen, nitrogen, chlorine or sulfur in the backbone. Commercial interests are paid to silicon based polymers as well. The backbone is that part of the chain on the main “path” linking a large number of repeat units together. To vary the properties of plastics, both the repeat unit with different molecular groups “hanging” or “pendant” from the backbone, (usually they are “hung” as part of the monomers before

linking monomers together to form the polymer chain). This customization by repeat unit's molecular structure has allowed plastics to become such an indispensable part of twenty first-century life by fine tuning the properties of the polymer.

1.3.2 Cyclo-olefin polymer (COP)

Recently, COPs have also received attention because of their high chemical stability and optical transparency, which make them promising materials for applications in analytical chemistry, chemical engineering, molecular biotechnology and optical industry. The market of COP is growing because of its excellent properties, primarily in optical applications. COP exhibits high optical transparency to visible light, low specific gravity, low water absorbency, good insulating property, low birefringence and high heat resistance. Furthermore, excellent precision molding is possible with COP. Details of such COPs properties are described as follows.

a) Optical properties

Light transmission in the visible light range (400 – 800 nm) is as high as that of PMMA, exhibiting 90 % or higher throughout the whole visible light range. The refractive index of COP is 1.53 and is placed midway between PMMA and PC. Its Abbe's number of 56 is greater than PC and closer to PMMA. COP exhibits the characteristics as a ring structure polymer with a relatively great Abbe's number. Considering its refractive index, it gives this material a small chromatic aberration.

b) Thermal resistance

COP with T_g of 140°C demonstrates 122°C of deflection temperature under load, which is almost the same as PC and higher than PMMA by over 20°C. Therefore, molded products

made with this material can be used across a wide temperature range.

c) Electric properties

Over a broad frequency range up to 1 GHz, it exhibits a low dielectric constant and dielectric dissipation tangent, with no fluctuation against changes in temperature and humidity. It also demonstrates an excellent insulation property.

d) Other properties

COP is a unique polymer. Its volatile chemical content, which causes molecular contamination, is extremely low as small as 1/200–1/300 of conventional polymers. Furthermore, it also exhibits a dry-down (desorption) rate as fast as that for stainless steel, and extremely low residual metal. Its only shortcoming is the possible occurrence of solvent cracks when touched by greasy hands because of residual stress. For applications requiring direct handling, the residual strain must be eliminated at the time of molding.

1.3.3 Applications of COP

a) Optical applications for lenses and prisms

COP properties of excellent transparency, high heat resistance, low water absorbency, stable and guaranteed refractive index, and low birefringence are fully utilized in the optical applications. COP has become the de-facto standard material, especially for camera lenses/prisms, lenses for a built-in camera of mobile phones, pick-up lenses of optical memory disk systems.

b) Medical and food container use

Due to excellent transparency, low impurity content, low water permeability, low water absorbency, and strength comparable to glass, COP is used for medical vials, syringes, optical lab test cells, syringes pre-filled with pharmaceutical content, and packaging. COP is especially suitable for the use in medical devices that undergo autoclave sterilization at 121°C. Recently, many problems have been identified relating to the impact on human health of substances that are suspected of disrupting endocrine action. Since COP does not contain such substances and has a low outgas property (low content of extremely volatile chemicals). Thus, the COP is now well recognized and used as a clean material for infant feeding bottles, tableware for school children.

c) Semiconductor industry

Applications in semiconductor industry take advantage of the same COP characteristics that make the product practical for medical uses, including its status as a clean material with low degassing, low metal content, and good dry-down property (a desorption rate as fast as that of metals). Therefore, COP began to appear in silicone wafer containers used in production and shipment, and in materials for clean room interiors as an important component in semiconductor manufacturing in response to the trend for increasing refinement.

d) Liquid crystal display components

Liquid crystal displays (LCDs) are replacing conventional cathode-ray tubes (CRTs) in the IT industry, with rapid growth in demand in large markets for such everyday applications as mobile phones, car navigation systems, laptop computers, monitors, and LCD TVs. These LCD devices rely on optical components such as light guide plates and diffusers that evenly disperse light, polarizing plates that control the screen, brightness-improving films that make

the screen more brilliant, and wide viewing films that broaden the viewable angle for screens. COP characteristics of transparency, low birefringence, lightweight, and capability in precision molding, are highly suitable for molded components with high precision that include light guide plates and diffusers. More components made with COP continue to be used in personal computers and LCD TVs with large-size screens. The use of COP particularly for light guide plates in mobile laptop computers is becoming the de-facto standard as well.

1.4 Aim of the study

1.4.1 Background

As mentioned in the previous sections, a number of organic materials, including alkylsilane SAMs and polymers, have been served as samples for the VUV surface processing. In the previous studies [55,59,63,64], both the reaction, i.e. (i) the direct VUV-excitation of the alkylsilane SAM and (ii) the oxidation of the SAM with the active oxygen generated by the VUV-excitation of oxygen molecules, were considered to proceed chemical reactions on the sample surface. In other words, the sample surface was directly irradiated with VUV light coming from the lamp window and, at the same time, the sample surface was exposed to active oxygen species (e.g. ozone and atomic oxygen) generated in the air layer in the vicinity of the sample surface. While these studies were performed successfully as a development of novel microfabrication technique, some questions remained on the exact roles of VUV light and active oxygen species.

Thus, we have planned a series of new experiments based on such consideration. The experimental set-up employed for the present study was quite different from the previous VUV exposure system. We placed a sample 30 mm below the lamp window. As shown

Figure 1.5 this distance was determined based on the following consideration. The optical absorption coefficient of VUV light at 172 nm was reported to be $10 - 15 \text{ cm}^{-1} \text{ atm}^{-1}$ (at a partial pressure of 0.2 atm, namely, ambient air) [65]. Thus, the transmittance of 172 nm light through an air layer of 10 mm thick is estimated to be 5 – 13%. In fact, we have measured the transmittance and confirmed that value was about 10%. Thus, the transmittance at 172 nm through an air layer of 30 mm is estimated to be less than 0.1%. At this distance, the VUV light does not reach to the sample surface, substantially. Accordingly, chemical reactions on the alkylsilane SAM surface are concluded to be only oxidation with active oxygen species generated in the space above the sample where the VUV light is completely absorbed.

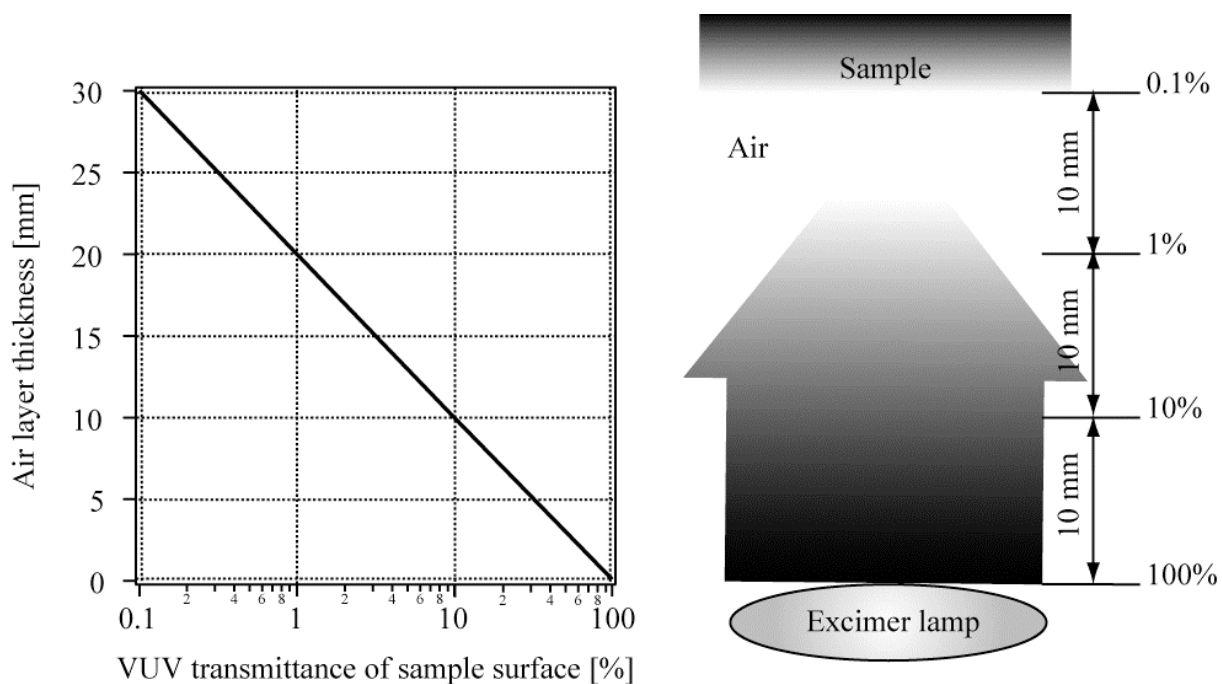


Figure 1.5. Schematic illustration for VUV transmittance of oxygen in the atmosphere.

1.4.2 Aim of this thesis

The aim of this study is to highlight the role of the VUV-generated active oxygen and to

demonstrate the surface modification of the sample with VUV-generated active oxygen. Through the VUV photo-degradation, this study have been accomplished for the fabrication of multilayer film and the development of polymer bonding technology.

1.4.3 Scope

Chapter 1 includes general information on photochemical surface modification processing, organosilane SAMs, and plastic resins. In Chapter 2, a new concept in order to stack SAM layers without using complicated procedures and/or special precursors was proposed. This method employed VUV light at 172 nm for the photochemical process to convert the monolayer surface CH₃-terminated to be a hydrophilic surface covered with a certain concentration of oxygen-containing polar functional groups. The conditions of this VUV photochemical conversion process were optimized in order to fabricate dual-layered films. In the work described in Chapter 3, alkylsilane self-assembled multilayers with more than ten layers were fabricated only by repeating the stacking of the alkylsilane layer on the modified SAM surface and the hydrophilic conversion of the stacked layer. Structures and properties of the fabricated multilayers were examined in detail using a contact angle meter, ellipsometry, X-ray photoelectron spectroscopy, fourier transform infrared spectroscopy, grazing incidence X-ray reflectivity measurement, and atomic force microscopy. Chapter 4 gives the results on the photochemical conversion of the surface of COP into a hydrophilic surface consisting of oxygen-containing polar functional groups such as C–O, C=O, and COO components by simple irradiation with a VUV light in the presence of atmospheric oxygen molecules. The VUV photochemical conversion conditions for the COP surface were studied in detail. Furthermore, capability in VUV-activation bonding of COP plates was investigated by using a hot press machine. Chapter 5 summarizes this research.

References

- [1] R. Srinivasan and V. Mayne-Banton, *Appl. Phys. Lett.*, **41**, 576 (1982).
- [2] R. Srinivasan and W. J. Leigh, *J. Am. Chem. Soc.*, **104**, 6784 (1982).
- [3] A. T. Barfknecht, J. P. Partridge, C. J. Chen, and C. -Y. Li (Eds), *Advanced Electronic Packaging Materials, Mater. Res. Symp. Soc. Proc.*, **167** (1990).
- [4] I. Higashikawa, M. Nonaka, T. Sato, M. Nakase, S. Ito, K. Horioka, and Y. Horiike, *Mater. Res. Soc. Symp. Proc.*, **101**, 3 (1990).
- [5] H. Esrom and U. Kogelschatz, *Appl. Surf. Sci.*, **54**, 440 (1992).
- [6] R. Srinivasan and B. Braren, in: *Lasers in Polymer Science and Technology: Applications III*, J. -P. Fouassier and J. F. Rabek (Eds). CRC Press, Boca Raton, Florida (1989).
- [7] B. J. Garrison and R. Srinivasan, *Appl. Phys. Lett.*, **44**, 849 (1984).
- [8] R. Srinivasan, E. Sutcliffe, and B. Braren, *Appl. Phys. Lett.*, **51**, 1285 (1987).
- [9] P. A. Robertson and W. I. Milne, *Electron. Lett.*, **22**, 603 (1986).
- [10] S. D. Baker, W. I. Milne, and P. A. Robertson, *Appl. Phys. A*, **46**, 243 (1988).
- [11] J. Marks and R. E. Robertson, *Appl. Phys. Lett.*, **52**, 810 (1988).
- [12] Z. Yu, Z. Luo, T. Y. Sheng, H. Zarnani, C. Lin, and G. J. Collins, *IEEE Trans. Plasma Sci.*, **18**, 753 (1990).
- [13] C. S. Dulcey, J. H. Georger Jr., V. Krauthamer, D. A. Stenger, T. L. Fare, and J. M. Calvert, *Science*, **252**, 551 (1991).
- [14] R. A. George, D. H. Martin, and E. G. Wilson, *J. Phys. C*, **5**, 871 (1972).
- [15] S. Onari, *J. Phys. Soc. Japan*, **26**, 500 (1969).
- [16] F. Truica-Marasescu and M. R. Wertheimer, *Macromol. Chem. Phys.*, **206**, 744 (2005).
- [17] A. C. Fozza, J. Roch, J. E. Klemberg-Sapieham, A. Kruse, A. Höllander, and M. R.

- Wertheimer, *Nucl. Instrum. Meth. Phys. Res. B*, **131**, 205 (1997).
- [18] R. P. Roland, M. Bolle, and R. W. Anderson, *Chem. Mater.*, **13**, 2493 (2001).
- [19] T. Ye, E. A. McArthur, and E. Borguet, *J. Phys. Chem. B*, **109**, 9927 (2005).
- [20] A. Ulman, *An Introduction to Ultrathin Organic Films From Langmuir-Blodgett to Self-Assembly*, Academic Press, San Diego, (1991).
- [21] D. K. Schwartz, *Surf. Sci. Rep.*, **27**, 245 (1997).
- [22] D. L. Allara and R. G. Nuzzo, *Langmuir*, **1**, 45 (1985).
- [23] R. G. Nuzzo, F. A. Fusca, and D. L. Allara, *J. Am. Chem. Soc.*, **109**, 2358 (1987).
- [24] S. C. Minne, P. Flueckiger, H. T. Soh, and C. F. Quate, *J. Vac. Sci. Technol. B*, **13**(3), 1380 (1995).
- [25] G. G. Roberts, *Adv. Phys.*, **34**, 475 (1985).
- [26] J. D. Swalen, D. L. Allara, J. D. Andrade, E. A. Chandross, S. Garoff, J. Israelachvili, T. J. McCarthy, R. Murray, R. F. Pease, J. F. Rabolt, K. J. Wynne, and H. Yu, *Langmuir*, **3**, 932 (1987).
- [27] A. Ulman, *Chem. Rev.*, **96**, 1533 (1996).
- [28] F. Schreiber, *Prog. Surf. Sci.*, **65**, 151 (2000).
- [29] S. Flink, F.C.J.M. van Veggrl, and D. N. Reinhoudt, *Adv. Mater.*, **12**, 1315 (2000).
- [30] J. C. Love, L. A. Estroff, J. K. Kriebel, R. G. Nuzzo, and G. M. Whitesides, *Chem. Rev.*, **105**, 1103 (2005).
- [31] W. C. Biegelow, D. L. Pickett, and W. A. Zisman, *J. Colloid Sci.*, **1**, 513 (1946).
- [32] L. O. Brockway and J. Karle, *J. Colloid Sci.*, **2**, 277 (1947).
- [33] E. G. Shafrin and W. A. Zisman, *J. Colloid Sci.*, **4**, 571 (1949).
- [34] E. P. Plueddemann, *Silane Coupling Agents*; 2nd Ed. Plenum Press: New York and London (1991).

- [35] E. E. Polymeropoulos and J. Sagiv, *J. Chem. Phys.*, **69**, 1836 (1978).
- [36] J. Sagiv, *J. Am. Chem. Soc.*, **102**, 92 (1980).
- [37] N. Tillman, A. Ulman, and T. L. Penner, *Langmuir*, **5**, 101 (1989).
- [38] R. Maoz and J. Sagiv, *Langmuir*, **3**, 1045 (1987).
- [39] L. Netzer and J. Sagiv, *J. Am. Chem. Soc.*, **105**, 674 (1983).
- [40] P. Connolly, J. Cooper, G. R. Moores, J. Shen, and G. Thompson, *Nanotechnology*, **2**, 160 (1991).
- [41] S. Britland, E. Perez-Arnaud, P. Clark, B. McGinn, P. Connolly, and G. Moores, *Biotechnol. Prog.*, **8**, 155 (1992).
- [42] N. Ichinose, H. Sugimura, T. Uchida, N. Shimo, and H. Masuhara, *Chem. Lett.*, 1961 (1993).
- [43] M. J. Lercel, R. C. Tiberio, P. F. Chapman, H. G. Craighead, C. W. Sheen, A. N. Parikh, and D. L. Allara, *J. Vac. Sci. Technol. B*, **11**, 2823 (1993).
- [44] P. C. Rieke, B. J. Tarasevich, L. L. Wood, M. H. Engelhard, D. R. Baer, G. E. Fryxell, C. M. John, D. A. Laken, and M. C. Jaehnig, *Langmuir*, **10**, 619 (1994).
- [45] N. Mino, S. Ozaki, K. Ogawa, and M. Hatada, *Thin Solid Films*, **243**, 374 (1994).
- [46] Y. Xia, M. Mrksich, E. Kim, and G. M. Whitesides, *J. Am. Chem. Soc.*, **117**, 9576 (1995).
- [47] A. Takahara, K. Kojima, S. -R. Ge, and T. Kajiyama, *J. Vac. Sci. Technol. A*, **14**, 1747 (1996).
- [48] H. Sugimura and N. Nakagiri, *J. Am. Chem. Soc.*, **119**, 9226 (1997).
- [49] Z. Huang, P. -C. Wang, A. G. MacDiarmid, X. Xia, and G. M. Whitesides, *Langmuir*, **13**, 6480 (1997).
- [50] R. Youkin, K. K. Berggren, K. S. Johnson, M. Prentiss, D. C. Ralph, and G. M. Whitesides, *Appl. Phys. Lett.*, **71**, 1261 (1997).

- [51] C. R. K. Marrian, F. K. Perkins, S. L. Brandow, T. S. Koloski, E. A. Dobisz, and J. M. Calvert, *Appl. Phys. Lett.*, **64**, 390 (1994).
- [52] F. K. Perkins, E. A. Dobisz, S. L. Brandow, T. S. Koloski, J. M. Calvert, K. W. Rhee, J. E. Kosakowski, and C. R. K. Marrian, *J. Vac. Sci. Technol. B*, **12**, 3725 (1994).
- [53] H. Sugimura and N. Nakagiri, *Langmuir*, **11**, 3623 (1995).
- [54] H. Sugimura, K. Okiguchi, N. Nakagiri, and M. Miyashita, *J. Vac. Sci. Technol. B.*, **14**, 4140 (1996).
- [55] H. Sugimura and N. Nakagiri, *Jpn. J. Appl. Phys.*, **36**, L968 (1997).
- [56] S. L. Brandow, J. M. Calvert, E. S. Snow, and P. M. Campbell, *J. Vac. Sci. Technol. B*, **15**, 1455 (1997).
- [57] H. Sugimura and N. Nakagiri, *Appl. Phys. A*, **66**, S427 (1998).
- [58] S. L. Brandow, M. -S. Chen, R. Aggarwal, C. S. Dulcey, J. M. Calvert, and W. J. Dressick, *Langmuir*, **15**, 5429 (1999).
- [59] H. Sugimura, K. Ushiyama, A. Hozumi, and O. Takai, *Langmuir*, **16**, 885 (2000).
- [60] B. Lee and N. A. Clark, *Langmuir*, **19**, 5495 (1998).
- [61] A. E. Moser and C. J. Eckhardt, *Thin Solid Films*, **382**, 202 (2001).
- [62] A. Kumar, H. A. Biebuyck, and G. M. Whitesides, *Langmuir*, **10**, 1498 (1994).
- [63] L. Hong, H. Sugimura, T. Furukawa, and O. Takai, *Langmuir*, **19**, 1966 (2003).
- [64] L. Hong, H. Sugimura, O. Takai, N. Nakagiri, and M. Okada, *Jpn. J. Appl. Phys.*, **42**, L394 (2003).
- [65] K. Watanabe, E. C. Y. Inn, and M. Zelikoff, *J. Chem. Phys.*, **21**, 1028 (1953)

Chapter 2

Surface chemical conversion of organosilane SAMs

2.1 Introduction

Organosilane self-assembled monolayers (SAMs) are expected to be used as high-resolution resist films because they provide a compact ultrathin layer. In addition, organosilane SAMs are of particular interest in a variety of applications, for example, corrosion protection [1], microfluidics [2,3], protein adsorption [4], chromatography [5], chemical sensors [6,7], and molecular electronics [8-11]. Organosilane films produced by self-assembly offer the great advantage of structural stabilization via multiple covalent and hydrogen bonds [12]. In contrast, self-assembled multilayers are expected to have functionalities that are not present in monolayers. For example, it is inferred that, owing to their in-plane molecular mobility, silane films might have the ability to self-heal to prevent structural defects in individual layers in a multilayer structure. These extremely robust and versatile materials are therefore remarkable candidates for the design of complex molecular architecture that might have a large impact on future nanotechnologies [12-14].

Such multilayers have been formed through a layer-by-layer self-assembly process, which can usually be carried out using one of two methods. One method is the forming of a SAM on a SAM that has active functional terminal groups [15-19]. In the other method, the top surface, *i.e.*, the terminal groups, of the first SAM, are modified before the formation of the second SAM [20-22]; here, SAMs are reformed through various types of irradiation, such as UV-light [23,24], X-ray [25,26], electron [20,27,28], and plasma irradiation [29-31]. However, the surface modification of organosilane SAMs has hardly been studied.

In our previous paper [21,22], we investigated the vacuum ultraviolet (VUV)

photodegradation of alkyl monolayers in the presence of atmospheric oxygen molecules. Here, VUV light of 172 nm in wavelength excites atmospheric oxygen molecules, resulting in the generation of ozone molecules as well as oxygen atoms in singlet and triplet states [O(1D) and O(3P), respectively], as described in the Equation 2.1 [32].



Since these active oxygen species, particularly O(1D), have strong oxidative reactivity, the surface terminating $-\text{CH}_3$ groups on the monolayer are oxidized to polar functional groups, such as $-\text{COOH}$ and $-\text{CHO}$. However, in the previous studies, the sample surface was directly irradiated with VUV light while the sample surface was exposed to active oxygen species. Therefore, in addition to the oxidation of the SAM with the active oxygen, a VUV excitation of the alkylsilane SAM might be induced. Questions have remained concerning the exact roles of VUV light and active oxygen species.

In the present study, VUV light and VUV-light-generated active oxygen species were used to chemically introduce polar functional groups on the surface of alkylsilane SAMs. For the VUV irradiation of these SAMs, we have employed a particular set up, in which VUV light did not directly irradiate the SAM surface. Consequently, only the VUV-light-generated active oxygen participated in the oxidation of the SAMs, as schematically illustrated in Figure 2.1. Furthermore, we attempted to stack another organosilane SAM on the VUV-light-treated SAMs using the silane coupling method [33-37], in which the introduced functional groups work as reaction sites.

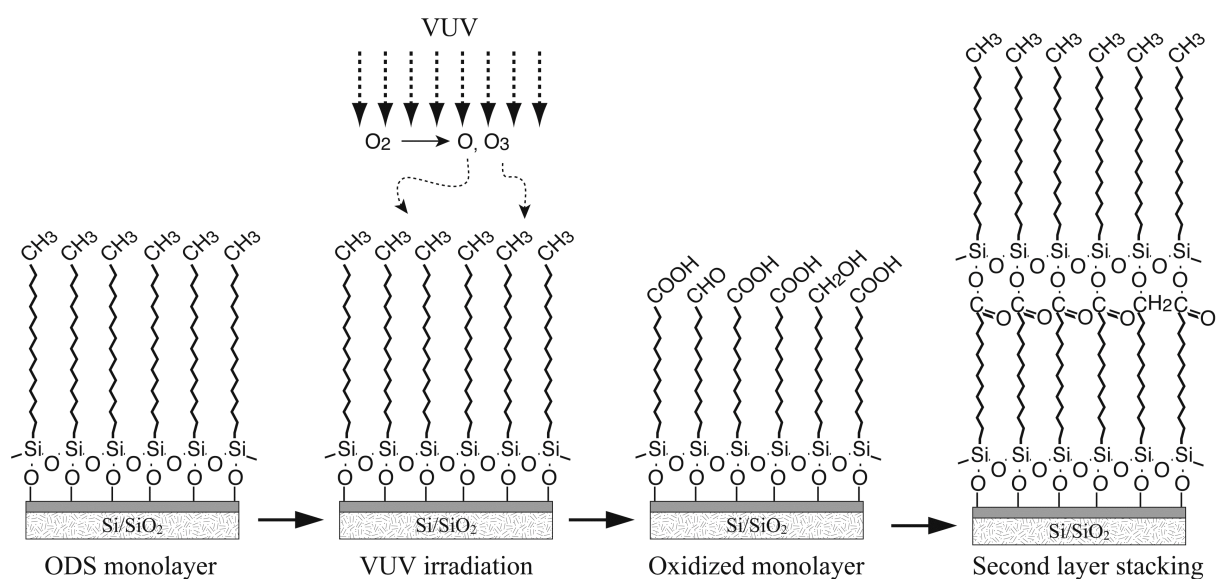


Figure 2.1. Schematic illustration of layer-by-layer chemical self-assembly of ODS/(oxidized ODS)/Si films, where oxidized ODS means ODS-SAM treated with VUV-light-generated active oxygen in order to convert terminal methyl groups to active groups such as carboxyl group.

2.2 Experimental procedure

The *n*-octadecyltrimethoxysilane self-assembled monolayers (ODS-SAMs) were prepared on silicon (Si) substrates by chemical vapor deposition [38]. Si(100) substrates (phosphorus-doped n-type wafers with a resistivity in the range of 1-10 Ω cm) covered with a native thin oxide layer (ca. 2 nm) were cleaned using a UV/ozone cleaning method [39] and hydroxylated simultaneously. Carbonaceous contamination was removed and consequently, the substrate surfaces became hydrophilic with a water contact angle of almost 0° so as to be terminated with hydroxyl (OH) groups. The cleaned and -OH terminated silicon substrates were placed together with a glass cup containing *n*-octadecyltrimethoxysilane [ODS; CH₃(CH₂)₁₇Si(OCH₃)₃, Gelest Inc.] liquid into a Teflon container with a volume of 120

cm³. The container was tightly sealed with a screw cap and heated in an oven kept at 150 °C. Under this condition, the ODS liquid in the container vaporized and reacted with the OH groups on the substrate surface. The molecules were immobilized onto the substrate surface and also connected to adjacent ODS molecules through siloxane bridges. The reaction time for SAM formation was fixed at 3 h. ODS-SAM formation was confirmed by the increase in the contact angle from 0 to 104° on average, and the thickness estimated by ellipsometry was about 1.5 nm. Detailed properties of the vapor-phase grown ODS-SAMs have already been reported [40,41].

The VUV-light-exposure apparatus for ODS-SAM-coated samples is illustrated in Figure 2.2. We used an excimer lamp as a source of VUV light at a wavelength of 172 nm (Ushio., UER20-172V; intensity at the lamp window, 10 mW cm⁻²) as a light source. In our VUV-light-exposure system, the chamber was filled with ambient air, and the distance between the lamp window and the sample surface was fixed at 30 mm. The optical absorption coefficient at 172 nm in wavelength was reported to be in the range of 10 - 15 cm⁻¹ atm⁻¹ (at a partial pressure of 0.2 atm, namely, in ambient air) [41]. The transmittance of 172 nm light through a 10 mm-thick air layer was calculated to be in the range of 5 – 13%. Its experimental value was about 10%, according to our measurement. Consequently, the transmittance at 172 nm through an air layer of 30 mm is estimated to be less than 0.1%. At a distance of 30 mm, VUV light was concluded to be absorbed almost completely by atmospheric oxygen molecules, which are converted to active oxygen species such as ozone and atomic oxygen. The light intensity at the sample surface was calculated to be less than 0.010 mW cm⁻². No substantial amount of VUV light reached the sample surface. Hence, the direct irradiation of ODS-SAMs with VUV photons can't be expected in the present system. Only the VUV-light-generated active oxygen can participate in the surface

modification of the ODS-SAMs. After VUV-light treatment, we attempted to stack another ODS-SAM using a similar silane coupling method, in which the oxidized SAM surface terminal groups acted as reaction sites.

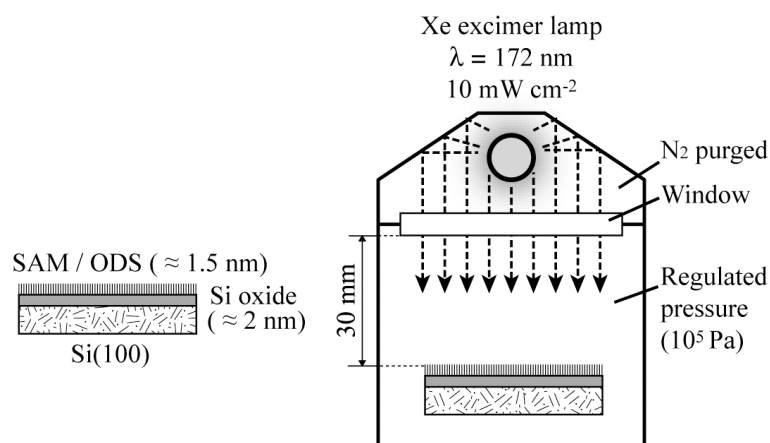


Figure 2.2. Schematic illustration of VUV-irradiation apparatus.

The samples were characterized using a contact angle meter (Kyowa Interface Science., CA-X), and by ellipsometry (Otsuka Electronics., FE-5000), X-ray photoelectron spectrometry (XPS; Kratos Analytical., ESCA-3400), and atomic force microscopy (AFM; SII Nanotechnology., SPA-300HV + SPI-3800N). The static water contact angles of the sample surfaces were measured in an atmospheric environment. SAM thickness was measured by ellipsometry. The chemical bonding states of each sample were examined by XPS using a Mg K α X-ray source of 10 mA and 10 kV. The morphology and surface roughness of the samples were measured by AFM.

2.3 Results and discussion

2.3.1 Surface chemical conversion of a alkylsilane monolayer

Figure 2.3 shows that both the water contact angles and film thicknesses of the *n*-octadecyltrimethoxysilane self-assembled monolayers (ODS-SAMs) decreased monotonically with an increase in irradiation time. The decrease in the water contact angle is due to the progressive introduction of polar functional groups onto the monolayer surface toward a VUV-irradiation time of 900 s. After 900 s, the contact angle settled at zero, indicating that the polar functional groups were also completely removed from the surface. Here, we can divide the changes in water contact angle and thickness into three regions labeled [a], [b], and [c] in Figure 2.3. In region [a], the water contact angle decreased rapidly, whereas in region [b] it maintained intermediate values at approximately 31 - 44°. In region [c], it continued to decrease, approaching 0°. Although the decreasing rate in region [c] is almost identical to that in region [b], these regions can be clearly separated from the results, as shown in Figure 2.3(b). The thickness gradually decreased in regions [a] and [b], and its decreasing rate became more rapid at the boundary of regions [b] and [c]. Finally, the water contact angle remained at approximately 0°. The concomitant change in film thickness also indicated that the ODS-SAM is gradually removed by VUV-light-generated active oxygen. As can be understood from Figure 2.1 that a monolayer of siloxane remained on the substrate even when all organic parts are degraded from the ODS-SAM. The thickness estimated by ellipsometry was 0.2 – 0.4 nm, as shown in Figure 2.3(b).

This VUV-irradiated surface chemical conversion of ODS-SAMs was studied in more detail using XPS. Figure 2.4 shows the C 1s and Si 2p XPS spectra of ODS-SAM samples prior to and after VUV irradiation for 200, 400, 900, and 1500 s. By VUV irradiation for 200, 400, 900, and 1500 s, the amount of carbon on the sample decreased, whereas the amount of silicon on the sample increased. The C 1s peak of VUV-irradiated ODS-SAMs can be deconvoluted into four components centered at 285.0, 286.1, 287.4, and 288.7 eV, as

demonstrated in Figure 2.5. The later three components correspond to C–O, C=O, and COO components, respectively, while the first component is a C–C component. Thus, it was shown that polar functional groups containing oxygen, that is, the origin of the hydrophilicity in this sample, are formed by the VUV-light treatment; therefore, XPS results as a function of VUV-irradiation time also indicate progressive functionalization, as confirmed by water contact angle measurements. Note that the intensities of the C 1s peaks for 900 and 1500 s are almost the same. This indicates that these peaks are due to contamination, that is, atmospheric impurities stuck on the sample, as is often the case with the XPS of samples transferred in ambient atmosphere. Therefore, also from the XPS spectra, we considered that the monolayer is almost decomposed at an irradiation time of 900 s, as indicated by the contact angle measurement. The spectrum of the ODS-SAM sample irradiated for 400 s, that is, region [b], showed characteristic features. A distinctive feature appeared in the range of approximately 286-289 eV in the C 1s XPS spectra, as indicated in Figure 2.4(a), which corresponded to oxidized organic components, *i.e.*, those originating from polar functional groups (OH, CHO, and COOH). From the deconvolution of this spectrum (Figure 2.5), we confirmed that the concentration of the C–C component decreased, while those of the oxidized components increased, compared with the values for unirradiated ODS-SAMs. The C 1s atomic percentage data summarized in Table 2.1 show progressive increases in the surface densities of polar functional groups (detected as C–O, C=O, and COO components) with VUV-light irradiation until 400 s; however, for longer VUV-light irradiation times, there was a decrease in their percentages. We have tried to confirm the presence of OH, CHO and COOH on the sample surfaces based on infrared (IR) spectroscopy as well. However, we could obtain no IR spectra with a sufficient signal-to-noise ratio both in attenuated total reflection and reflection absorption spectroscopy methods, because of the background noise

due to water vapor and the low IR reflectivity of Si substrates. As a consequence, we can consider that the monolayer after a VUV-light treatment of 400 s maintains the largest number of polar functional groups on the surface.

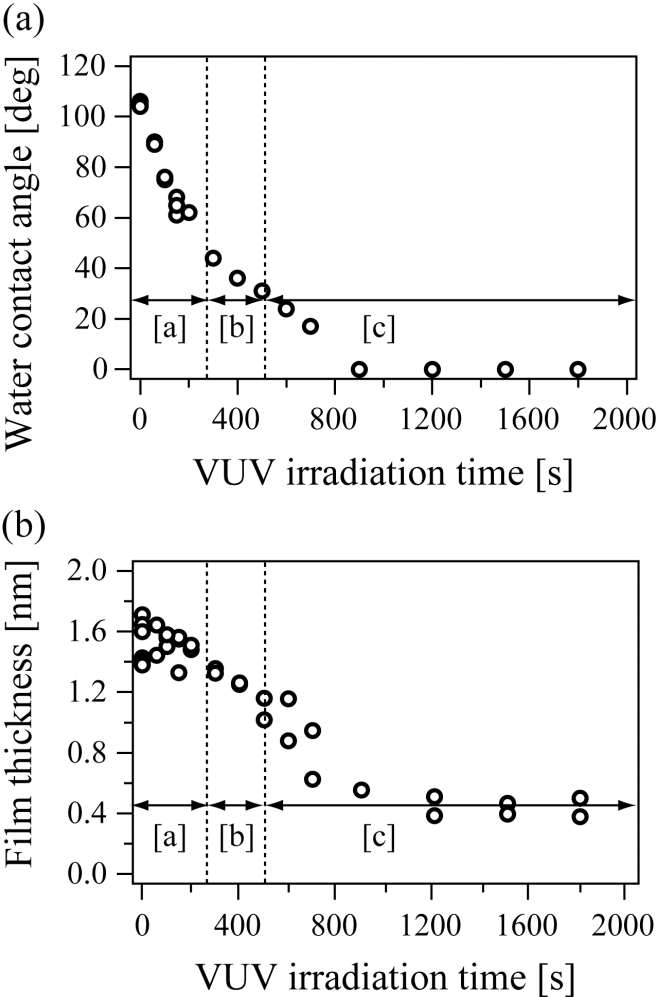


Figure 2.3. Changes in (a) water contact angles and (b) thickness of ODS-SAM with irradiation time of VUV light.

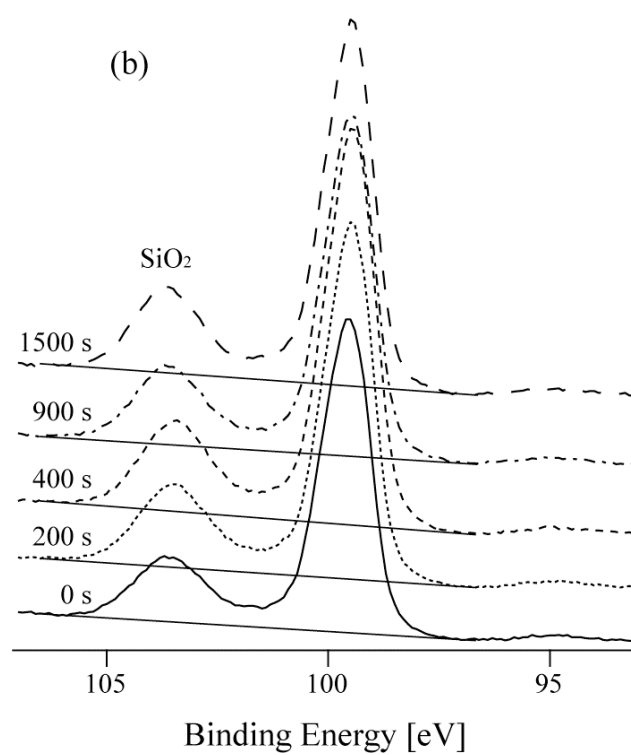
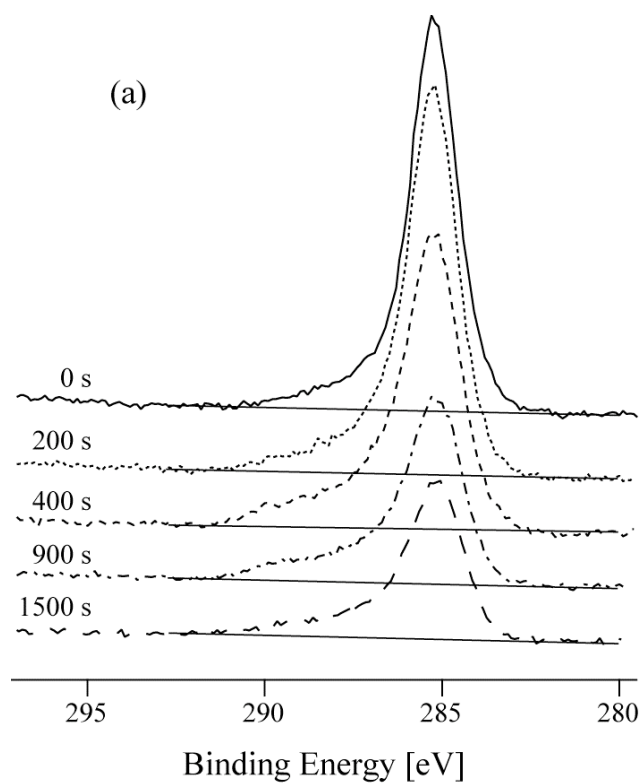


Figure 2.4. (a) C 1s and (b) Si 2p XPS spectra of ODS-SAM surfaces before and after irradiation with VUV light for 200 – 1500 s.

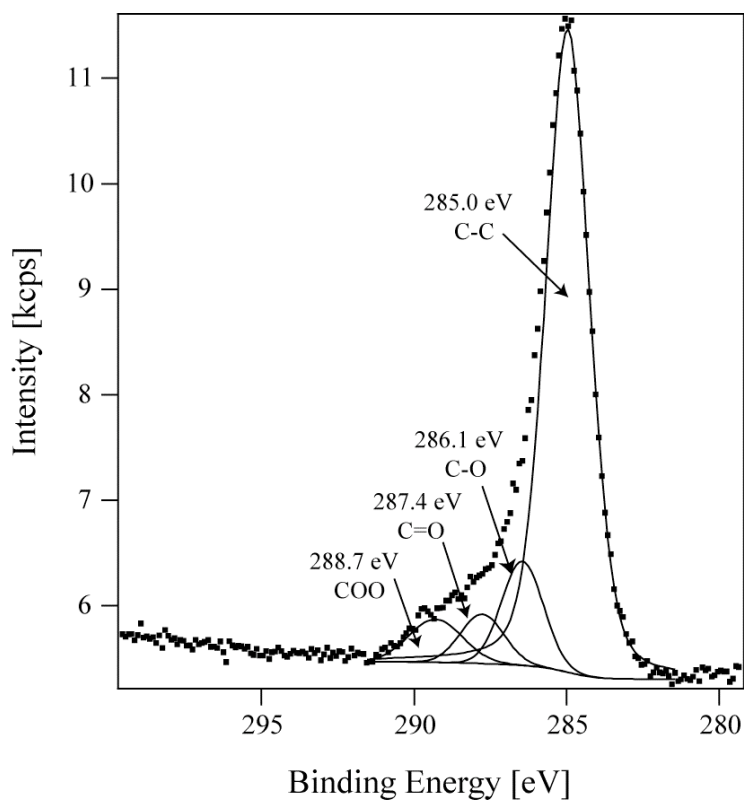


Figure 2.5. Deconvoluted C 1s XPS spectrum of ODS-SAM surface that underwent VUV irradiation for 400 s.

Table 2.1. Atomic percentages of four elements including C 1s of different carbon moieties determined by XPS versus VUV-light treatment time.

VUV-light treatment time [s]	Si [%]	C [%]				O [%]	C/O
		C-C [%]	C-O [%]	C=O [%]	COO [%]		
0	40	25	5	2	1	27	1.2
200	40	20	5	2	2	31	0.9
400	40	15	6	1	3	35	0.7
900	43	14	3	1	2	37	0.6

The surface structure of the VUV-light-treated monolayer was monitored using AFM. Topography images (Figure 2.6) indicate that VUV-light treatments of 200, 400, and 900 s do not significantly alter the initial surface structure of the monolayer. RMS roughnesses were all approximately 0.1 nm. The oxidation and etching of the ODS-SAMs using VUV-light-generated active oxygen was found to proceed uniformly.

The chemical changes induced on the ODS-SAMs by the VUV-light irradiation under the experimental conditions in this paper are considered to be primarily due to the VUV-light-generated active oxygen, since there was no substantial VUV light intensity reaching the sample surface, as explained in the experimental section. The VUV light intensity at the sample surfaces was less than 0.010 mW cm^{-2} . This very low intensity VUV light might cause a small number of chemical changes in the ODS-SAMs if the irradiation is prolonged for 200 – 500 s. We have estimated the packing density of our vapor-phase-grown ODS-SAM to be in the range of $7 \times 10^{13} - 8 \times 10^{13}$ ODS molecules cm^{-2} from the occupied area of one ODS molecule, which we reported to be 1.2 – 1.5 $\text{nm}^2/\text{molecule}$ [39]. When irradiated for 100 s at an intensity of 0.010 mW cm^{-2} with photons of 7.2 eV, *i.e.*, the photon energy of 172 nm light, the total photon flux becomes $9 \times 10^{14} \text{ cm}^{-2}$, corresponding to approximately 10 photons per ODS molecule. This number might not be negligible. On the other hand, the VUV absorption edge of polyethylene (PE), that is, a saturated hydrocarbon similar to ODS, is known to be about 160 nm [42]. In order to dissociate C-C and C-H bonds in PE, VUV light with a wavelength shorter than this absorption edge wavelength is required [43]. Indeed, it has been reported that under a high vacuum condition on the order of 10^{-4} Pa no chemical change was induced on a PE substrate by VUV irradiation at 172 nm, while the substrate was etched with irradiation at 124 or 146 nm [44]. Thus, VUV light at 172 nm is

expected to hardly be absorbed by ODS-SAMs, that consist of saturated hydrocarbon molecules [45]. We have also confirmed that no apparent change was recognized in the ODS-SAMs by VUV irradiation at 172 nm in vacuum. Therefore, we conclude that such a small number of photons, that is, tens of photons per molecule, had almost no effect on the chemical changes of the ODS-SAMs.

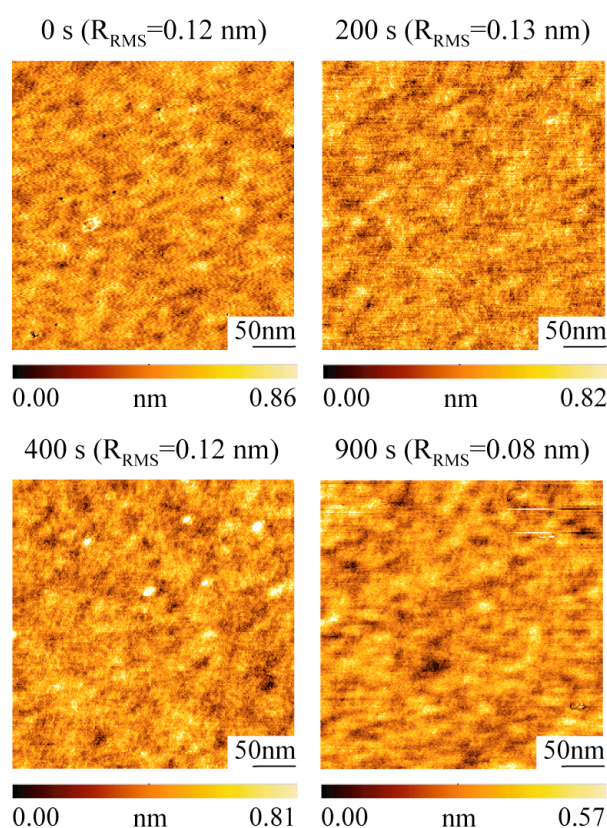


Figure 2.6. AFM topography images and RMS roughnesses of ODS-SAM surfaces prepared using four different VUV-light treatment times (tapping mode; image size, $500 \times 500 \text{ nm}^2$).

2.3.2 Stacking of a second alkylsilane SAM

In order to prove the ability to graft another set of organic compounds onto the VUV-light-functionalized SAM, a second layer of ODS molecules was grafted. The evolution

of the surface conversion was studied by measuring the water contact angle and film thickness (Figure 2.7). The presence of polar functional groups on the modified surface should allow the grafting of alkylsilane molecules. Indeed, as shown in Figure 2.7(a), the deposition of the second ODS-SAM onto the ODS-SAM/Si substrate modified with the VUV-generated active oxygen was possible for all the VUV treatment times, and the water contact angles of the second layer of the ODS-SAM substrates reached 100° on average. The primary chemistry behind this second layer deposition is most likely hydrogen bonding between hydrolyzed ODS molecules consisting of the second layer and the polar functional groups on the first modified layer surface. It is plausible that silane coupling reactions proceed further and that some of the hydrogen bonds are converted to Si-O-C bonds. As clearly demonstrated in Figure 2.7(b), however, the thickness of the films grown on VUV-light-treated ODS-SAM substrates increased until 400 s and decreased after 400 s until a treatment time of 1200 s, and then a plateau was observed at an average of 1.5 nm. A film of 2.8 nm thickness on average was grown with a VUV-light-treatment time of 400 s; therefore, we considered that 400 s was the most suitable VUV-light-treatment time as an optimum condition. Under this condition, we can attain a maximum density for the polar functional groups, which serve as sites for second monolayer growth, and minimize the loss of the thickness of the first monolayer due to etching.

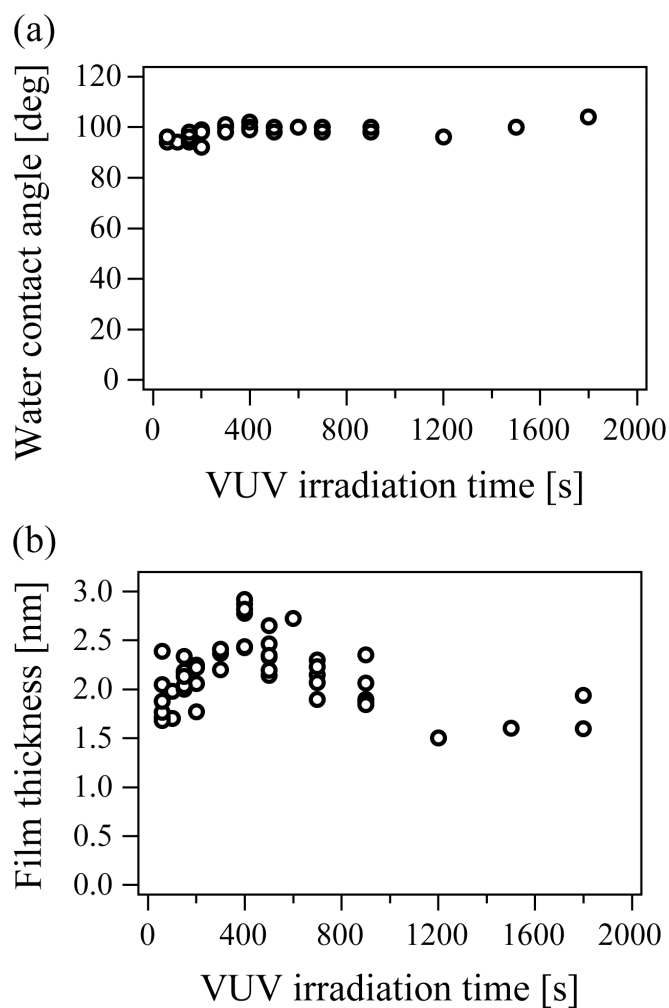


Figure 2.7. Changes in (a) water contact angles and (b) thicknesses of ODS bilayer with irradiation time of VUV light.

2.4 Summary

The surface chemical conversion of *n*-octadecyltrimethoxysilane self-assembled monolayers (ODS-SAMs) with active oxygen species generated by the VUV-light excitation of atmospheric oxygen molecules has been investigated by water contact angle analysis, film thickness analysis, XPS, and AFM. In the VUV-light treatment experiments, an ODS-SAM sample placed in air was irradiated with a Xe excimer lamp located 30 mm above the sample

surface. At this distance, the VUV light emitted from the lamp was almost completely absorbed by atmospheric oxygen molecules, which were converted to active oxygen species such as ozone and atomic oxygen. Finally, the VUV light intensity at the sample surface was attenuated to less than 0.1% of the initial intensity at the lamp window. Hence, the ODS-SAM surface was not substantially irradiated with VUV light in our experimental set up. Since all the VUV light was adsorbed by oxygen molecules in the space above the sample and was consumed to generate active oxygen, the primary photochemical reaction proceeding on the ODS-SAM was its oxidation with the VUV-light-generated active oxygen. Polar functional groups such as $-\text{COOH}$, $-\text{CHO}$, and $-\text{OH}$ were consequently formed on the sample surface. When the VUV-light treatment was further prolonged, the ODS-SAM was gradually etched and all of its alkyl region was removed completely in the end. We have also demonstrated that the oxidized groups served as reaction sites for immobilizing additional organosilane molecules. For bilayer fabrication, we have optimized conditions of the VUV-light treatment by which maximum polar functional group density the minimum etching depth were attainable. This method will be applicable to the fabrication of multilayers consisting of a variety of organosilane molecules. In addition, our investigation helps to clarify the role of active oxygen in the photoreactivity of SAMs.

References

- [1] P. E. Laibinis and G. M. Whitesides, *J. Am. Chem. Soc.*, **114**, 9022 (1992).
- [2] B. Zhao, J. S. Moore, and D. J. Beebe, *Science*, **291**, 1023 (2001).
- [3] Y. Feng, Z. Zhou, X. Ye, and J. Xiong, *Sens. Actuators A Phys.*, **108**, 138 (2003).
- [4] P. Ying, G. Jin, and Z. Tao, *Colloids Surf. B*, **33**, 259 (2004).
- [5] M. J. Wirth, R. W. P. Fairbank, and H. O. Fatunmbi, *Science*, **275**, 44 (1997).

- [6] Y. Cui, Q. Wei, H. Park, and C. M. Lieber, *Science*, **293**, 1289 (2001).
- [7] D. Niwa, T. Homma, and T. Osaka, *Jpn. J. Appl. Phys.*, **43**, L105 (2004).
- [8] J. Collet, M. Bonnier, O. Bouloussa, F. Rondelez, and D. Vuillaume, *Microelectron. Eng.*, **36**, 119 (1997).
- [9] S. Lenfant, C. Krzeminski, C. Delerue, G. Allan, and D. Vuillaume, *Nano Lett.*, **3**, 741 (2003).
- [10] S. Kobayashi, T. Nishikawa, T. Takenobu, S. Mori, T. Shimoda, T. Mitani, H. Shimotani, N. Yoshimoto, S. Ogawa, and Y. Iwasa, *Nat. Mater.*, **3**, 317 (2004).
- [11] M. Halik, H. Klauk, U. Zschieschang, G. Schmid, C. Dehm, M. Schütz, S. Maisch, F. Effenberger, M. Brunnbauer, and F. Stellacci, *Nature*, **431**, 963 (2004).
- [12] A. Baptiste, A. Gibaud, J. F. Bardeau, K. Wen, R. Maoz, J. Sagiv, and B. M. Ocko, *Langmuir*, **18**, 3916 (2002).
- [13] R. Maoz, E. Frydman, S. R. Cohen, and J. Sagiv, *Adv. Mater.*, **12**, 725 (2000).
- [14] R. Maoz, S. R. Cohen, and J. Sagiv, *Adv. Mater.*, **11**, 55 (1999).
- [15] R. Buller, H. Cohen, T. R. Jensen, K. Kjaer, M. Lahav, and L. Leiserowitz, *J. Phys. Chem. B*, **105**, 11447 (2001).
- [16] I. Weissbuch, S. Guo, R. Edgar, S. Cohen, P. Howes, K. Kjaer, J. Als-Nielsen, M. Lahav, and L. Leiserowitz, *Adv. Mater.*, **10**, 117 (1998).
- [17] H. Yonezawa, K. H. Lee, K. Murase, and H. Sugimura, *Chem. Lett.*, **35**, 12 (2006).
- [18] A. Hatzor, T. van der Boom-Moav, S. Yoshelis, A. Vaskevich, A. Shanzer, and I. Rubinstein, *Langmuir*, **16**, 4420 (2000).
- [19] J. A. Libera, R. W. Gurney, S. T. Nguyen, J. T. Hupp, C. Liu, R. Conley, and M. J. Bedzyk, *Langmuir*, **20**, 8022 (2004).
- [20] K. Ogawa, N. Mino, H. Tamura, and M. Hatada, *Langmuir*, **6**, 851 (1990).

- [21] L. Hong, H. Sugimura, T. Furukawa, and O. Takai, *Langmuir*, **19**, 1966 (2003).
- [22] H. Sugimura, L. Hong, and K. H. Lee, *Jpn. J. Appl. Phys.*, **44**, 5185 (2005).
- [23] S. V. Roberson, A. J. Fahey, A. Sehgal, and A. Karim, *Appl. Surf. Sci.*, **200**, 150 (2002).
- [24] T. Ye, D. Wynn, R. Dudek, and E. Borguet, *Langmuir*, **17**, 4497 (2001).
- [25] S. R. Wasserman, G. M. Whitesides, I. M. Tidswell, B. M. Ocko, P. S. Pershan, and J. D. Axe, *J. Am. Chem. Soc.*, **111**, 5852 (1989).
- [26] T. K. Kim, X. M. Yang, R. D. Peters, B. H. Sohn, and P. F. Nealey, *J. Phys. Chem. B*, **104**, 7403 (2000).
- [27] S. Hou, Z. Li, Q. Li, and Z. F. Liu, *Appl. Surf. Sci.*, **222**, 338 (2004).
- [28] J. Park and H. Lee, *Mater. Sci. Eng. C*, **24**, 311 (2004).
- [29] J. -D. Liao, M. -C. Wang, C. -C. Weng, R. Klauser, S. Frey, M. Zharnikov, and M. Grunze, *J. Phys. Chem. B*, **106**, 77 (2002).
- [30] M. Tatoulian, O. Bouloussa, F. Moriere, F. Arefi-Konsari, J. Amouroux, and F. Rondelez, *Langmuir*, **20**, 10481 (2004).
- [31] C. -C. Weng, J. -D. Liao, Y. -T. Wu, M. -C. Wang, R. Klauser, M. Grunze, and M. Zharnikov, *Langmuir*, **20**, 10093 (2004).
- [32] R. P. Roland, M. Bolle, and R. W. Anderson, *Chem. Mater.*, **13**, 2493 (2001).
- [33] S. L. Brandow, M. -S. Chen, R. Aggarwal, C. S. Dulcey, J. M. Calvert, and W. J. Dressick, *Langmuir*, **15**, 5429 (1999).
- [34] N. Ichinose, H. Sugimura, T. Uchida, N. Shimo, and H. Masuhara, *Chem. Lett.*, 1961 (1993).
- [35] B. Lee and N. A. Clark, *Langmuir*, **14**, 5495 (1998).
- [36] H. Sugimura and N. Nakagiri, *Appl. Phys. A*, **66**, S427 (1998).
- [37] H. Sugimura, K. Ushiyama, A. Hozumi, and O. Takai, *Langmuir*, **16**, 885 (2000).

- [38] H. Sugimura, A. Hozumi, T. Kameyama, and O. Takai, *Surf. Interface Anal.*, **34**, 550 (2002).
- [39] K. Hayashi, N. Saito, H. Sugimura, O. Takai, and N. Nakagiri, *Langmuir*, **18**, 7469 (2002).
- [40] H. Sugimura and N. Nakagiri, *J. Photopolym. Sci. Technol.*, **10**, 661 (1997).
- [41] K. Watanabe, E. C. Y. Inn, and M. Zelikoff, *J. Chem. Phys.*, **21**, 1026 (1953).
- [42] S. Onari, *J. Phys. Soc. Jpn.*, **26**, 500 (1969).
- [43] R. A. George, D. H. Martin, and E. G. Wilson, *J. Phys. C*, **5**, 871 (1972).
- [44] F. Truica-Marasescu and M. R. Wertheimer, *Macromol. Chem. Phys.*, **206**, 744 (2005).
- [45] At 172 nm, the optical transparency of a PE film with a thickness in the range of 1 - 2 nm is greater than 99.99%, similarly to ODS-SAM, as estimated from the optical densities of PE reported in R. H. Partridge, *J. Chem. Phys.*, **45**, 1685 (1966).

Chapter 3

Organosilane self-assembled multilayer formation

3.1 Introduction

Organized molecular films have attracted growing attention owing to their functionalities in a wide variety of science and engineering fields [1-3]. Such films provide the opportunity for developing new material surface functions leading to improved performance or crucial functions. As a technique for the fabrication of organized molecular films, self-assembly, that is, the spontaneous organization of organic molecules at a solid substrate surface, has been indispensable, as has the Langmuir-Blodgett (LB) method. The self-assembling process is a powerful means for the fabrication on films of a monomolecular thickness, that is, self-assembled monolayer (SAM). However, the process has difficulties in fabricating multilayers compared with the LB method by which multilayers are readily fabricated. Multilayers are expected to yield fruitful functions which cannot be obtained by the monolayers alone. One promising approach to fabricate self-assembled multilayers is the use of coordination chemistry [4]. For example, several types of multilayers have been fabricated through coordination bonds between metal ions with isocyanide or amino groups [5-8]. Mallouk and coworkers developed a promising method in which monolayers of alkyl-bisphosphonic acid and zirconium (Zr) ions were alternately stacked [9]. Besides phosphonic acid, carboxylic acid has been employed in order to fabricate multilayers with Cu(II) or Zr(IV), Ti(IV) ions [10-12]. Although this coordination multilayer chemistry is successful, it lacks versatility to some extent since the method needs a bisphosphoric or biscalboxylic molecule as a component of multilayers.

Organosilane SAMs formed on oxide surfaces through the silane coupling chemistry

have become a major category of SAM [13-16], and a variety of organosilane precursors are commercially available at present. Thus, multilayer stacking of organosilane SAMs is of special interest. There have been several reports on the fabrication of self-assembled multilayers by the use of an organosilane SAM as the bottom layer of the multilayers [17-26]. In these reported methods, an activation process-step of the bottom SAM surface via chemical or photochemical treatments is frequently applied before stacking an upper layer on it. Thus, there are some requirements for the surface functional groups terminating the bottom SAM. The surface groups must be chemically reactive, or convertible, through some chemical treatment processes. If a more general way independent of specific functional groups on a SAM for its activation is available, we can fabricate multilayers more freely. We have reported previously a photochemical surface modification method which could activate even methyl groups on an alkylsilane SAM surface. Organosilane self-assembled bilayers have been fabricated by this method [27-29]. Our photochemical process employs a vacuum ultra-violet (VUV) light at 172 nm in wavelength as a light source. When an organosilane SAM surface is irradiated with VUV light in the presence of atmospheric oxygen molecules, the VUV light excites oxygen molecules, resulting in the generation of ozone molecules as well as oxygen atoms in singlet and triplet states [30]. Since these active oxygen species, particularly singlet oxygen atoms, have strong oxidative reactivity, the species oxidize and etch the monolayer [31]. At the initial stage of this VUV-induced photochemical degradation amplified with atmospheric oxygen, surface terminating functional groups of a SAM, e.g., $-\text{CH}_3$ or $-\text{CH}_2\text{Cl}$ groups, are converted to polar functional groups such as $-\text{COOH}$ and $-\text{CHO}$. Consequently, the SAM surface becomes hydrophilic to some extent. This hydrophilically modified SAM surface provides silane coupling sites for stacking a second organosilane monolayer in order to fabricate a bilayer.

In this paper, we report on a further extension of the VUV-photochemical method to the fabrication of multilayers with more than ten layers. Alkylsilane self-assembled multilayers were successfully fabricated by repeated stacking of alkylsilane layers on the modified SAM surface with hydrophilic conversion of the stacked layer. The structures and properties of the fabricated multilayers are investigated in detail.

3.2 Experimental procedure

We employed an organosilane self-assembled monolayer (SAM) prepared on a silicon (Si) substrate from ODS (*n*-octadecyltrimethoxysilane, $\text{CH}_3(\text{CH}_2)_{17}\text{Si}(\text{OCH}_3)_3$, Gelest Inc.) as the first layer for multilayer formation. By using a chemical vapor deposition (CVD) method [32], an ODS-SAM was prepared on Si(100) substrates (phosphorus-doped n-type wafers with a resistivity of 1-11 Ω cm) and Si(111) substrates (phosphorus-doped n-type wafers with a resistivity of 1-10 Ω cm) covered with a 2.3-nm-thick native oxide layer. The Si(111) substrates were used for fourier transform infrared spectroscopy (FTIR) and grazing incidence X-ray reflectivity (GIXR) measurements as described later. All the substrates cut from the wafer were cleaned ultrasonically with ethanol and ultrapure water for 20 min in this order and then photochemically cleaned by exposing in air to vacuum ultraviolet (VUV) generated from an excimer lamp (Ushio. Inc., UER20-172V; intensity at lamp window 10 mW cm^{-2}) for 20 min at a lamp-sample distance of 5 mm. This photochemical cleaning method is described in detail elsewhere [32]. In a nitrogen-filled glove with a regulated humidity of around 17%, the sample and 60 μL of ODS liquid in a glass cup with a volume of 3 cm^3 were placed in a Teflon container with a capacity of 120 cm^3 . The container was then sealed with a screw cap and placed in an electric oven maintained at 150 $^\circ\text{C}$ for 3 h. The ODS liquid in the vessel vaporized and reacted with the OH groups on the silicon sample surfaces. The molecules

were fixed onto the sample surfaces and connected to adjacent ODS molecules through siloxane bonds. ODS-SAM formation was confirmed by the increase in the contact angle from 0 to 104° on average, and the thickness estimated by ellipsometry was about 1.4 – 1.5 nm using a model of Air/SiO₂/Si. Detailed properties of the vapor-phase grown ODS-SAMs have already been reported [33,34].

The resulting ODS-SAM on the Si substrate was then treated with another VUV-light process as described later. After the VUV-light treatment, we attempted to stack another ODS-SAM using a silane coupling method, in which the terminal groups of the oxidized ODS-SAM surface, –COOH, –CHO, and/or –CH₂OH groups, acted as new reaction sites. To build a multilayer, the procedure of oxidizing and deposition described above was sequentially repeated. In the final step, the film was capped with an ODS monolayer, creating a chemically inert and nonwetable outer film surface.

The static water contact angles of the sample surfaces were measured with a contact angle meter (Kyowa Interface Science, CA-X) in an atmospheric environment; here, we fixed the size of water droplets at about 1.5 mm in diameter. SAM thickness was measured by ellipsometry (Otsuka Electronics, FE-5000). The measured region was 400 – 800 nm in wavelength. The incident angle was set to be 70°. The model of Air/SiO₂/Si was used for the analysis of raw data. Since the resulting value was the sum of the thickness of the monolayer and the native oxide, the actual monolayer thickness was determined by subtracting the oxide thickness from the total value. Before monolayer coating, the thickness of the native oxide layer of each sample was measured. The chemical bonding states of each sample were examined by X-ray photoelectron spectroscopy (XPS; Kratos Analytical, ESCA-3400) using a Mg K α X-ray source with 10 mA in emission current and 10 kV in accelerating voltage. The binding energy scales were referenced to 285.0 eV as determined by the locations of the

maximum peaks on the C 1s spectra of hydrocarbon (CH_x), associated with adventitious contamination. The LbL self-assembly process was also monitored by quantitative fourier transform infrared spectroscopy (FTIR; Digilab Japan Co., Ltd, Excalibur FTS-3000). We used transmittance mode and a single reflection ATR (attenuated total reflection) mode for measurement of the samples. The ATR IR spectra were obtained with 65° of incident angle, and hemispherical Ge ATR crystal with diameter of 2.5 cm (internal reflection element, from Harrick Scientific). The transmittance IR spectra were obtained on 0° incidence. IR Spectra were measured in a dry atmosphere of a sample compartment purged with nitrogen and were referenced to background spectra determined under the same conditions. All spectra were measured at a resolution of 4 cm^{-1} and with 1024 scan cycles. The density, thickness, and roughness of the films including oxide-layer on the samples were examined by grazing incidence X-ray reflectivity measurement (GIXR; Rigaku, ATX-G) performed using a high-resolution 18 kW rotating anode X-ray diffractometer. The Cu $\text{K}\alpha$ beam from the rotating anode was monochromatized with flat Ge(220) double crystals. The specular reflectivity curves were recorded with a $\theta/2\theta$ scan mode. To determine thickness and roughness with high accuracy, it is essential to precisely align the sample position with the X-ray beam direction. The sample was mounted on a vertical sample stage, which was installed on a high-resolution goniometer. The 2θ angular resolution of the instrument was 0.0001° . The alignment process was controlled by an attached computer and carried out automatically. By repeatedly adjusting z and ω (or θ) axes, the optimum sample position is located (at the center of the X-ray beam) and only half of the X-ray beam is detected by the detector. Then by setting the detector (2θ) at an appropriate position, the total external reflection adjustment starts. By further optimizing the z , ω and χ positions, maximum reflection intensity which equals the intensity of the incident beam is achieved. The

morphology and surface roughness of the samples were measured by atomic force microscopy (AFM; SII Nanotechnology, SPA-300HV + SPI-3800N) in tapping mode with a Si probe (Seiko Instruments Inc., SI-DF20, force constant of 15 N m^{-1}).

3.3 Results and discussion

3.3.1 Growth mechanism of a solid-immobilized multilayer

Figure 3.1 illustrates the growth mechanism of a solid-immobilized multilayer of oriented long-chain silane molecules, i.e. ODS. Here, “oxidized ODS” means ODS layer treated with VUV-generated active oxygen, and ODS(oxidized ODS)_{*n*} denotes the resulting multilayer consisting of *n*+1 monolayers in total. While the initial cleaning of the Si substrate was done by VUV-irradiation at a lamp-sample distance of 5 mm as described above, VUV-light treatment for the chemical conversion of ODS-SAMs was always carried out under the larger distance of 30 mm. We employed an excimer lamp as the source of VUV light with wavelength 172 nm, and the chamber was filled with ambient air. The optical absorption coefficient of the VUV light at wavelength 172 nm in ambient air with an oxygen partial pressure of 0.2 atm was reported to be in the range of $10\text{-}15 \text{ cm}^{-1} \text{ atm}^{-1}$ [34], indicating that the transmittance of light through a 10 mm-thick air layer would be in the range of 5 - 13%, and we observed a value of about 10%. Therefore, the transmittance for 30 mm was estimated to be less than 0.1%, which means that the light intensity at the ODS-SAM surface is less than 0.010 mW cm^{-2} . In other words, at the distance of 30 mm, VUV light was absorbed almost completely by atmospheric oxygen molecules, yielding active oxygen species such as ozone and atomic oxygen, hence no substantial amount of VUV-light reached the sample surface. The direct irradiation of ODS-SAMs with VUV photons is not expected in the present system, and only the VUV-light-generated active oxygen can participate in the

surface modification of the ODS-SAMs.

Using this VUV-light system, we have optimized the irradiation time for the chemical conversion [29]. In our previous tentative study [29], it was found that, under the VUV-light treatment, both the water contact angle and the film thickness of the ODS-SAM decreased monotonically with increasing irradiation time. This demonstrated that polar functional groups are evidently and progressively introduced through the treatment with the concomitant etching of the SAM. The introduction of the polar functional groups was also confirmed by XPS measurement [29]. As a result, it was thought that the surface density of polar functional groups, which serve as silane coupling sites for stacking a second monolayer, is insufficient if the irradiation time is too short. In contrast, if the irradiation time is too long, the second monolayer would be successfully prepared, but the total thickness of the resulting bilayer film will be small. In consequence, the total thickness of the bilayer films grown on VUV-light-treated ODS-SAM substrates was found to increase toward the irradiation time of 400 s and decrease after 400 s until a treatment time of 1200 s. We thus concluded that 400 s is the optimum VUV-light-treatment time. Under this condition, we can introduce maximum polar functional groups on the surface of the first monolayer and, at the same time, minimize the loss of the thickness of the monolayer due to etching.

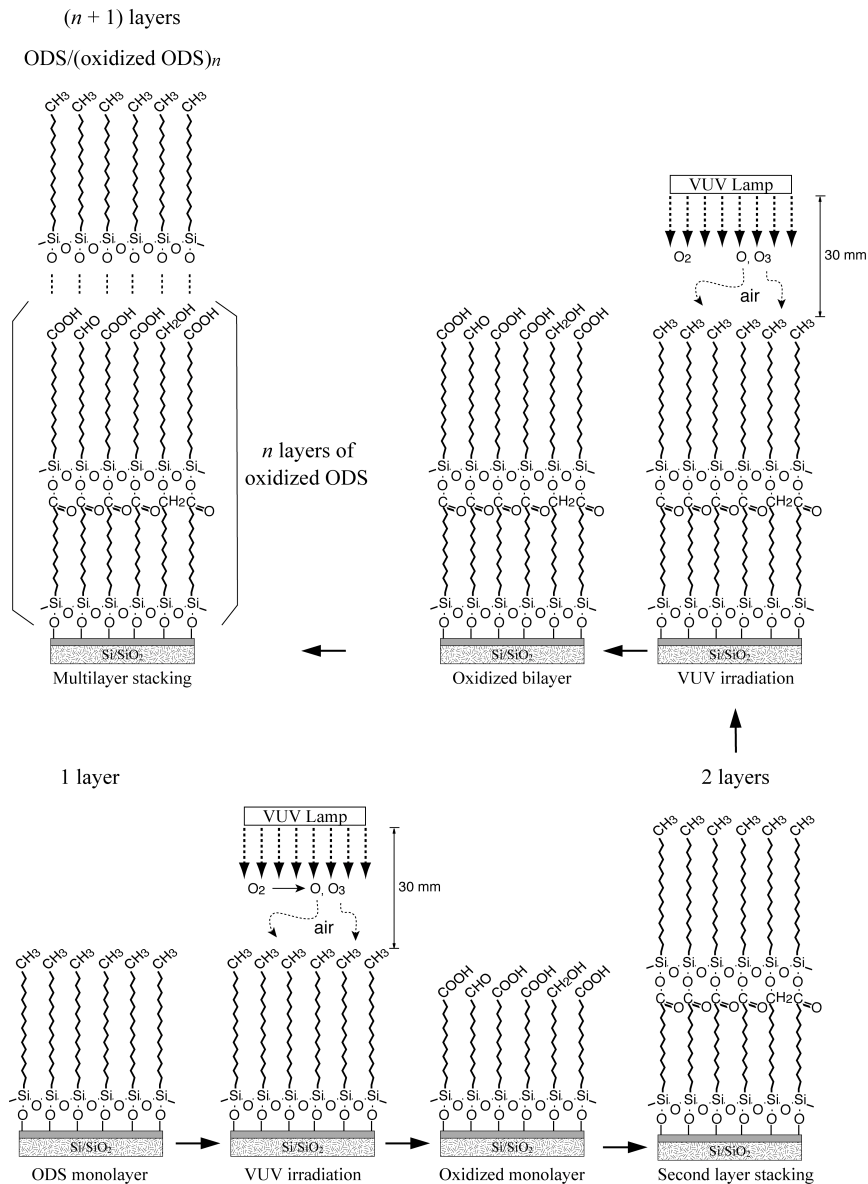


Figure 3.1. Conception illustration of the layer-by-layer chemical self-assembly of ODS/(oxidized ODS)_n/Si films, where oxidized ODS means ODS-SAM treated with VUV-generated active oxygen in order to convert terminal methyl groups into active groups such as a carboxyl group. Built-up multilayer structures of this kind are composed mainly of oxidized ODS, rather than ODS. Deposition of a final layer of saturated ODS, instead of oxidized ODS, will stabilize the final multilayer structure ((n+1) layers, with a top ODS monolayer, shown on the upper left of figure.).

3.3.2 Surface analysis of monolayer/multilayers

We prepared eleven different monolayer/multilayers, i.e. ODS(oxidized ODS)_{*n*}, *n* = 0-10, through the LbL growth process. Figure 3.2 shows the change in water contact angle and thickness of the ODS/(oxidized ODS)_{*n*}/Si (with *n* = 0, 3, 6, 10) films. The film thickness increased throughout the LbL growth process, and an almost proportional relationship was found between the film thickness and the layer number, indicating that a series of multilayers were successfully fabricated on the silicon wafer through the LbL approach. The water contact angle is an indicator of surface wettability, which reflects the surface functional group(s). It is known that the water contact angle for a hydrophobic methyl-terminated surface, e.g. ODS-SAM, is about 105° or more, while that for a surface terminated with a polar functional group is much smaller; for example, oxidized ODS monolayer obtained by the VUV-light-treatment for 400 s was 36° [29]. In the *n* range of 0 to 10, that is 1 to 11 layers, the water contact angles were around 100°, suggesting that the layers were thoroughly terminated with -CH₃ groups. However, the value followed a slightly decreasing trend from 104° to 98°, which means that the packing density of terminating -CH₃ groups gradually decreases with *n*. This is attributed to a gradual accumulation of disorder in the monolayer structure as was also indicated by GIXR analysis and AFM observation described later.

Figure 3.3 shows XPS C 1s and Si 2p spectra of initial monolayer (*n* = 0; 1 layer) and multilayer samples of 4 (*n* = 3), 7 (*n* = 6), and 11 layers (*n* = 10). With increasing layer number, the analyzed amount of carbon at the sample surface increased whereas that of silicon at 99.6 eV, which is mainly due to the Si substrate underneath, decreased, indicating that layers are successfully deposited throughout the LbL self-assembly process, as shown by the water contact angle measurement and the ellipsometric measurement. Here, the difference

in C 1s peak intensity between 7 and 11 layers is very small. XPS is a surface sensitive analysis and our system has a detection depth of about 5 nm for organic compounds. As shown in Figure 3.2b, the thickness for 11 layers far exceeds 10 nm, resulting in little difference in C 1s intensity between the two samples. For the same reason, the bulk Si peak at 99.6 eV almost disappeared in the case of 11 layers.

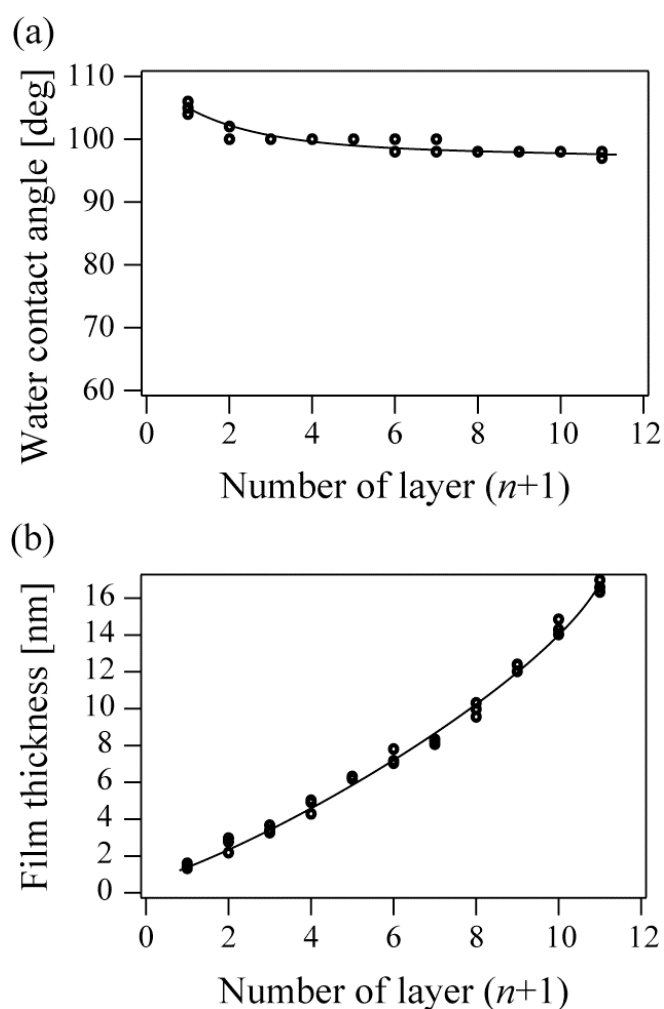


Figure 3.2. Change in (a) water contact angle and (b) thickness of ODS multilayer against number of layers. Measurements were taken with three different samples.

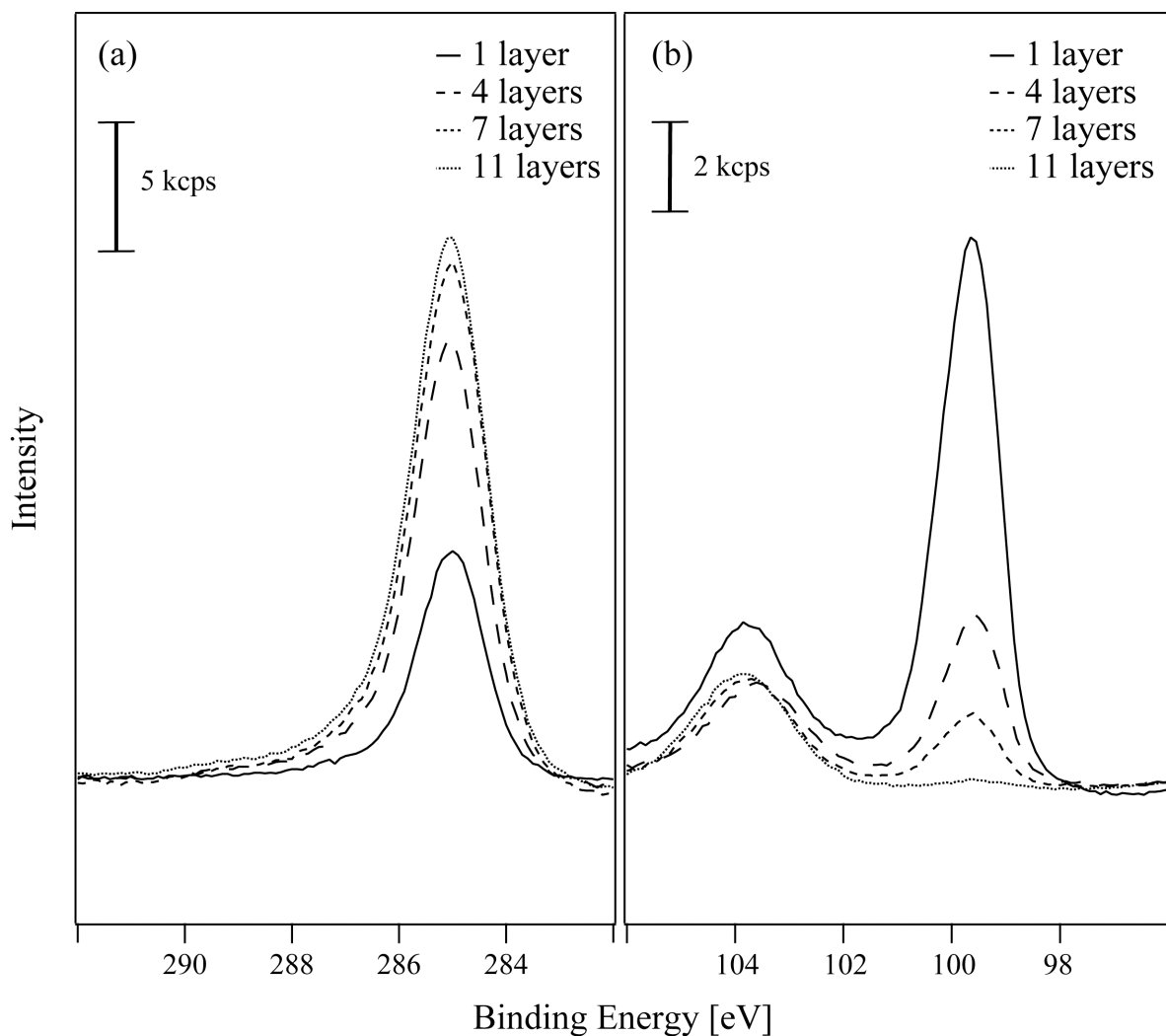


Figure 3.3. XPS (a) C 1s and (b) Si 2p spectra of ODS monolayer/multilayer samples with four different numbers of stacked layers.

The stepwise growth of multilayer films, according to the sequence of surface oxidizing and layer deposition, is also demonstrated by FTIR spectra after each deposition operation of the layer. The FTIR data provide direct evidence for the total amount of film-forming moieties of ODS molecules which are deposited on the surface, and for the orientation and packing density of the ODS paraffinic tails in each deposited layer. Figure 3.4 shows FTIR-transmission spectra in the C-H stretching region for the series of the ODS/(oxidized

ODS)_n/Si (with $n = 0, 3, 6, 10$) films. The strong bands observed at 2924 cm⁻¹ and 2853 cm⁻¹ are assigned to the methylene antisymmetric ($\nu_a\text{CH}_2$) and symmetric ($\nu_s\text{CH}_2$) stretching modes, respectively. The observed increasing trends in both absorbance intensity of the CH₂ stretch bands arise from variations in the amount of hydrocarbon in the films. From this viewpoint, we can state that layers are deposited in the LbL manner as we predicted. In addition, we can discuss the information that can be obtained from the peak position of these two bands: The peak position of these bands is known to depend on chain-length and the conformation of the paraffinic tails, i.e. hydrocarbon chains. For example, a shift to higher frequency in the peak positions of the $\nu_a\text{CH}_2$ and $\nu_s\text{CH}_2$ bands is indicative of packing density reduction [35]. In the case of Figure 3.4 the peak positions of the $\nu_a\text{CH}_2$ and $\nu_s\text{CH}_2$ bands in all of the spectra are recognized at almost constant wavenumbers of 2924 and 2853 cm⁻¹. Besides the peak positions, the full width at half height of the 2924 cm⁻¹ peak lies between 20.7 and 24.2 cm⁻¹ and that of the 2853 cm⁻¹ between 16.1 and 17.2 cm⁻¹. The peak positions of the CH₂ stretching modes, at 2924 and 2853 cm⁻¹, correspond to a disordered, liquid-like state of the hydrocarbon tails, contrary to the hexagonal (“rotator”) phase, which yields values not higher than 2917 and 2850, respectively [36-38]. These results agree with the other experimental facts that relatively thinner thicknesses and lower water contact angles of the stacked monolayers compared with those of a highly ordered monolayer, that is, more than 2 nm and near 110°.

The assembly of mono- and multilayer films, according to the build-up process shown in Figure 3.1, was followed by the FTIR measurement in the attenuated total reflection (ATR) mode, with spectra being taken after the adsorption of each new monolayer, as demonstrated in Figure 3.5. By using sufficiently thin Si substrates, thickness 525 μm , in the ATR mode, it became possible to explore the spectral region below 1400 cm⁻¹, which provides important

information on the modes of intra- and interlayer bindings. The spectral region below 1400 cm^{-1} is usually inaccessible, because of the strong absorption of the Si substrate itself. The CH_2 stretch bands of the paraffinic chains, peaking at 2926 and 2854 cm^{-1} , which are indicative of the amount of absorbed hydrocarbon material on the surface, were also observed as in the case of FTIR with transmittance mode. From the spectra given in Figure 3.5, the bandwidths and peak positions of the CH_2 stretch bands, at 2926 and 2854 cm^{-1} , did not change against the number of stacked layers, implying that the organization of the hydrocarbon molecular tails is the same in all films regardless of total film thickness. The CH_3 peak at 2955 cm^{-1} was clearly recognized only in the 1 layer spectrum, however, and was hardly seen in the spectra for 4, 7, and 11 layers, since the relative amount of CH_3 groups, the terminal groups of the top layer, was smaller than in these three samples. The CH_3 peak is, accordingly, hidden in the CH_2 peak shoulder. The 1850 - 750 cm^{-1} spectral region, displayed on the right side in Figure 3.5, provides information on functional groups involved in the intralayer, interlayer, and film-to-surface binding. The presence of both siloxane (Si-O-Si) stretching modes around 1129 cm^{-1} and a Si-OH stretch band at 880 cm^{-1} indicates the presence of incomplete intra- and interlayer covalent bonding of the silane groups. The broad bands at around 1129 cm^{-1} are characteristic of the Si-O-Si stretching mode of partially condensed oligomeric polysiloxanols. The positions, widths, and intensities of the Si-O-Si bands depend on many structural parameters, such as the extent of polymerization, branching, and the nature of the alkyl substituents on the silicon. Most probably, each layer of silane head groups in the present films may be viewed as a two-dimensional network made up of various linear and cyclic polysiloxanol species, which together contribute to the complex features observed in this spectral region. The distribution of siloxane structures in the initial monolayer (1 layer) differs from that in the spectra of the 4, 7, and 11 layer samples, implying

differences in the amounts of siloxane bonds originating from bonds in the interfaces of each layer. The broad band at around 880 cm^{-1} in 1, 4, 7, and 11 layer spectra arises from the Si-OH stretching vibration of unreacted silanols, with contributions from the out-of-plane deformation of the acid OH groups. The feature near 1465 cm^{-1} in all of the spectra is assigned to CH_2 scissoring (δ) vibrations of the alkyl chains. The $\delta(\text{CH}_2)$ bending mode is dependent on the lateral packing order of the chains. Thus, the identical peak positions of $\delta(\text{CH}_2)$ in Figure 3.5 further confirm the similar two-dimensional ordering of these samples, regardless of the structure on the film which would change against the total number of stacked layers.

Excellent depth resolution at the nm level is required for surface chemical analysis techniques, where high quality reference material, such as multilayered thin films, is desirable for the optimization of sputter depth profiling. Therefore, precise detection of growth processes from the viewpoint of layer thickness, surface and interface roughness with high resolution is an important task. Grazing incidence X-ray reflectivity (GIXR) is a powerful technique for such objectives. GIXR offers high spatial resolution at the sub-nanometer level for the measurement of roughness and thickness. Its high penetration and non-destructive capabilities are very suitable for probing buried interfaces. Here we demonstrate the GIXR characterization of the samples, and the thickness determined by GIXR was compared with that found by ellipsometry. The different interface roughness features and evolution with depth were also characterized by fitting techniques. X-ray reflectivity profiles on the samples of 1, 4, 7, and 11 layer films are shown in Figure 3.6. The dotted and solid curves represent the experimental and fitted data, respectively. Obviously, the 1 layer film has the minimum number of the oscillations. From 1 layer to 11 layers, the number of the oscillations gradually increases. This increase clearly demonstrates that increase of the thickness was achieved by

the LbL self-assembly process, as indicated by the ellipsometry measurement. However, no Bragg peaks, which are expected to be appeared in a X-ray reflectivity curve of a well-ordered multilayer [36], are discernible in the X-ray reflectivity curves of our multilayers as shown in Figure 3.6. This is due to a poor regularity in the periodicity of the multilayers caused by the interface roughness and the unevenness of layer thickness as summarized in Table 3.1. Table 3.1 shows the optimized values of parameters of film density, thickness, and surface and interface roughness obtained from the sample of 11 layers. It should be noted that the average thickness of each layer is 1.3 nm, which is almost consistent with that obtained from ellipsometric analysis, that is, 1.4 nm per layer. The data in Table 1.3 also shows a slightly decreasing trend in the density values of each layer with deposition layer from eleventh. This is possibly because of the accumulation of voids or other defects in the films with increasing layer number, as shown by the water contact angle measurement. The surface roughness of 0.40 nm on the eleventh layer was slightly smaller than that of the interfacial layers. The lower roughness of the top layer compared to the interfaces is probably due to a reaction, like oxidation, which took place on the surface after the film was exposed to VUV-light-generated active oxygen species. For the surface roughness obtained by GIXR, we also employed a supplemental roughness measurement by using atomic force microscopy. The morphology and roughness on the sample surfaces of the 1, 4, 7 and 11 layer films are shown in Figure 3.7. The surface roughness of the 1 layer film is about 0.18 nm, which is almost same as that of the substrate without covering ODS-SAM. With increasing number of stacked layers, the surface roughness gradually increases. It reaches be 0.29 nm for 11 layers, indicating the increase of disordering in each monolayer by layer stacking.

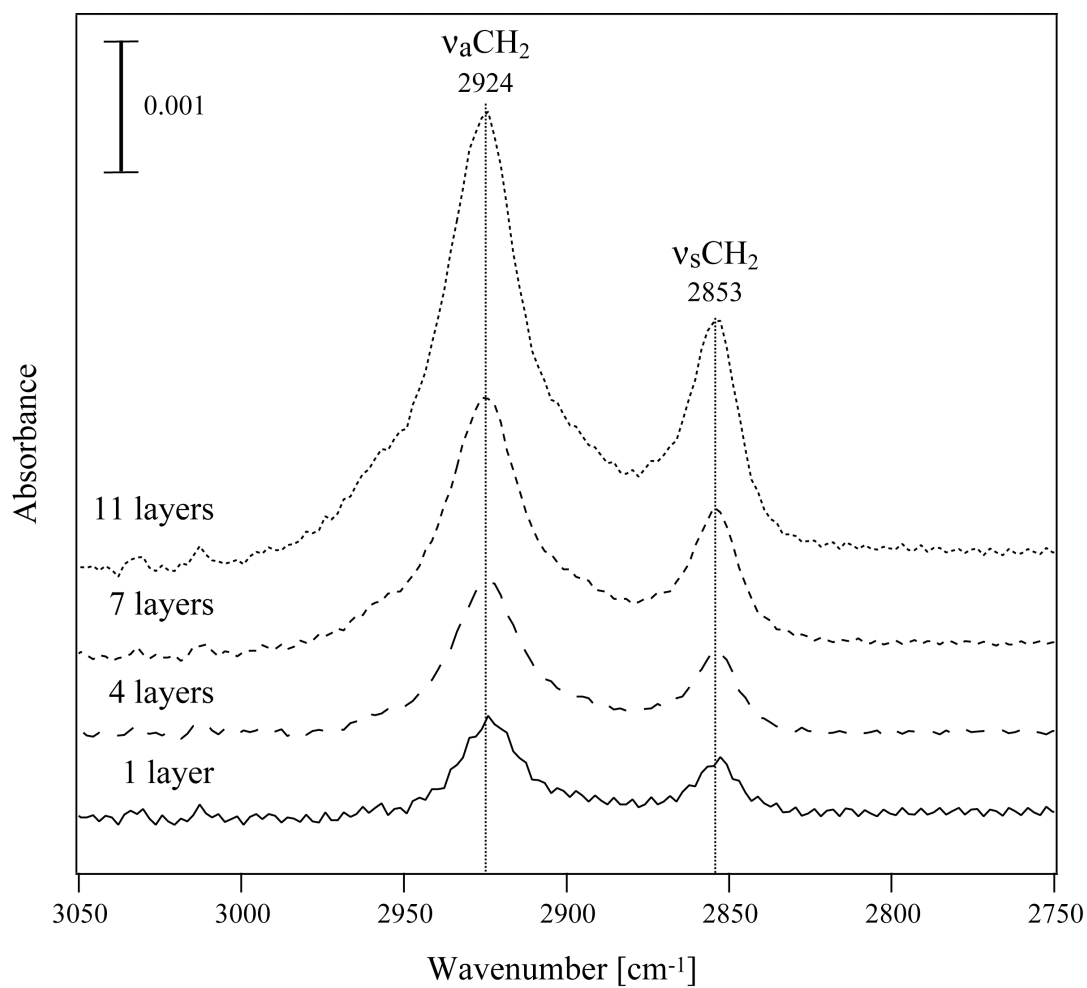


Figure 3.4. FTIR-transmission spectra for ODS monolayer/multilayer samples with four different numbers of stacked layers in the region of 2750 - 3050 cm⁻¹. The spectra were referenced to a common background, and obtained with resolution of 4 cm⁻¹ and 1024 scan cycles.

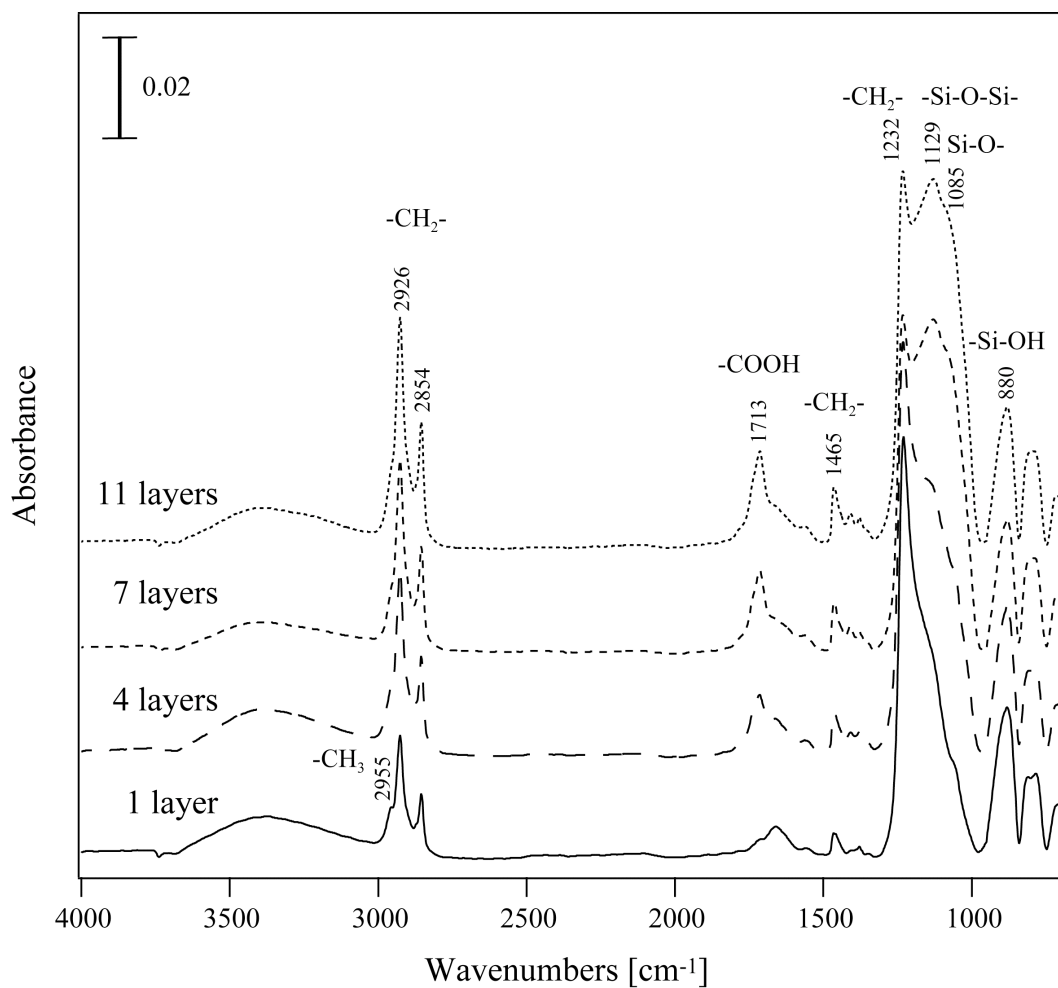


Figure 3.5. FTIR-ATR spectra for ODS monolayer/multilayer samples with four different numbers of stacked layers. All the spectra were collected using the same ATR crystal and were referenced to a common background. The resolution was 4 cm⁻¹ and the number of scan cycles was 1024.

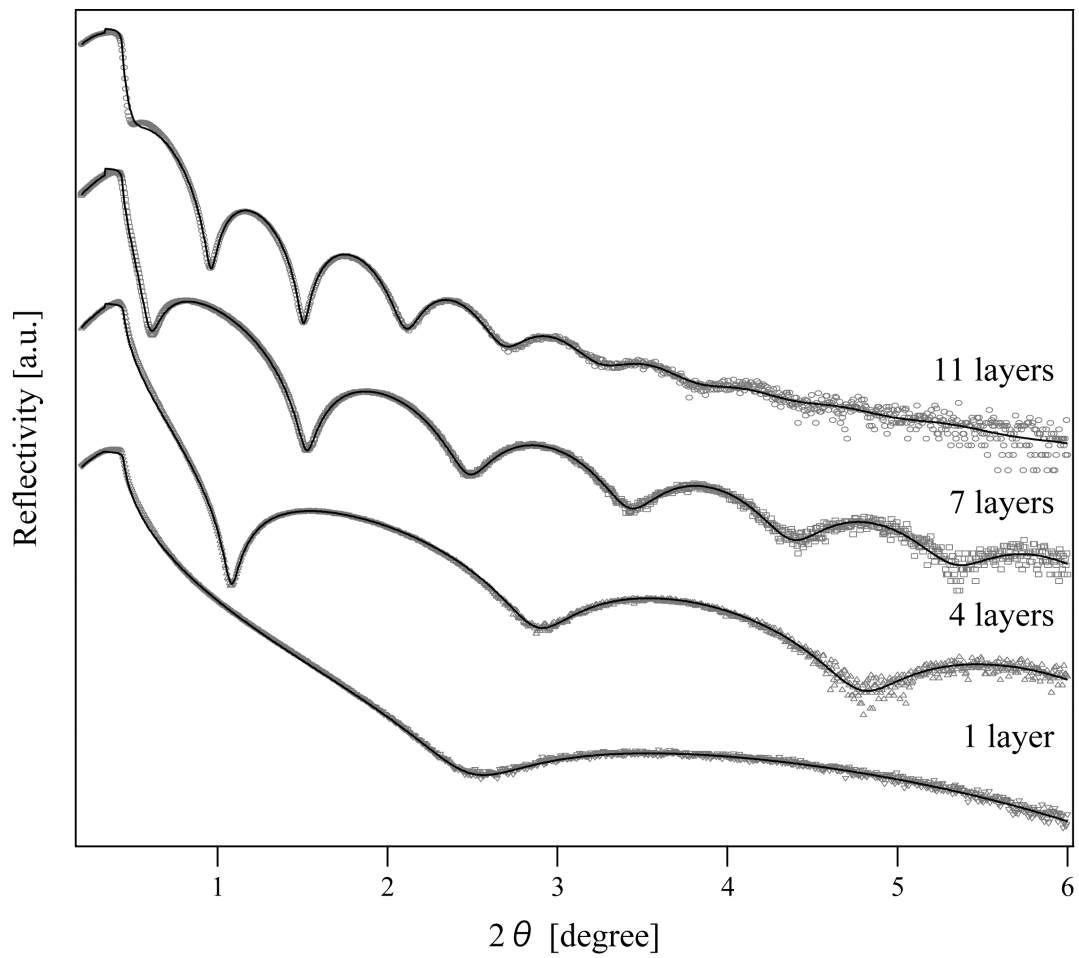


Figure 3.6. A set of measured X-ray reflectivity profiles (dotted curves) and the fitted curves (solid line) for ODS monolayer/multilayer samples with four different numbers of stacked layers.

Table 3.1. Structural parameters for the 11 layers film determined by the fitting of GIXR profile.

Layer	Density (g/cm ³)	Thickness (nm)	RMS roughness (nm)
11 th layer	0.64	1.2	0.40
10 th layer	0.78	1.2	0.42
9 th layer	0.82	1.3	0.72
8 th layer	0.84	1.3	0.65
7 th layer	0.89	1.4	0.77
6 th layer	0.91	1.2	0.74
5 th layer	0.94	1.2	0.70
4 th layer	1.03	1.3	0.73
3 rd layer	1.15	1.3	0.70
2 nd layer	1.24	1.3	0.69
1 st layer	1.23	1.2	0.60
SiO ₂	1.08	0.8	0.83
Si	2.25	—	1.18

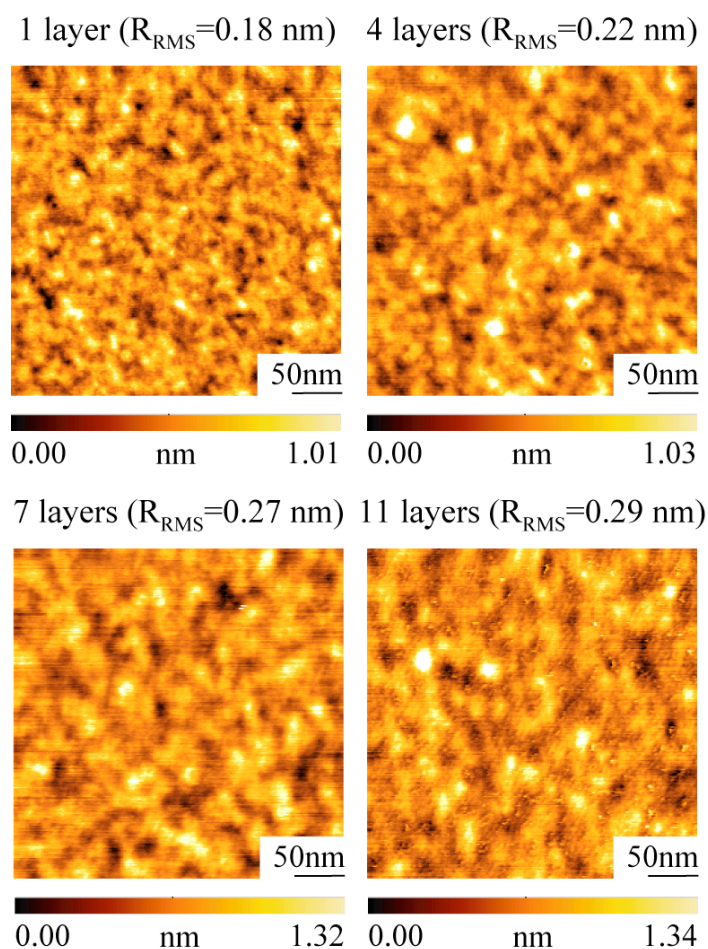


Figure 3.7. AFM topographic images with RMS roughness of ODS monolayer/multilayer samples with four different numbers of stacked layers.

3.4 Summary

The *n*-octadecyltrimethoxysilane (ODS) self-assembled multilayer formation based on activation of the methyl-terminated surface with reactive oxygen species generated by vacuum ultra-violet excitation of atmospheric oxygen molecules was investigated by water contact angle, ellipsometry, XPS, FTIR, GIXR, and AFM measurements. Although, the molecular ordering state in the multilayers is not so high compared with that of well-ordered organosilane monolayers and multilayers, we have succeeded in fabricating multilayers with a

relatively large thickness (16 nm scale and above) by the simple method in which a sample is treated in gas-phase throughout the process and, thus, no solvent is required to be used. It should be noted that any types of organosilane precursors, even methyl-terminated ones, are compatible to our method. These features of the LbL method here we have demonstrated is thought to be advantageous in practical. Furthermore, since we have employed an optical method for surface activation, the LbL method will be readily extendable to micro-fabrication processes [27,28,31] by activating a selected area with the use of a photomask.

References

- [1] J. D. Swalen, D. L. Allara, J. D. Andrade, E. A. Chandross, S. Garoff, J. Israelachvili, T. J. McCarthy, R. Murray, R. F. Pease, J. F. Rabolt, K. J. Wynne, and H. Yu, *Langmuir*, **3**, 932 (1987).
- [2] A. Ulman, *Chem. Rev.*, **96**, 1533 (1999).
- [3] F. Schreiber, *Prog. Surf. Sci.*, **65**, 151 (2000).
- [4] M. Haga and T. Yutaka, *Trends in Molecular Electrochemistry*, A. J. L. Pombeiro and C. Amatore Eds., Marcel Dekker, 311 (2004).
- [5] M. Maskus and H. D. Abruña, *Langmuir*, **12**, 4455 (1996).
- [6] M. A. Ansell, E. B. Cogan, and C. J. Page, *Langmuir*, **16**, 1172 (2000).
- [7] M. Altman, A. D. Shukla, T. Zubkov, G. Evmenenko, P. Dutta, and M. E. van der Boom, *J. Am. Chem. Soc.*, **128**, 7374 (2006).
- [8] M. Wanunu, S. Livne, A. Vaskevich, and I. Rubinstein, *Langmuir*, **22**, 2130 (2006).
- [9] H. Lee, L. J. Kepley, H. -G. Hong, and T. E. Mallouk, *J. Am. Chem. Soc.*, **110**, 618 (1988).
- [10] S. D. Evans, A. Ulman, K. E. Goppert-Berarducci, and L. J. Gerense, *J. Am. Chem. Soc.*, **113**, 2130 (1991).

- [11] H. Yonezawa, K. -H. Lee, K. Murase, and H. Sugimura, *Chem Lett.*, **35**, 1392 (2006).
- [12] H. Sugimura, H. Yonezawa, S. Asai, Q. -W. Sun, T. Ichii, K. -H. Lee, K. Murase, K. Noda, and K. Mastushige, *Colloid Surf. A*, **321**, 249 (2008).
- [13] J. Sagiv, *J. Am. Chem. Soc.*, **102**, 92 (1980).
- [14] K. Ogawa, N. Mino, K. Nakajima, Y. Azuma, and T. Ohmura, *Langmuir*, **7**, 1473 (1991).
- [15] S. Onclin, B. J. Ravoo, and D. N. Reinhoudt, *Angew. Chem. Int. Ed.*, **44**, 6282 (2005).
- [16] H. Sugimura, *Nanocrystalline Materials: Their Synthesis -Structure-Property Relationships and Applications*, Edited by S.C. Tjong, Elsevier, Oxford, 75 (2006).
- [17] L. Netzer, R. Iscovici, and J. Sagiv, *Thin Solid Films*, **99**, 235 (1983).
- [18] N. Tillman, A. Ulman, and J. F. Elman, *Langmuir*, **5**, 1020 (1989).
- [19] K. Ogawa, N. Mino, H. Tamura, and M. Hatada, *Langmuir*, **6**, 851 (1990).
- [20] W. Lin, W. Lin, G. K. Wong, and T. J. Marks, *J. Am. Chem. Soc.*, **118**, 8034 (1996).
- [21] T. Takahagi, Y. Nagasawa, and A. Ishitani, *Jpn. J. Appl. Phys.*, **35**, 3542 (1996).
- [22] S. Heid and F. Effenberger, *Langmuir*, **12**, 2118 (1996).
- [23] S. Katom and C. Pac, *Langmuir*, **14**, 2372 (1998).
- [24] J. Naciri, J. Y. Fang, M. Moore, D. Shenoy, C. S. Dulcey, and R. Shashidhar, *Chem. Mater.*, **12**, 3288 (2000).
- [25] M. -T. Lee and G. S. Ferguson, *Langmuir*, **17**, 762 (2001).
- [26] T. Lummerstorfer and H. Hoffmann, *J. Phys. Chem. B*, **108**, 3963 (2004).
- [27] L. Hong, H. Sugimura, T. Furukawa, and O. Takai, *Langmuir*, **19**, 1966 (2003).
- [28] H. Sugimura, L. Hong, and K. -H. Lee, *Jpn. J. Appl. Phys.*, **44**, 5185 (2005).
- [29] Y. -J. Kim, K. -H. Lee, H. Sano, J. Han, T. Ichii, K. Murase, and H. Sugimura, *Jpn. J. Appl. Phys.*, **47**, 307 (2008).
- [30] R. P. Roland, M. Bolle, and R. W. Anderson, *Chem. Mater.*, **13**, 2493 (2001).

- [31] H. Sugimura, K. Ushiyama, A. Hozumi, and O. Takai, *Langmuir*, **16**, 885 (2000).
- [32] H. Sugimura, A. Hozumi, T. Kameyama, and O. Takai, *Surf. Interf. Anal.*, **34**, 550 (2002).
- [33] H. Sugimura and N. Nakagiri, *J. Photopolym. Sci. Technol.*, **10**, 661 (1997).
- [34] K. Watanabe, E. C. Y. Inn, and M. Zelikoff, *J. Chem. Phys.*, **21**, 1026 (1953).
- [35] C. Naselli, J. F. Rabolt, and J. D. Swalen, *J. Chem. Phys.*, **82**, 2136 (1985).
- [36] K. Wen, R. Maoz, H. Cohen, J. Sagiv, A. Gibaud, A. Desert, and B. M. Ocko, *ACS Nano*, **2**, 579 (2008).
- [37] H. Hoffmann, U. Mayer, and A. Krischanitz, *Langmuir*, **11**, 1304 (1995).
- [38] T. Koga, M. Morita, H. Ishida, H. Yakabe, S. Sasaki, O. Sakata, H. Otsuka, and A. Takahara, *Langmuir*, **21**, 905 (2005).

Chapter 4

Surface modification and bonding of cyclo-olefin polymer (COP)

4.1 Introduction

In recent years, cyclo-olefin polymer (COP) resins have been used in a variety of applications according to their various properties and low cost, and the market for these resins growing every year [1]. The properties of COP, such as excellent transparency, high heat resistance, low water absorbency, stable and guaranteed refractive index, and low birefringence are fully utilized in many applications, especially for camera lenses/prisms, lenses for cameras incorporated into mobile phones, and pick-up lenses. COP is also suitable for medical devices that undergo autoclave sterilization at 121°C, such as medical vials, syringes, and optical lab test cells.

Extensive work to develop practical and economical methods for the surface modification of COP have been carried out by many researchers. For improvements in adhesivity, dyeability, and wettability, surface photografting modification in a gas- or liquid-phase has attracted wide-spread attention [2-6]. In particular, adhesion is a critical design feature of many commercially available products. In order to obtain better adhesion properties, it is necessary to form adhesive chemical bonds at the interface. This can be done by introducing oxygen polar functional groups on the COP surface through an appropriate surface treatment.

For this purpose, polymeric materials, especially in continuous formats like films, have been treated with several different oxidative processes, such as corona discharge treatment [7-9], plasma etching [10,11], ultraviolet irradiation [12], and chemical solution etching

[13]. These processes can modify the surface composition, morphology, and surface energy, which are associated with adhesive bonding, wettability, biocompatibility, and some other surface-related properties. While the above processes attempt to give new functions to polymer surfaces, it is also important to modify polymer material surfaces without affecting their bulk characteristics, such as their mechanical, thermal, and other intrinsic properties. Ultraviolet irradiation should be the best method in this respect, since ultraviolet irradiation interacts only with the polymer surface and does not penetrate into the centre of the material. Ultraviolet irradiation is also efficient and economical and hence is a potentially practical oxidative process for polymer surface modification. In particular, ultraviolet light with shorter wavelengths, i.e vacuum ultraviolet (VUV; $\lambda < 200$ nm), plays an important role in the near-surface chemistry of plasma-treated polymers [14,15]. One possible advantage of VUV photochemistry over its plasma counterparts is that a more specific surface chemistry is achieved using monochromatic radiation because of more specific and selective (photo) chemistry both on the solid surface and in the gas phase [16-19]. However, the VUV photochemistry of COP has not been elucidated so far.

For this study, we investigated whether and how VUV-light treatment modifies the COP surface to produce a hydrophilic surface. The resulting functional groups on the COP surfaces generated by the treatment are discussed in terms of the VUV irradiation distance and treatment duration. Here, we have employed X-ray photoelectron spectroscopy (XPS) for qualitative and quantitative chemical analysis of the polymer surfaces. However, when utilized alone XPS has some major weaknesses, hence the XPS data is discussed in combination with the results of Fourier transform infrared spectroscopy (FTIR). Using XPS and FTIR, the generation of hydroxyl, carbonyl, and carboxyl groups on the surface of COP samples treated with VUV-light was analyzed.

4.2 Experimental procedure

Materials – The test material used in this study was a transparent cyclo-olefin polymer (COP, 480R, Zeon Co.). Sheets of this COP resin with a thickness of 1 mm were fabricated by injection molding. Detailed properties of COP have been reported previously [1]. The test samples underwent VUV-light treatment (see “VUV-Light Treatment” section) and the modified samples were analyzed by several different techniques (see “Chemical and Physical Properties Analysis” section). The dimensions of the test samples were dependent on the analysis method employed.

VUV-light treatment – A schematic of the VUV-irradiation apparatus is shown in Figure 4.1. An excimer lamp was the source of VUV light at a wavelength of 172 nm (Ushio., UER20-172V; intensity at the lamp window, 10 mW cm^{-2}). The lamp consisted of two (inner and outer) quartz glass tubes filled with a discharge gas. The metal electrode was mounted within the inner tube, while the metal mesh electrode was located outside the outer tube.

The COP samples were placed on the sample stage in the irradiation chamber in the presence of ambient air. The distance between the lamp window and the sample surface was fixed at 5 or 30 mm. Since oxygen molecules absorb VUV light efficiently at 172 nm, the VUV light is attenuated when propagating through an air layer with a certain thickness. The optical absorption coefficient of the light at 172 nm in ambient air was reported to be in the range of $10\text{-}15 \text{ cm}^{-1} \text{ atm}^{-1}$ [20], so light transmittance through a 5 mm-thick air layer was estimated to be less than 50%, which means that the light intensity at the COP surface was less than 5 mW cm^{-2} . In other words, at a distance of 5 mm the sample surface was directly irradiated with VUV light from the lamp window while there was an absorption loss of about 50%. At the same time, the sample surface was exposed to active oxygen species (e.g. ozone and atomic

oxygen) generated in the air layer in the vicinity of the sample surface. Hence, two kinds of reactions; (i) direct VUV-excitation and (ii) indirect oxidation by the active oxygen, were considered to proceed on the sample surface. In contrast, the transmittance at 30 mm was estimated to be less than 0.1%, which means that the light intensity at the sample surface was less than 0.010 mW cm^{-2} . In other words, at a distance of 30 mm, VUV light was absorbed almost completely by atmospheric oxygen molecules yielding active oxygen species and almost no VUV-light reached the sample surface. Direct irradiation of COP surfaces with VUV photons was not expected to occur under an air layer of 30 mm, and only the VUV-light-generated active oxygen species could participate in the surface modification of COP.

Chemical and physical properties analysis – After VUV-light treatment, the modified COP surfaces were examined using a combination of analytical techniques. The static water contact angles of the sample surfaces were measured with a contact angle meter (Kyowa Interface Science, CA-X) in an atmospheric environment with the size of water droplets fixed at about 1.5 mm in diameter. At least four different measurements on the sample surfaces were obtained and the average values for water contact angles were calculated. The chemical bonding states of each sample were examined by X-ray photoelectron spectroscopy (XPS; Kratos Analytical, ESCA-3400) using a Mg $K\alpha$ X-ray source with a 10 mA emission current and a 10 kV accelerating voltage. The background pressure in the analytical chamber was 8.0×10^{-7} Pa. The X-ray spot diameter was 6 mm. The binding energy scales were referenced to 285.0 eV as determined by the location of the maximum peaks on the C1s spectra of hydrocarbon (CH_x), associated with adventitious contamination. The C1s and O1s spectra were decomposed by fitting a Gaussian-Lorentzian mixture function (mixture rate, 20:80). The surface modification process of COP samples were also monitored by

quantitative Fourier transform infrared spectroscopy (FTIR; Digilab Japan Co., Ltd, Excalibur FTS-3000). We used a single reflection ATR (attenuated total reflection) mode for measurement of the samples. The ATR IR spectra were obtained with a 65° angle of incidence and a hemispherical Ge ATR crystal with a diameter of 2.5 cm (internal reflection element, from Harrick Scientific). IR Spectra were measured in a dry atmosphere of a sample compartment purged with nitrogen and were referenced to background spectra determined under the same conditions. All spectra were measured at a resolution of 4 cm^{-1} and with 1024 scan cycles. The morphology and surface roughness of the samples were measured by atomic force microscopy (AFM; SII Nanotechnology, SPA-300HV + SPI-3800N) in tapping mode at a scan rate of 0.5 Hz using a silicon cantilever probe (Seiko Instruments Inc., SI-DF20, force constant of 15 N m^{-1}). From the analysis of the images, the root-mean-squared roughness (R_{RMS}) for the topographic profiles measured on $5 \times 5\ \mu\text{m}^2$ images was evaluated.

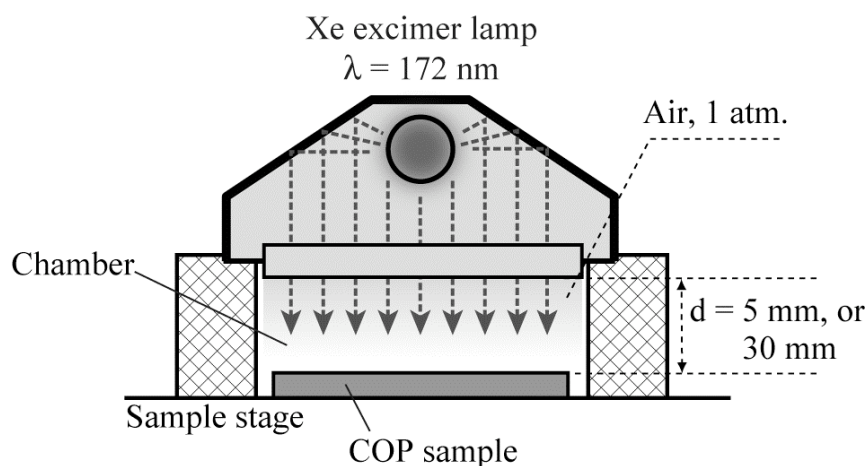


Figure 4.1. Schematic illustration of VUV-irradiation apparatus.

4.3 Results and discussion

4.3.1 Water contact angle of direct and remote VUV-light treated COP surface

The water contact angles of the COP surfaces treated with VUV-light at distances of 5 and 30 mm are shown in Figure 4.2. The COP surface treated at a distance 5 mm gave a larger decrease in the contact angle and became hydrophilic more rapidly than that at 30 mm. When comparing COP surfaces after an irradiation time of 5 min, the decrease in water contact angles from the initial value were 78% and 44% for the distances of 5 and 30 mm, respectively. At a distance of 5 mm, the water contact angle settled at zero after an irradiation time of 20 min, while in the case of the 30 mm distance, it decreased more gradually but leveled off from 40 min at approximately 14°. In either case, it was expected that the oxygen-containing functional groups were more or less introduced at the COP surfaces.

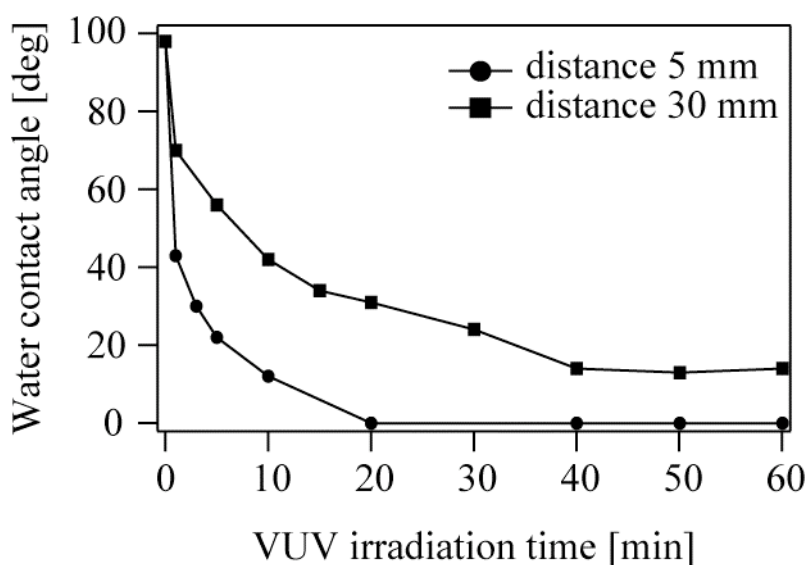
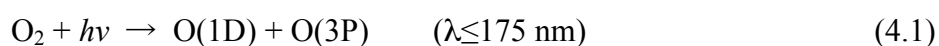


Figure 4.2. Changes in water contact angles of the COP surface with irradiation time of VUV light.

4.3.2 Chemical composition of direct and remote VUV-light treated COP surface

The chemical state of the VUV-irradiated surface was examined in more detail using

XPS. This study investigated the dependency of surface oxygenation of COP on different experimental conditions, VUV irradiation distance, and treatment duration, and used the O1s/C1s atomic ratio, which was calculated from the intensities of O1s and C1s spectra, as a measure of the extent of surface oxygenation. The increase in the extent of surface oxidation with VUV irradiation time is shown in Figure 4.3. Initial by faster oxidation was observed with a distance of 5 mm, and the O1s/C1s atomic ratio reached 0.7 within 20 min. Such a fast oxidation is of importance for the commercial use of this process in the future. The most reasonable explanation for the results is that active oxygen species can attack the COP surface only at a relatively lower rate compared to direct VUV-excitation. In other words, a photolytic activation is needed for the increase in COP oxidation rate. In our previous paper [21,22], the VUV photodegradation of alkyl monolayers in the presence of atmospheric oxygen molecules was reported. Here, VUV light of 172 nm wavelength excited atmospheric oxygen molecules resulting in the generation of ozone and/or oxygen atoms in singlet and triplet states [O(1D) and O(3P), respectively], as described in the Equation 4.1 [23]:



These active oxygen species, particularly O(1D), have strong oxidative reactivity. At a distance of 5 mm, the sample surface was directly irradiated with VUV light with concurrent exposure to active oxygen species. Therefore, in addition to oxidation of the sample surface by active oxygen, VUV excitation of the sample surface can be induced and the overall oxidation rate is accelerated. The O1s/C1s atomic ratio indicates the quantity of polar functional groups introduced onto the surface. From Figure 4.3, as for the O1s/C1s atomic ratio, neither distance showed significant change after 40 min. In other words, it is thought

that quantity of functional groups introduced onto the surface after 40 min does not change. Thus, 40 min-irradiation was found to be sufficient to obtain the maximally hydrophilic surfaces at each VUV-irradiation distance.

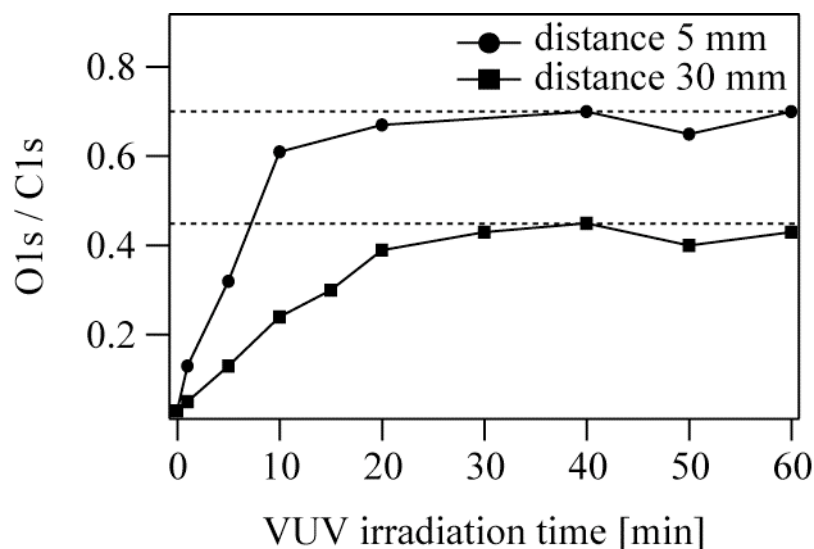


Figure 4.3. Changes of O1s / C1s atomic ratio obtained from XPS.

In addition to providing the total heteroatom concentration on the surfaces of VUV-treated COP presented above, XPS was also used to characterize their chemical bonding states. Remarkable differences between the distance of 5 and 30 mm were found not only in the rate of oxygen incorporation and the final oxygen concentration but also in the evolution of the polar functional groups. Figures 4.4 and 4.5 show the C1s and O1s XPS spectra of the COP samples after VUV irradiation for 5, 10, 40, and 60 min. In Figures 4.4 and 4.5, the spectra for untreated samples are also shown for comparison. The tail on the high binding energy side of the main C1s peak for COP showed that oxygen incorporation onto the COP surfaces gave rise to a variety of functional groups. These C1s peaks can be decomposed into four main components at 285.0 (C–H groups), 286.5 (C–O groups), 288.0 (C=O groups), and

289.5 eV (COO). The O1s peaks can be decomposed into two peaks, which are assigned as follows: O1s 532.4 eV (C=O or C–O groups) and 533.8 eV (O=C–O–H or O=C–O–C groups). These XPS results clearly demonstrated that after VUV-light treatment polar functional groups such as carbonyl, ether, and carboxyl appeared on the COP surface. By VUV irradiation for 5, 10, and 40 min, the amount of carbon on the sample decreased, whereas the amount of oxygen on the sample increased, indicating a progressive functionalization as a function of VUV-light treatment duration. The C1s atomic percentage data summarized in Table 4.1 and 4.2 also showed progressive increases in the surface densities of polar functional groups (detected as C–O, C=O, and COO components) with VUV-light irradiation until 40 min. Differences between the samples with VUV irradiation times of 40 and 60 min are not evident. This suggests that the functionalization of COP by VUV-light treatment remains almost constant for VUV irradiation times longer than 40 min, being in agreement with the reduction in the water contact angles shown in Figure 4.2. VUV-light treatment also has a more obvious effect with the short irradiation distance: A much higher concentration of polar functional groups was observed for a distance of 5 mm than for the corresponding times with a distance of 30 mm. For a distance of 5 mm, the COO component appeared within the first 5 min. However, in the case of the 30 mm distance only prolonged VUV-light treatment (>10 min) resulted in the appearance of COO components.

For the surface chemical-analysis, we also employed a supplemental measurement using FTIR. The FTIR-ATR spectra of untreated and treated COP are presented in Figures 4.6 and 4.7. Here, the sampling depth of the present FTIR-ATR technique (0.13 mm and below) is large compared with the estimated depth of VUV-light treatment effects. The VUV-light treatment introduced three new IR bands, i.e. O–H, C=O, and C–O valence vibrations. A very broad band located between 3750 and 3050 cm^{-1} , centered at about 3450

cm^{-1} , could be attributed to the O–H stretching in alcohols and/or phenols. A relatively sharp band between 1897 and 1519 cm^{-1} had a doublet structure, subpeaks being centered at 1716 and 1624 cm^{-1} , respectively. This feature could be assigned to C=O stretching in aliphatic ketones (1725-1705 cm^{-1}) and C=C and C=O in unsaturated ketones (1705-1665 cm^{-1}). A broad band between 1290 and 1180 cm^{-1} could be assigned to C–O–C antisymmetric stretching in esters. A broad band between 1000 and 900 cm^{-1} with a peak at 940 cm^{-1} could be assigned to C–H out-of-plane deformation (1000-950 cm^{-1}), CH_2 out-of-plane wagging (950-900 cm^{-1}) in vinyl ($-\text{CH}=\text{CH}_2$), and/or CH out-of-plane deformation (980-955 cm^{-1}) in vinylene ($-\text{CH}=\text{CH}-$) with a high level of confidence. As mentioned above, Figures 4.6 and 4.7 show increases in the C=C double bond concentration on the sample surface. C=C double bond formation was explained by the abstraction of hydrogen, known as the dominant mechanism during VUV irradiation of hydrocarbon polymers [24-26]. Figures 4.6 and 4.7 show that the vibrational bands that are most perturbed as a function of VUV irradiation time are the carbonyl band vibrations at about 1897-1519 cm^{-1} . It should be pointed out that no spectrum is free from carbonyl band vibrations except for the non-treated sample, but the intensity of this band increased as a function of VUV irradiation time. Note that, in our FTIR analysis, the word “intensity” means the height of the peak and not the area. In contrast, the carbonyl band area was measured relative to the hydrocarbon (C–H) band area, and the result is shown in Figure 4.8 as a function of VUV irradiation time. In this figure, a substantial increase in the $[\text{C}=\text{O}]/[\text{C}-\text{H}]$ area ratio until 40 min could be observed. This fact corroborates the activation/functionalization effect of VUV-light treatment on the COP surface. However, differences between the samples with VUV irradiation times of 40 and 60 min were not evident. This behavior was in agreement with the XPS results although XPS and FTIR analysis have different sampling depths. The increase in the XPS O1s/C1s atomic ratio

(Figure 4.3) and the $[C=O]/[C-H]$ area ratio (Figure 4.8) meant that the sample has been largely oxidized and the total amount of oxygen-containing moieties had increased, while the proportion of oxygen-containing moieties gradually increased from the outermost layers during the reaction.

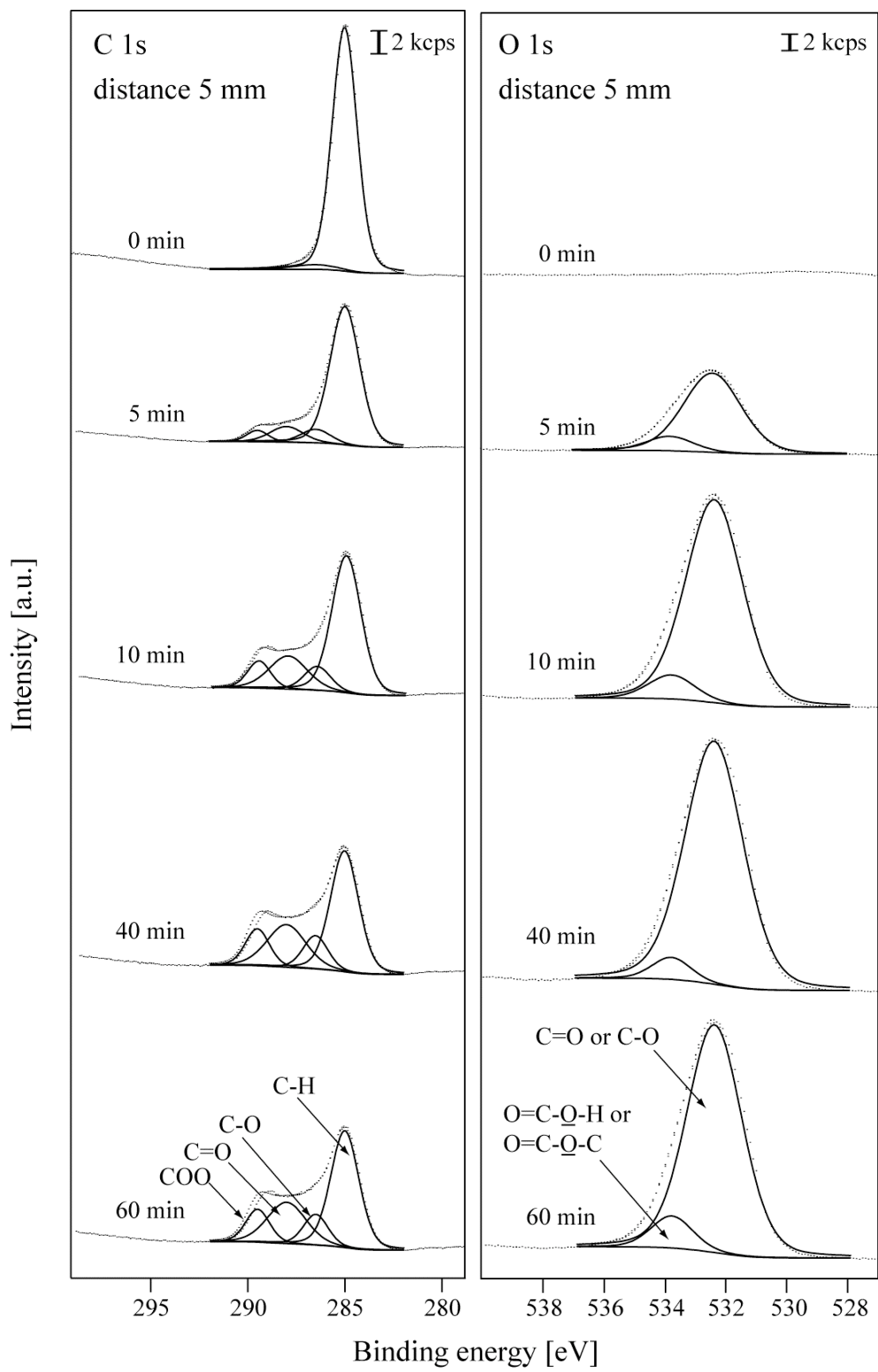


Figure 4.4. Deconvoluted C1s and O1s XPS spectra obtained from COP surfaces before and after VUV irradiation at a distance of 5 mm for 5 - 60 min.

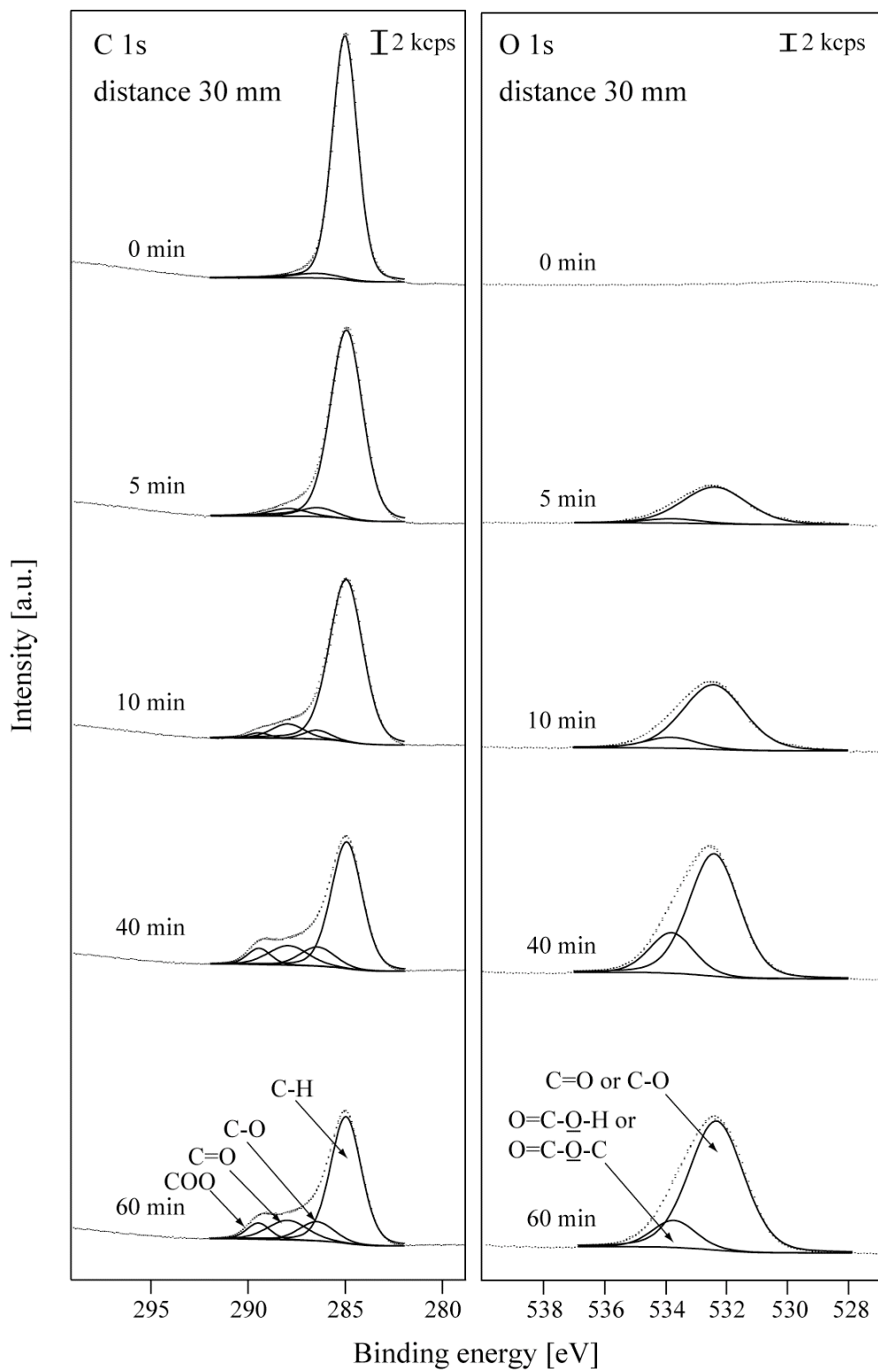


Figure 4.5. Deconvoluted C1s and O1s XPS spectra obtained from COP surfaces before and after VUV irradiation at a distance of 30 mm for 5 - 60 min.

Table 4.1. Atomic percentages of four elements including C 1s of different carbon moieties determined by XPS versus VUV-light treatment time for distance 5 mm.

VUV-light treatment time [min]	C [%]				O [%]
	C-H [%]	C-O [%]	C=O [%]	COO [%]	
0	94	3	-	-	3
5	59	7	7	3	24
10	37	6	13	6	38
20	33	7	13	7	40
40	30	7	15	7	41
60	30	7	15	7	41

Table 4.2. Atomic percentages of four elements including C 1s of different carbon moieties determined by XPS versus VUV-light treatment time for distance 30 mm.

VUV-light treatment time [min]	C [%]				O [%]
	C-H [%]	C-O [%]	C=O [%]	COO [%]	
0	94	3	-	-	3
5	82	3	3	-	12
10	71	3	6	1	19
20	51	9	9	3	28
40	47	9	9	4	31
60	48	9	9	4	30

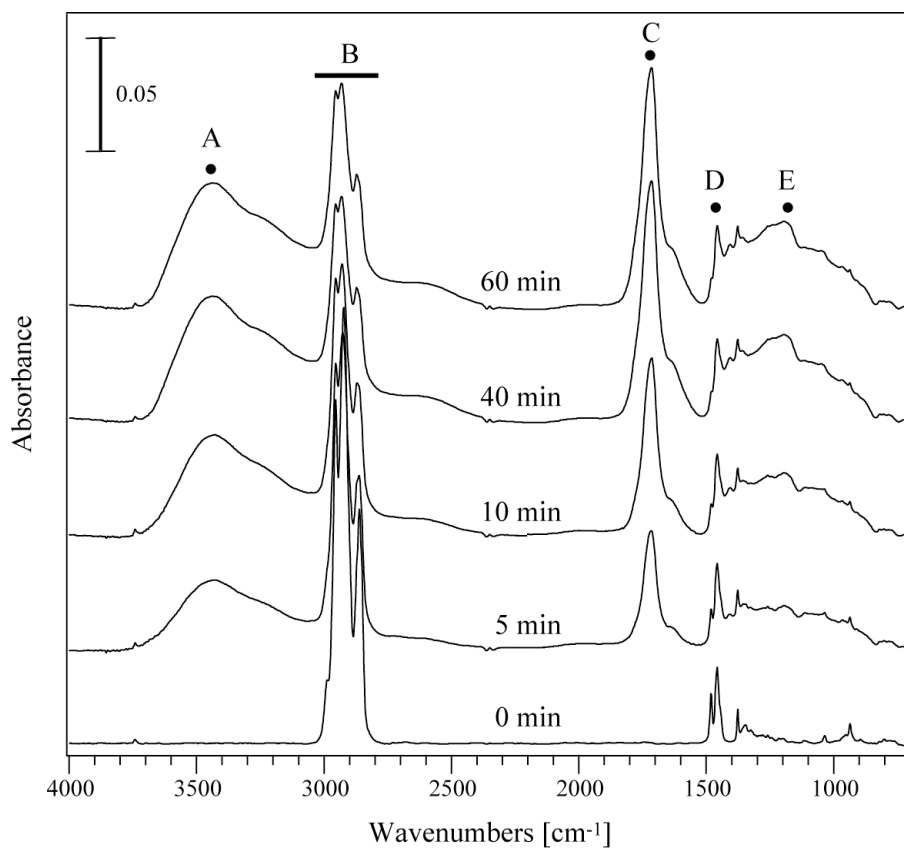


Figure 4.6. FTIR-ATR spectra on COP surfaces before and after VUV irradiation at a distance of 5 mm for 5 - 40 min: (A) O–H valence vibration; (B) C–H valence vibration; (C) C=O valence vibration; (D) CH₂ deformation vibration; (E) C–O valence vibration.

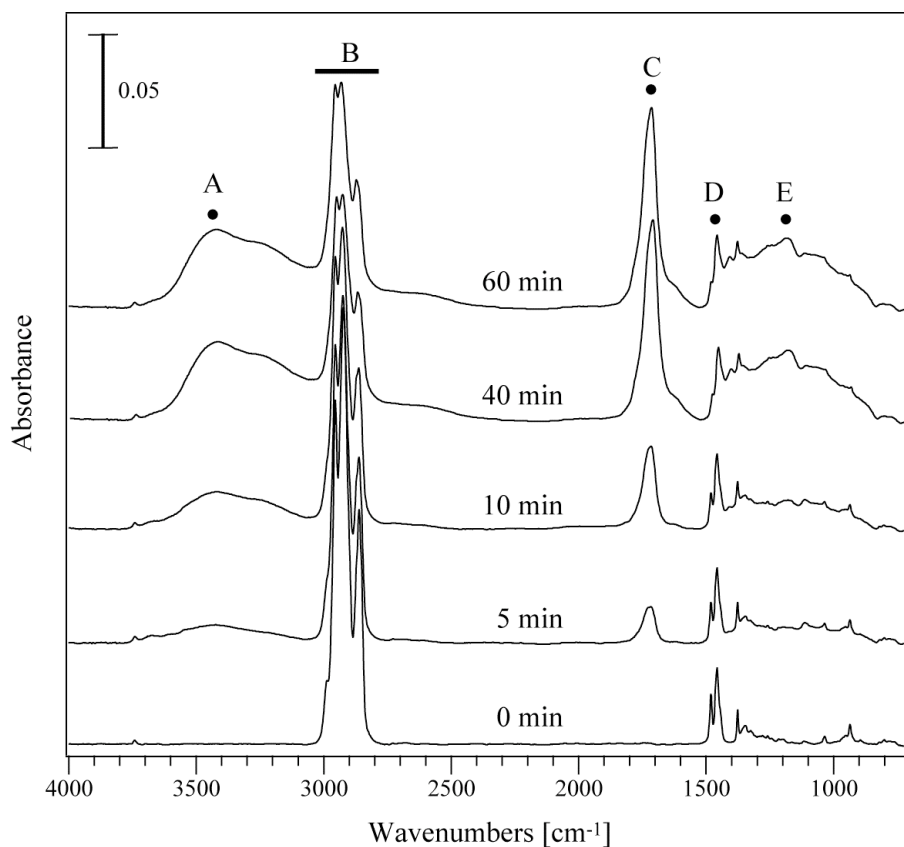


Figure 4.7. FTIR-ATR spectra on COP surfaces before and after VUV irradiation at a distance of 30 mm for 5 - 40 min: (A) O-H valence vibration; (B) C-H valence vibration; (C) C=O valence vibration; (D) CH₂ deformation vibration; (E) C-O valence vibration.

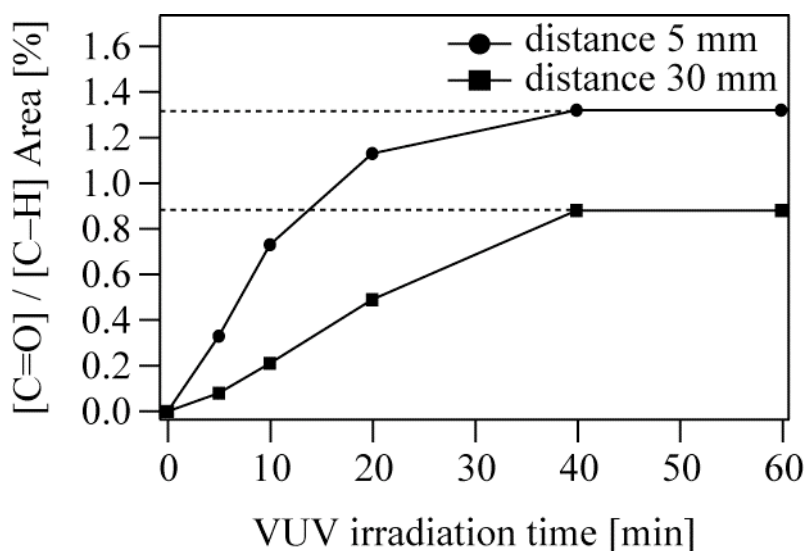


Figure 4.8. Carbonyl band ($1897\text{-}1519\text{ cm}^{-1}$, valence vibration), relative to hydrocarbon band ($3050\text{-}2750\text{ cm}^{-1}$, valence vibration) area, as a function of the time for VUV irradiation.

4.3.3 Topography of direct and remote VUV-light treated COP surface

The surface structure of the VUV-light-treated COP was monitored using AFM, which is the most suitable technique for the characterization of nonconductive VUV treated surfaces and to obtain 3D surface topography and roughness data. Figures 4.9 and 4.10 show topography images of COP samples prior to and after VUV irradiation for 5, 10, 20, 40, and 60 min. The smoothness of the sample surface increased with the increase in the VUV irradiation time. That is, VUV-light treatment of the sample caused changes in the surface topography. In the case of a distance of 5 mm, both of the reaction types, VUV-excitation of the COP surface and oxidation of the COP surface by active oxygen species, can promote significant surface topography changes while in the case of the 30 mm distance, only the oxidation of the COP surface by active oxygen species can change the surface topography. In particular in the case of the 5 mm distance, the surface topography of COP treated for 5 or 10 min showed structures like bubbles; however, for longer VUV irradiation times, a smooth

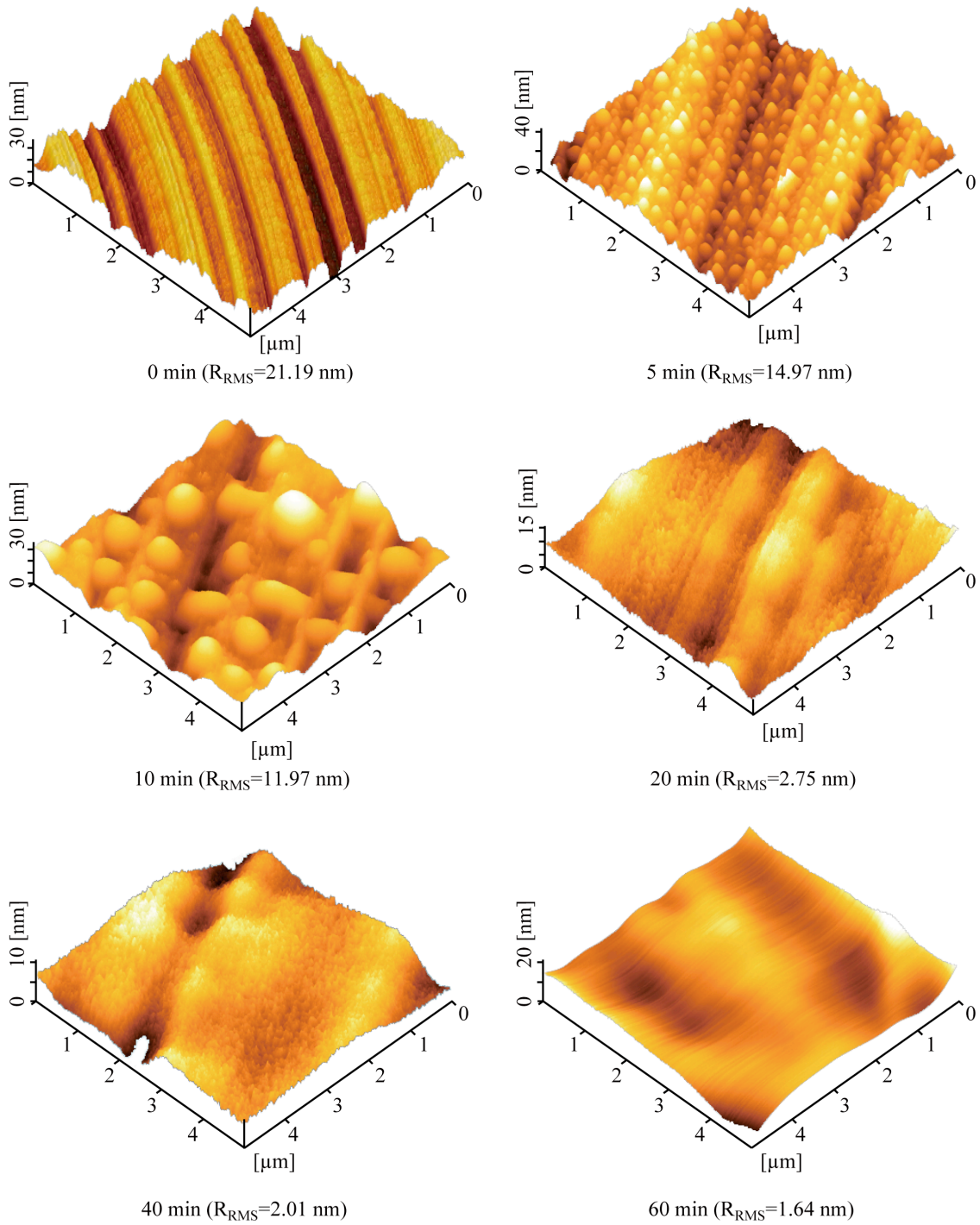


Figure 4.9. AFM topography images and RMS roughness on COP surfaces of distance 5 mm before and after irradiation with VUV light for 5 - 60 min (tapping mode; image size, $5 \times 5 \mu\text{m}^2$).

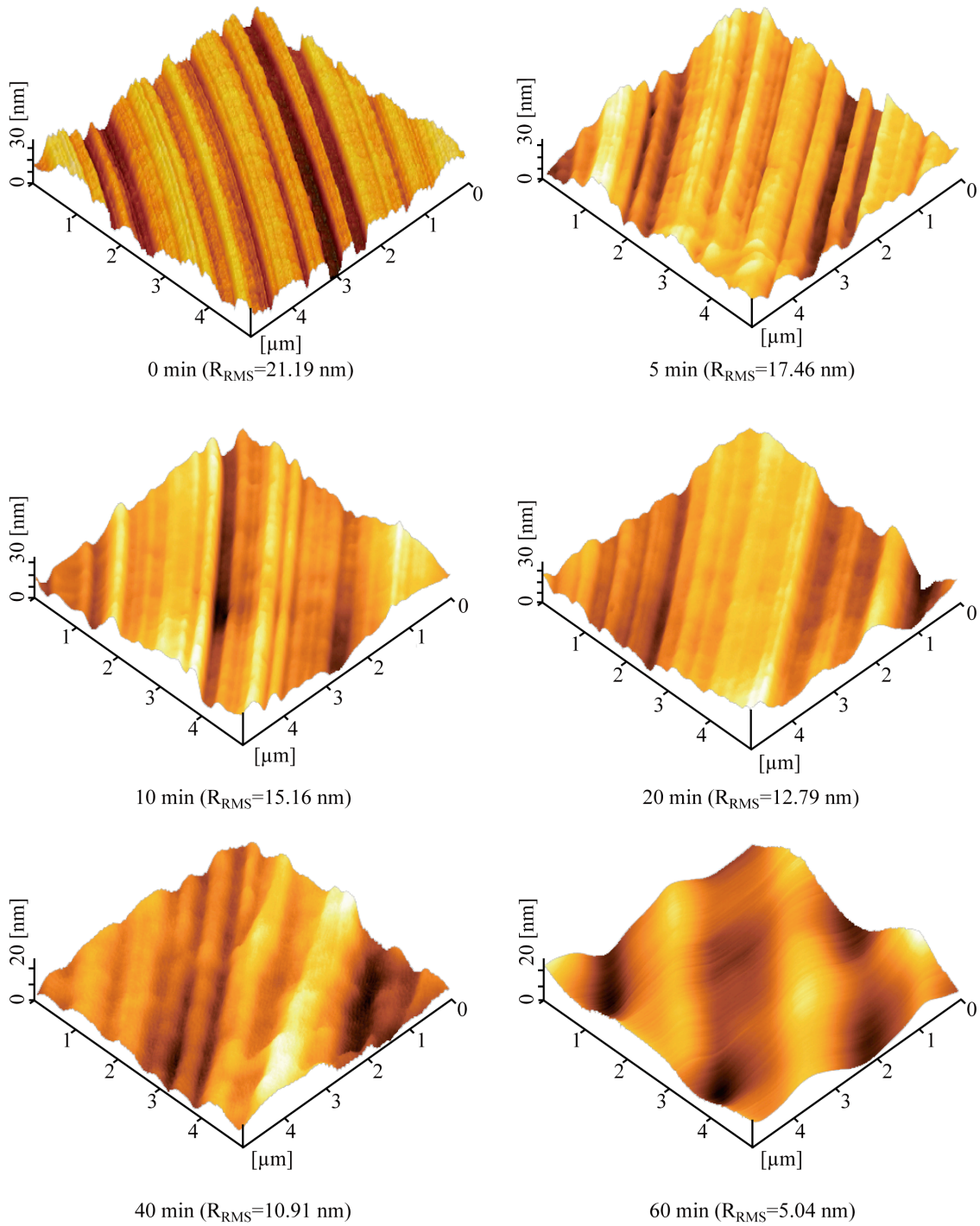


Figure 4.10. AFM topography images and RMS roughness on COP surfaces of distance 30 mm before and after irradiation with VUV light for 5 - 60 min (tapping mode; image size, $5 \times 5 \mu\text{m}^2$).

structure without bubbles emerged. Although the detailed mechanism of the formation of the bubble-like structures is still unclear, it may be attributed to high energy photons of 172 nm (i.e. 7.2 eV) direct irradiation onto the surface. However, in both cases the surface roughness gradually decreased with increasing VUV irradiation time. The change in surface roughness contributed in a significant way to improve wettability as confirmed by Figure 4.2. In addition, the AFM results suggested that surface oxidation had occurred uniformly.

4.3.4 Temporal change of VUV-light treated COP surface

Temporal change of COP surfaces after VUV irradiation at a distance of 5 mm for 20 min was investigated by water contact angle, XPS, and FTIR-ATR, as shown in Figure 4.11 ~ 4.14. All data do not change greatly until 100 days at time. This shows that the COP surface is stabilized. That is to say, the VUV-light treated hydrophilic COP surface has a life at least 100 days.

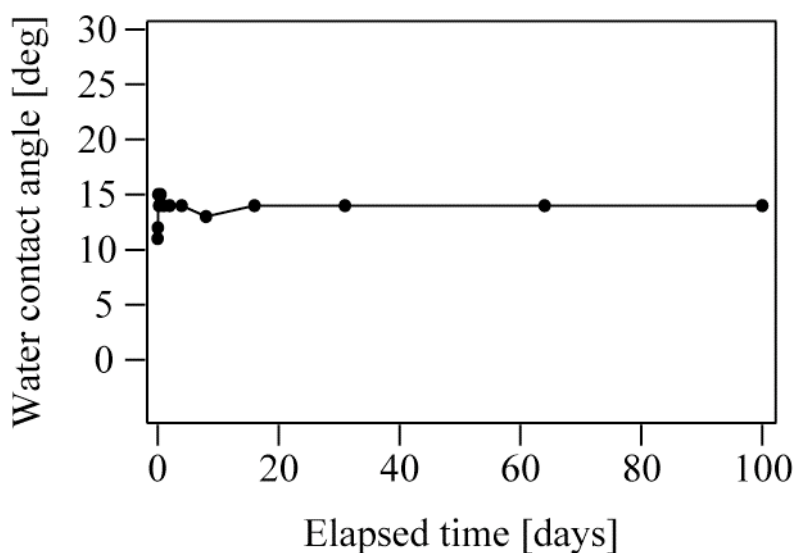


Figure 4.11. Changes in water contact angles of the VUV-light treated COP surface with temporal change.

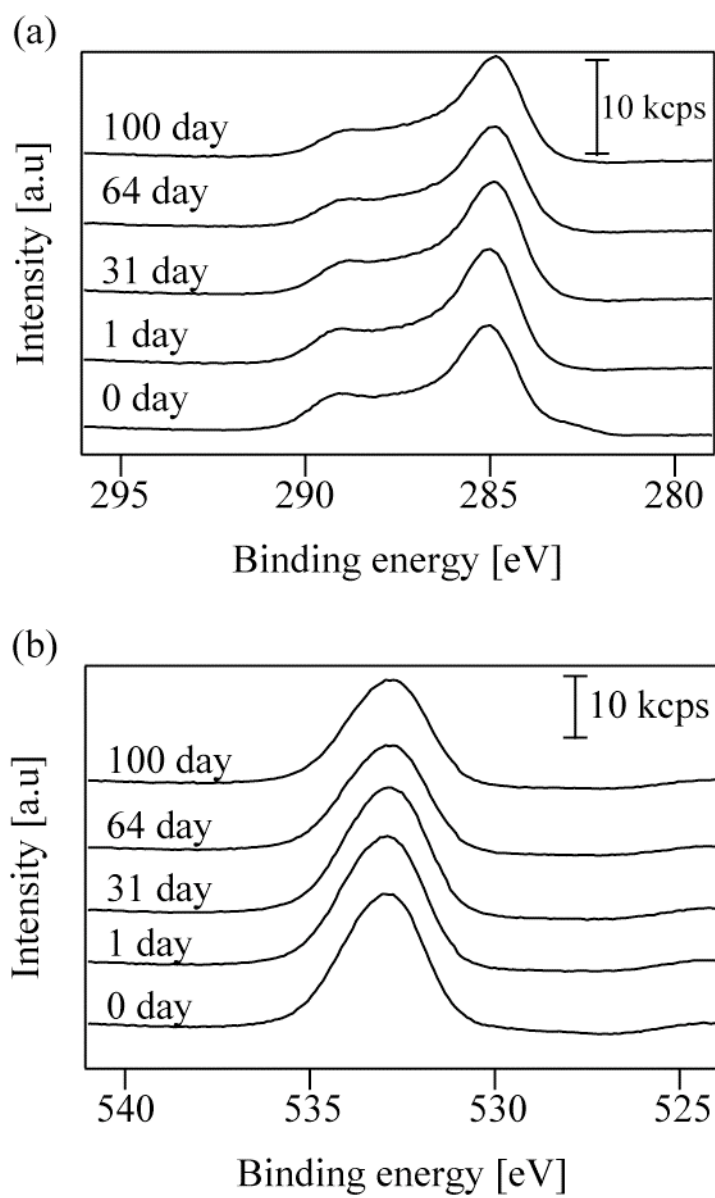


Figure 4.12. Changes in (a) C 1s and (b) O 1s XPS spectra of the VUV-light treated COP surface with temporal change.

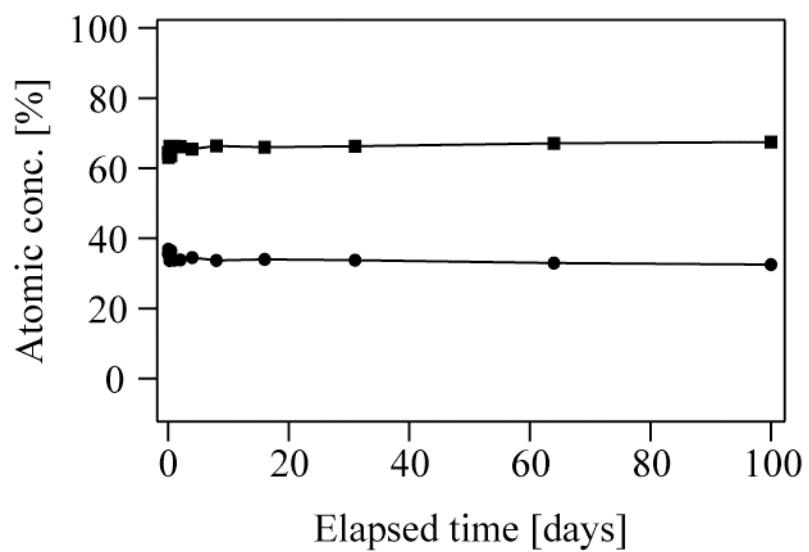


Figure 4.13. Changes in surface concentrations on C 1s and O 1s XPS spectra of the VUV-light treated COP surface with temporal change.

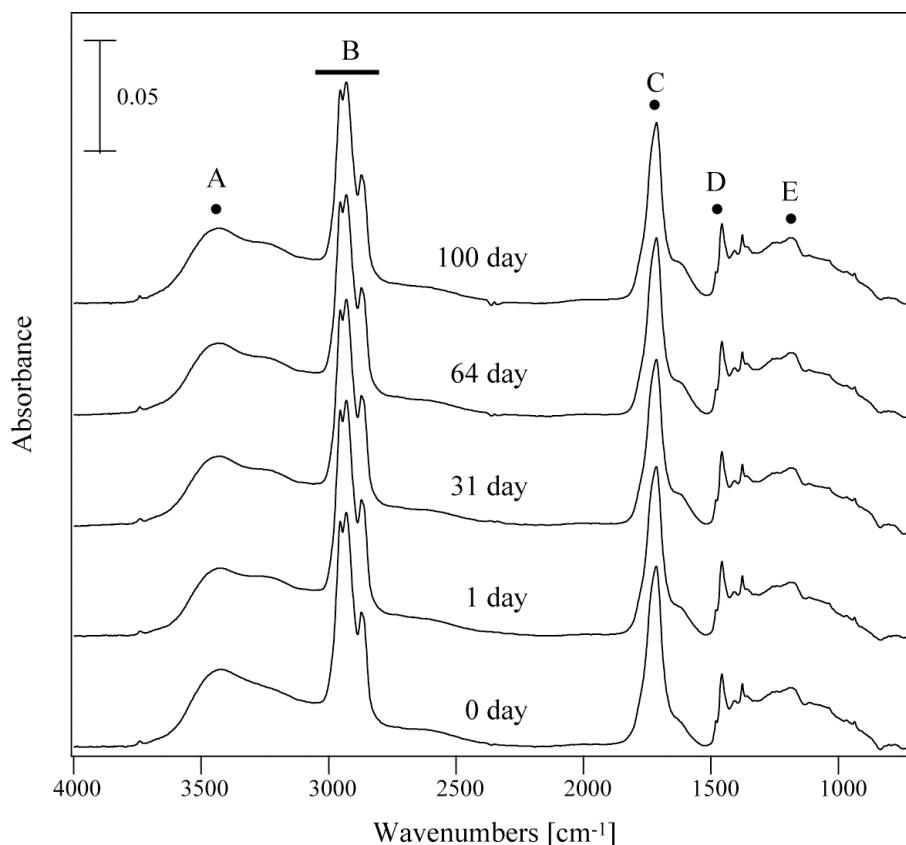


Figure 4.14. Changes in FTIR-ATR spectra of the VUV-light treated COP surface with temporal change: (A) O–H valence vibration; (B) C–H valence vibration; (C) C=O valence vibration; (D) CH₂ deformation vibration; (E) C–O valence vibration.

4.3.5 Photochemical activation bonding of COP

Research of photochemical activation bonding was conducted by using a press machine with COP surfaces after VUV irradiation at a distance of 30 mm for 5, 40 min was conducted. Procedures of bonding between COP plates is shown in Figure 4.15. The COP samples were placed on the sample stage in the press machine. Then, COP bonding experiments was conducted in various conditions, as shown in Table 4.3. The COP bonding was possible from temperature 90 °C in the case of VUV irradiation time 40 min. This shows that the COP bonding has close relation to VUV irradiation time. In fact, Figure 4.16 show

cross section SEM photo of after bonding COP plates in the condition of VUV irradiation at a distance of 5 mm for 10min.

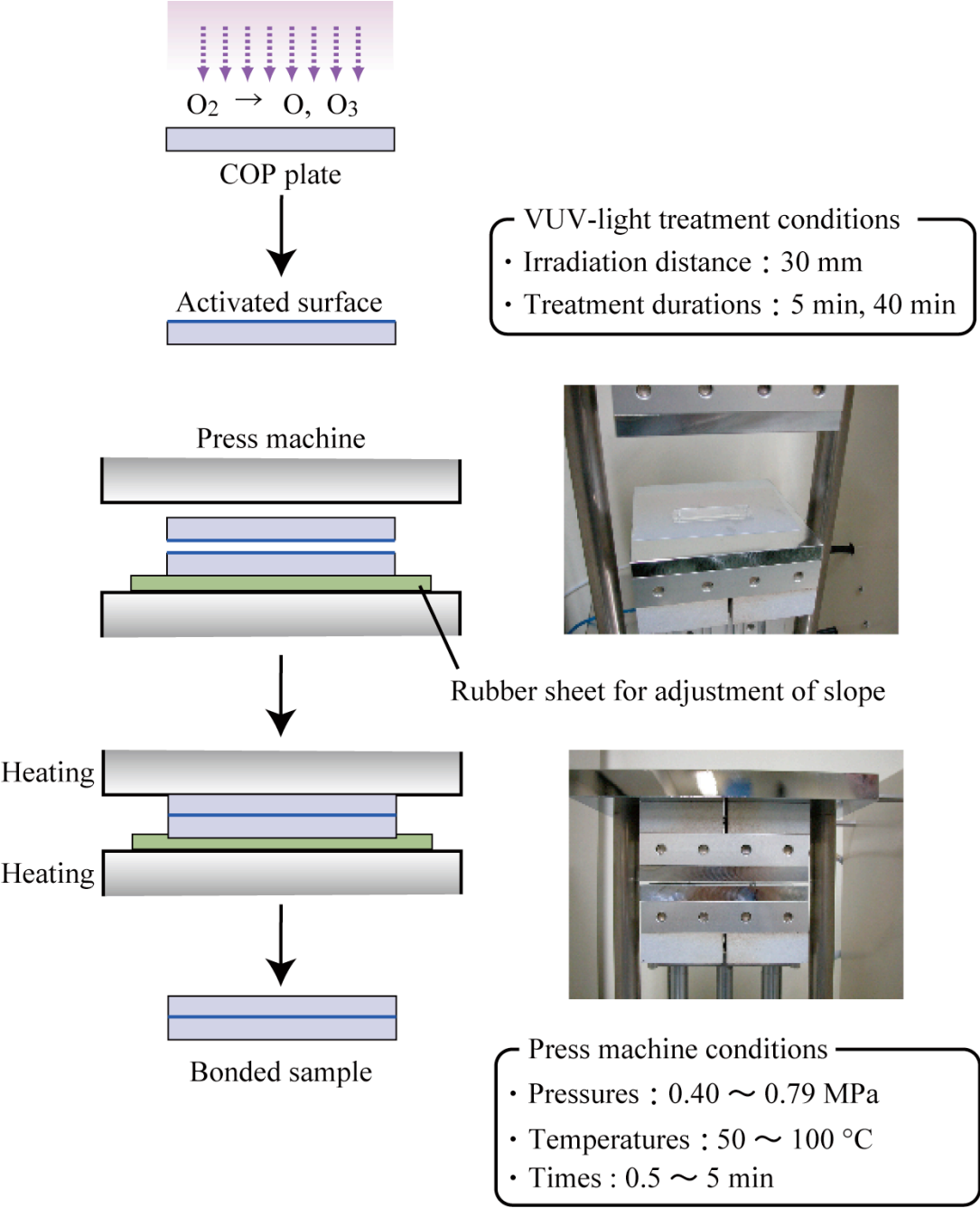


Figure 4.15. Procedures of bonding between COP plates.

Table 4.3. Presence or absence of bonding between COP plates.

(a) VUV irradiation : 0 min

Pressure [MPa]		0.79			
	Time [min]	0.5	1	3	5
Temp. [°C]	70	×	×	×	×
	80	×	×	×	×
	90	×	×	×	×
	100	×	×	×	×

(b) VUV irradiation : 5 min

Pressure [MPa]		0.40				0.53				0.66				0.79			
	Time [min]	0.5	1	3	5	0.5	1	3	5	0.5	1	3	5	0.5	1	3	5
Temp. [°C]	50	×	×	×	×	×	×	×	×	×	×	×	×	×	×	×	×
	60	×	×	×	×	×	×	×	×	×	×	×	×	×	×	×	×
	70	×	×	×	×	×	×	×	×	×	×	×	×	×	×	×	×
	80	×	×	×	×	×	×	×	×	×	×	×	×	×	×	×	×
	90	×	×	×	×	×	×	×	×	×	×	×	×	×	×	×	×
	100	×	×	×	×	×	×	×	×	×	×	×	×	×	×	×	×

(c) VUV irradiation : 40 min

Pressure [MPa]		0.40				0.53				0.66				0.79			
	Time [min]	0.5	1	3	5	0.5	1	3	5	0.5	1	3	5	0.5	1	3	5
Temp. [°C]	50	×	×	×	×	×	×	×	×	×	×	×	×	×	×	×	×
	60	×	×	×	×	×	×	×	×	×	×	×	×	×	×	×	×
	70	×	×	×	×	×	×	×	×	×	×	×	×	×	×	×	×
	80	×	×	×	×	×	×	×	×	×	×	×	×	×	×	×	×
	90	×	×	○	○	×	×	○	○	×	×	○	○	×	×	○	○
	100	×	×	○	○	×	○	○	○	×	○	○	○	○	○	○	○

Bonding states : ○ Good (Bonded surface does not come off under pulling it by hand.), × Fault (Bonded surface comes off under pulling it by hand.)

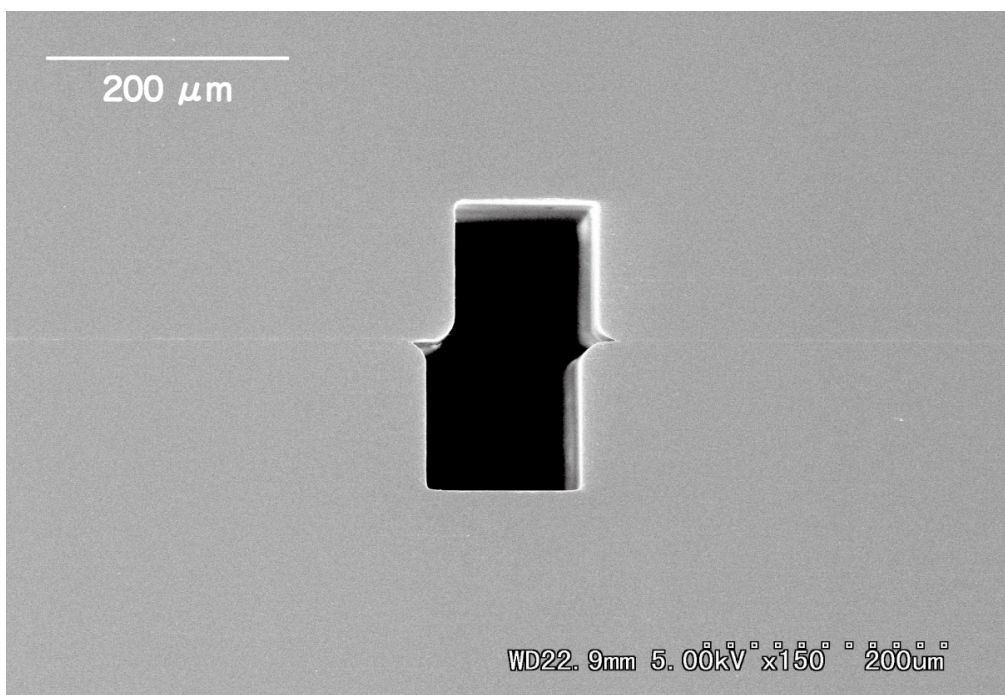


Figure 4.16. Cross section SEM photo of after bonding between COP plates.

4.4 Summary

In this study, COP surfaces were irradiated using an excimer lamp as a source of VUV light at a wavelength of 172 nm. Polar functional groups appeared as ether, ketone, and carboxyl groups on the COP surface after VUV-light treatment. These groups formed hydrophilic polymer surfaces. The amount of functional groups introduced onto the COP surfaces by VUV-light treatment was dependent on the experimental parameters, i.e. VUV irradiation distance and treatment duration. A higher concentration of polar functional groups was observed for the 5 mm distance than for the 30 mm distance for the corresponding periods of VUV-light treatment. The O1s/C1s atomic ratio of XPS spectra and the [C=O]/[C-H] area ratio of FTIR-ATR spectra were taken as a measure of the degree of surface oxidation following VUV. From these analyses, the optimum experimental

time-length for irradiation distances of 5 and 30 mm was found to be 40 min. When assessed from the data on the two different distances, it was found that COP appeared to be more stable against active oxygen, hence photochemical activation seemed to be more effective for the surface functionalization. From the present investigation, VUV-light treatment technology was found to be effective for COP surface modification similarly to other polymers [27,28]. Furthermore, onto the COP surfaces, a modified layer with a high amount of polar functional groups is formed by the process. The COP plates are bonded through attractive interactions between the modified layers on the plates at a low temperature and a low pressure without deforming microstructures performed on the plates. Our study achievements are expectable as the base for the development of fundamental manufacturing techniques applicable to micro-chemical, micro-optical and micro-mechanical systems made of various materials. The advantages of the technology are: 1) the equipment is simple and cheap; 2) the equipment can be safely and easily operated; 3) no chemical reagents are required; and 4) there are no residual polluting byproducts or time consuming after treatments.

References

- [1] M. Yamazaki, *J. Mol. Catal. A: Chem.*, **213**, 81 (2004).
- [2] S. Tazuke and H. Kimura, *Makromol. Chem.*, **179**, 2603 (1978).
- [3] K. Allmer, A. Hult, and B. Ranby, *J. Polym. Sci.: Part A: Polym. Chem.*, **26**, 2099 (1988).
- [4] K. Yamada, H. Tsutaya, S. Tatekawa, and M. Hirata, *J. Appl. Polym. Sci.*, **46**, 1065 (1992).
- [5] L. M. Hamilton, A. Green, S. Edge, J. P. S. Badyal, W. J. Feast, and W. F. Pacynko, *J. Appl. Polym. Sci.*, **52**, 413 (1994).
- [6] H. Mingbo and H. Xingzhou, *Polym. Degrad. Stab.*, **18**, 321 (1987).
- [7] D. K. Owens, *J. Appl. Polym. Sci.*, **19**, 3315 (1975).

- [8] J. F. Carly and P. T. Kitzel, *Polym. Eng. Sci.*, **20**, 330 (1980).
- [9] H. Iwata, A. Kishida, M. Suzuki, Y. Hata, and Y. Ikada, *J. Polym. Sci. Polym. Chem. Ed.*, **26**, 3309 (1988).
- [10] H. Yasuda, H. C. Marsh, S. Brandt, and C. N. Reilley, *J. Polym. Sci. Polym. Chem. Ed.*, **15**, 991 (1977).
- [11] H. Schonhorn and R. H. Hansen, *J. Appl. Polym. Sci.*, **11**, 1461 (1967).
- [12] M. Hudis, *J. Appl. Polym. Sci.*, **16**, 2397 (1972).
- [13] E. R. Nelson, T. J. Kilduff, and A. A. Benderly, *Ind. Eng. Chem.*, **50**, 329 (1958).
- [14] A. C. Fozza, J. E. Klemberg-Sapieha, and M. R. Wertheimer, *Plasmas Polym.*, **4**, 183 (1999).
- [15] A. C. Fozza, M. Moisan, and M. R. Wertheimer, *J. Appl. Phys.*, **88**, 20 (2000).
- [16] H. Esrom and U. Kogelschatz, *Thin Solid Films*, **218**, 231 (1992).
- [17] A. Hozumi, T. Masuda, K. Hayashi, H. Sugimura, O. Takai, and T. Kameyama, *Langmuir*, **18**, 9022 (2002).
- [18] F. -E. Truica-Marasescu and M. R. Wertheimer, *Macromol. Chem. Phys.*, **206**, 744 (2005).
- [19] Y. Li, A. Hayashi, M. Saito, M. Vacha, S. Murase, and H. Sato, *Polym. J.*, **38**, 395 (2006).
- [20] K. Watanabe, E. C. Y. Inn, and M. Zelikoff, *J. Chem. Phys.*, **21**, 1026 (1953).
- [21] L. Hong, H. Sugimura, T. Furukawa, and O. Takai, *Langmuir*, **19**, 1966 (2003).
- [22] H. Sugimura, L. Hong, and K. H. Lee, *Jpn. J. Appl. Phys.*, **44**, 5185 (2005).
- [23] R. P. Roland, M. Bolle, and R. W. Anderson, *Chem. Mater.*, **13**, 2493 (2001).
- [24] J. Hong, F. Truica-Marasescu, L. Martinu, and M. R. Wertheimer, *Plasmas Polym.*, **7**, 245 (2002).
- [25] R. Wilken, A. Holländer, and J. Behnisch, *Plasmas Polym.*, **7**, 185 (2002).

[26] A. Holländer, R. Wilken, and J. Behnisch, *Surf. Coat. Technol.*, **116-119**, 788 (1999).

[27] M. Charbonnier and M. Romand, *International Journal of Adhesion & Adhesives* **23**, 277 (2003).

[28] J. -Y. Zhang, H. Esrom, U. Kogelschatz, and G. Emig, *J. Adhesion Sci. Technol.*, **8**, 1179 (1994).

Chapter 5

Conclusions

The aim of this study was to highlight the role of the VUV-generated active oxygen and to demonstrate the surface modification of the sample with the active oxygen.

Chapter 1 describes general information on photochemical surface modification processing, organosilane SAMs, and plastic resins.

In Chapter 2, a new concept to stack a SAM without complicated procedures and/or special precursors was proposed. The surface chemical conversion of ODS-SAMs with active oxygen species generated by the VUV-light excitation of atmospheric oxygen molecules were investigated by water contact angle analysis, film thickness analysis, XPS, and AFM. In the VUV-light treatment experiments, an ODS-SAM sample placed in air was irradiated with a Xe excimer lamp located 30 mm above the sample surface. At this distance, the VUV light emitted from the lamp was almost completely absorbed by atmospheric oxygen molecules, which were converted to active oxygen species such as ozone and atomic oxygen. Using this VUV-light system, we optimized the irradiation time for the chemical conversion. It was found that, under the VUV-light treatment, both the water contact angle and the film thickness of the ODS-SAM decreased monotonically with increasing irradiation time. This demonstrated that polar functional groups are evidently and progressively introduced through the treatment with the concomitant etching of the SAM. The introduction of the polar functional groups was also confirmed by XPS measurement. As a result, it was thought that the surface density of polar functional groups, which serve as silane coupling sites for stacking a second monolayer, is insufficient if the irradiation time is too short. In contrast, if the irradiation time is too long, the second monolayer would be successfully prepared, but the

total thickness of the resulting bilayer film will be small. In consequence, the total thickness of the bilayer films grown on VUV-light-treated ODS-SAM substrates was found to increase toward the irradiation time of 400 s and decrease after 400 s until a treatment time of 1200 s. We thus concluded that 400 s is the optimum VUV-light-treatment time. Under this condition, we can introduce maximum polar functional groups on the surface of the first monolayer and, at the same time, minimize the loss of the thickness of the monolayer due to etching.

In Chapter 3, describes the fabrication of alkylsilane self-assembled multilayers with more than ten layers by only repeating the stacking of the alkylsilane layer on the modified SAM surface and the hydrophilic conversion of the stacked layer. Structures and properties of the fabricated multilayers were investigated in detail using a water contact angle analysis, and by film thickness analysis, XPS, FTIR, GIXR, and AFM. Film thickness and GIXR measurements revealed that multilayer films of up to 11 discrete monolayers were successfully obtained, indicating that the self-assembly is a viable technique for the construction of relatively thick (16 nm and above) multilayer films. Water contact angle measurement and AFM indicated, however, that disorder of the constitutive monolayer was increased with the number of the layers. Also, the peak positions of the CH₂ stretching modes, at 2924 and 2853 cm⁻¹, correspond to a disordered, liquid-like state of the hydrocarbon tails, contrary to the hexagonal (“rotator”) phase, which yields values not higher than 2917 and 2850 cm⁻¹, respectively, as shown in the FTIR-transmission spectra. These results agree well with the other experimental facts that both the thicknesses and water contact angles of the stacked monolayers are small compared with those of a highly ordered monolayers, if available. Although, the molecular ordering in the multilayers is not so high compared with that of well-ordered organosilane monolayers and multilayers, we have succeeded in

fabricating multilayers with a relatively large thickness (16 nm scale and above) by the simple method in which a sample is treated in gas-phase throughout the process and, thus, no solvent is required to be used.

Chapter 4 provides the results on photochemical conversion of hydrophobic COP surface to hydrophilic consisting of oxygen functional groups such as C–O, C=O, and COO components by simple irradiation with VUV in the presence of atmospheric oxygen molecules. The amount of functional groups introduced at the COP surfaces by VUV-light treatment was dependent on the experimental parameters, i.e. VUV irradiation distance and treatment duration. A higher concentration of oxygen functional groups was recognized for the 5 mm distance compared to the case of 30 mm distance for the corresponding periods of VUV-light treatment. The O1s/C1s atomic ratio of XPS spectra and the [C=O]/[C–H] area ratio of FTIR-ATR spectra were taken as a measure of the degree of surface oxidation by VUV irradiation. From these analyses, the optimum duration time for irradiation distances of 5 and 30 mm was found to be 40 min. When assessed from the data on the two different distances, it was found that COP appeared to be more stable against active oxygen, hence photochemical activation seemed to be more effective for the surface functionalization. Furthermore, the COP plates are bonded through attractive interactions between the modified layers on the plates at a low temperature and a low pressure without deforming microstructures performed on the plates.

From the present study, VUV-light treatment technology was found to be effective for surface modification of organosilane SAMs and COP resins. The author believes that my research achievements are expectable as the base for the development of fundamental manufacturing techniques applicable to micro-chemical, micro-optical and micro-mechanical

systems made of various materials.

Acknowledgements

I really thank Professor Hiroyuki SUGIMURA (Department of Materials Science and Engineering, Kyoto University) for giving me a great chance to perform the interesting subject and for supporting his earnest guidance, sincere encouragement and excellent research environments during the doctoral course at Kyoto University. Furthermore, he gave me the opportunity to present my work to an international audience at conferences.

I would like to thank Professor Yasuhiro AWAKURA (Department of Materials Science and Engineering, Kyoto University) and Professor Akira SAKAI (Department of Materials Science and Engineering, Kyoto University) for reviewing this thesis, and his valuable comments. I would deeply like to thank Professor Myeong-Hoon LEE (Department of Marine System Engineering, Korea Maritime University) who the first introduced me the academic world of ‘Material Surface Coating’ and has greatly encouraged me over a long time from the undergraduate to the doctoral course.

I would sincerely like to give my deep appreciation to Associate Professor Kuniaki MURASE (Department of Materials Science and Engineering, Kyoto University) for his in-depth discussions and kind comments in my research. I would also like to thank to Assistant Professor Takashi ICHII (Department of Materials Science and Engineering, Kyoto University) for his kind advice on the study in the doctoral course.

In particular, I would also like to thank Mr. Jiwon HAN and Mr. Hikaru SANO for their assistance and supports in the course of this work, and all other members of Professor SUGIMURA’s research group. I would like to express my thanks to Associate professor Seongjong KIM (Mokpo National Maritime University), Dr. Kyoungwang LEE (RIST), Dr. Hanjin RYU (POSCO), Dr. Yongsup YUN (AIST), Dr. Pilwon HEO (Nagoya University), Dr.

Sunhyung LEE (Shinshu University) for their advices on the research as well as the life in Korea and Japan.

Finally, my heartfelt thanks must go to my wife, Hyosoon PARK, for her constant encouragements and supports during last 6 years. I give my sincere gratitude to my parents, Sunchae KIM and Jeongsun BANG, for supporting me throughout the past years.

Curriculum Vitae

Personal KIM, Young-Jong

Date and place of birth: February 28th, 1979, in Suncheon, Jeonnam, Korea

Sexuality and Marital status: married male

Nationality: Korea

Education

October 2005 – September 2008 Doctor of Engineering, Department of Materials Science and Engineering, Graduate School of Engineering, Kyoto University (in Japan)

March 2003 – February 2005 Master of Engineering, Department of Marine System Engineering, Graduate School of Engineering, Korea Maritime University (in Korea)

March 1997 – February 2001 Bachelor of Engineering, Division of Marine Engineering, College of Maritime Sciences, Korea Maritime University (in Korea)

March 1994 – February 1997 High school student, Natural Science, Suncheon Maesan High School (in Korea)

Publications (in scientific journals)

Papers related to this thesis

[1] Y. J. Kim, K. H. Lee, H. Sano, J. Han, T. Ichii, K. Murase and H. Sugimura, “Surface chemical conversion of organosilane self-assembled monolayers with active oxygen species generated by vacuum ultraviolet irradiation of atmospheric oxygen molecules”, *Japanese Journal of Applied Physics*, **47**, 307-312 (2008).

[2] Y. J. Kim, J. Han, H. Sano, K. H. Lee, K. Noda, T. Ichii, K. Murase, K. Matsushige and H. Sugimura, “Organosilane self-assembled multilayer formation based on activation of methyl-terminated surface with reactive oxygen species generated by vacuum ultra-violet excitation of atmospheric oxygen molecules”, *Japanese Journal of Applied Physics*, Submitted.

[3] Y. J. Kim, Y. Taniguchi, K. Murase, Y. Taguchi and H. Sugimura, “Vacuum ultraviolet-induced surface modification of cyclo-olefin polymer substrates for photochemical activation bonding”, *Applied Surface Science*, Submitted.

Other paper

[1] J. Han, K. H. Lee, S. Fujii, H. Sano, Y. J. Kim, K. Murase, T. Ichii and H. Sugimura, “Scanning capacitance microscopy for alkylsilane monolayer covered-Si substrate patterned by scanning probe lithography”, *Japanese Journal of Applied Physics*, **46**, 5621-5625 (2007).

Conference presentations

1. International conferences

International conferences related to this thesis

[1] ○Y. J. Kim, K. H. Lee, K. Murase and H. Sugimura “Photochemical surface modification of alkyl monolayers by vacuum ultra-violet irradiation for stacking organosilane monolayers”, Joint Symposium on Materials Science and Engineering for the 21st Century, Miyagi, Japan (July, 20-23, 2006).

[2] ○Y. J. Kim, T. Ichii, K. Murase and H. Sugimura, “Photochemical surface oxidation of alkylsilane self-assembled monolayers for multilayer fabrication and micropatterning” 12th International Conference ORGANIZED MOLECULAR FILMS (LB-12), Kraków, Poland (July, 1-5, 2007).

[3] ○Y. J. Kim, T. Ichii, K. Murase and H. Sugimura, “Chemical modification of self-assembled monolayers for the preparation of multilayers”, The 100th Fall Meeting of the Korean Chemical Society, Daegu, Korea (October, 18-19, 2007).

[4] ○Y. J. Kim, H. Sugimura, Y. Taniguchi and Y. Taguchi, “Photochemical activation bonding of cyclo-olefin polymer plates”, Third International Conference of Processing Materials for Properties (PMP III), Bangkok, Thailand (December, 7-10, 2008).

Other international conferences

[1] ○J. Han, K. H. Lee, S. Fujii, H. Sano, Y. J. Kim, K. Murase, T. Ichii and H. Sugimura,

“Scanning capacitance microscopy for alkylsilane monolayer covered-Si substrate patterned by scanning probe lithography”, 14th International Colloquium on Scanning Probe Microscopy, Shizuoka, Japan (December, 7-9, 2006).

[2] ○J. Han, H. Sano, Y. J. Kim, T. Ichii, K. Murase, H. Sugimura, “Local modification of self-assembled monolayer/silicon samples with and without an interfacial oxide layer by scanning probe lithography”, The 15th International Colloquium on Scanning Probe Microscopy, Atagawa, Japan (December, 6-8, 2007).

2. Conferences in Japan

[1] ○金永鍾、李庚晷、 邑瀬邦明、杉村博之、“多層膜形成のための真空紫外光励起酸素による有機シラン SAM の光化学表面変換”、第 67 回応用物理学会学術講演会、立命館大学 (2006 年 8 月 29 日～9 月 1 日)

[2] ○金永鍾、佐野光、 李庚晷、 邑瀬邦明、 杉村博之、“真空紫外光を用いたアルキル基 SAM の光化学変換とマイクロパターニング”、2006 年電気化学秋季大会、同志社大学 (2006 年 9 月 14 日～15 日)

[3] ○金永鍾、一井崇、 邑瀬邦明、杉村博之、“有機シラン SAM の光化学表面変換とマイクロパターニング”、第 8 回関西表面技術フォーラム、近畿大学 (2006 年 12 月 7 日～8 日)

[4] ○金永鍾、 藺林豊、 杉村博之、 谷口義尚、 田口好弘、“真空紫外光照射によるシクロオレフィンポリマー基材の表面処理”、第 56 回高分子学会年次大会、京都国際

会議場 (2007年5月29日～31日)

[5] ○谷口義尚、田口好弘、金永鍾、菌林豊、杉村博之、“シクロオレフィンポリマー部材の光活性化接着”、第56回高分子学会年次大会、京都国際会議場 (2007年5月29日～31日)

[6] ○金永鍾、杉村博之、谷口義尚、田口好弘、“シクロオレフィンポリマー基材の光化学表面変換と接着”、表面技術協会第116回講演大会、長崎大学 (2007年9月18日～20日)

[7] ○金永鍾、杉村博之、谷口義尚、田口好弘、“シクロオレフィンポリマー基材の光化学表面変換と接着”、第9回関西表面技術フォーラム、近畿大学 (2007年12月11日～12日)

[8] ○金永鍾、一井崇、邑瀬邦明、杉村博之、“真空紫外光励起酸素による有機シランSAMの光化学表面改質と多層膜の形成”、2008年春季第55回応用物理学関係連合講演会、日本大学 (2008年3月27日～30日)

[9] ○金永鍾、杉村博之、谷口義尚、田口好弘、“シクロオレフィンポリマー基材表面の光化学活性化と接合技術への応用”、第57回高分子学会年次大会、パシフィコ横浜展示ホールD (2008年5月28日～30日)

[10] ○金永鍾、一井崇、邑瀬邦明、杉村博之、“光化学表面改質による有機シラン多層膜の形成”、第57回高分子学会年次大会、パシフィコ横浜展示ホールD (2008

年 5 月 28 日～30 日)

[11] ○谷口義尚、田口好弘、金永鍾、杉村博之、“シクロオレフィン系ポリマー基
材の光活性化接着と解体”、第 57 回高分子学会年次大会、パシフィコ横浜展示ホール
D (2008 年 5 月 28 日～30 日)